

METHODOLOGY ON COASTAL CONSTRUCTION
CONTROL LINE ESTABLISHMENT

by

T. Y Chiu

Beaches and Shores Resource Center
Institute of Science and Public Affairs
Florida State University
300 Johnston (Seminole) Bldg., Tallahassee FL 32306

and

R. G. Dean

Department of Coastal and Oceanographic Engineering
University of Florida
Gainesville FL 32606

through

Beaches and Shores Resource Center
Florida State University

BEACHES AND SHORES
TECHNICAL AND DESIGN MEMORANDUM NO. 84-6

COASTAL ZONE
INFORMATION CENTER

Funded by

A grant from the U. S. Office of Coastal Zone Management
National Oceanic and Atmospheric Administration
(under the Coastal Zone Management Act of 1972, as amended)

through

Florida Office of Coastal Management
Florida Department of Environmental Regulation
and

Florida Department of Natural Resources

GB
459

.F56b

no.84-6

GB459 .F56 b 78-84-6
11321368

FEB 3 1997

FOREWORD

This work provides description and documentation of advancements made in numerical modeling procedures used in recommending location of Coastal Construction Control Lines (Chapter 161, Florida Statutes). Work completed includes: 1. modification of the storm surge model for efficient processing on the Florida Department of Natural Resources NRMSS data center IBM 4341 Model Group 2 processor, 2. installation of refinements to the storm surge programs to increase coordination between one-dimensional and two-dimensional models, and 3. selection, development and installation of a beach-dune erosion model that can be used in conjunction with the storm surge modeling procedure. The contents of this document, in preliminary form, were presented to the public in a Department of Natural Resources workshop held July 11-12, 1984.

The present work is presented in partial fulfillment of contractual obligations of the Federal Coastal Zone Management Program (subject to provisions of the Coastal Zone Management Improvement Act of 1972, as amended) subject to provisions of contract CM-37 entitled "Engineering Support Enhancement Program". Under provisions of DNR contract C0037, this work is a subcontracted product of the Beaches and Shores Resource Center, Institute of Science and Public Affairs, Florida State University. The document has been adopted as a Beaches and Shores Technical and Design Memorandum in accordance with provisions of Chapter 16B-33, Florida Administrative Code.

At the time of submission for contractual compliance, James H. Balsillie was the contract manager and Administrator of the Analysis/Research Section, Hal N. Bean was Chief of the Bureau of Coastal Data Acquisition, Deborah E. Flack Director of the Division of Beaches and Shores, and Dr. Elton J. Gissendanner the Executive Director of the Florida Department of Natural Resources.

Deborah E. Flack

Deborah E. Flack, Director
Division of Beaches and Shores

July, 1984

Property of CSC Library

U. S. DEPARTMENT OF COMMERCE NOAA
COASTAL SERVICES CENTER
2234 SOUTH HOBSON AVENUE
CHARLESTON, SC 29405-2413

TABLE OF CONTENTS

Section	Page
I. INTRODUCTION	1
II. METHODOLOGY OF STORM SURGE CALCULATION	1
2.1 Introduction	2
2.2 Parameterized Hurricane	2
2.3 Classification by Path Relative to Shoreline	3
2.4 General Overview of Storm Surge Numerical Models and Procedures	16
2.5 Features and Solution of the Two-Dimensional Numerical Model	20
Governing Differential Equations For Two-Dimensional Numerical Model	22
Finite Difference Forms of Governing Differential Equations	24
Inlet and Barrier Island Representation as Hydraulic Elements	28
Boundary Conditions	35
Implicit Solution of the Finite Difference Equations.	36
Dynamic Wave Set-Up	40
2.6 Features of the One-Dimensional Numerical Model	42
Governing Differential Equations For One-Dimensional Numerical Model	42
Finite Difference Forms of Governing Differential Equations	47
Initial and Boundary Conditions For the One-Dimensional Model	47
Explicit Solution of the Finite Difference Equations	47
2.7 Long-Term Simulation	48
III. APPLICATIONS OF STORM SURGE METHODOLOGY WITH SPECIFIC ILLUSTRATION BY EXAMPLE TO CHARLOTTE COUNTY	50
3.1 Two-Dimensional Model (Appendix A)	50
Verification With Storms of Record	50
Generation of Data Base for Calibration of One-Dimensional Model	55
3.2 One-Dimensional Model (Appendix B)	67
Calibration With Two-Dimensional Model Results	67

TABLE OF CONTENTS (Cont'd.)

<u>Section</u>	<u>Page</u>
3.3 Long-Term Simulations	68
IV. EROSION CALCULATION METHODOLOGY	78
4.1 Introduction	78
4.2 Equilibrium Beach Profiles	78
4.3 Cross-shore transport Models	87
4.4 Prediction of Beach and Dune Erosion Due to Severe Storms by Kriebel's Model	89
Profile Schematization	89
Governing Equations	89
Method of Solution of Finite Difference Equations	92
Application of Method to Computation of Idealized Beach Response	93
Application of Method to Long-Term Beach and Dune Response Simulations	102
4.5 Prediction of Beach and Dune Erosion Due to Severe Storms by Simple Model	108
4.6 Augmentation of the Erosion Predicted by the Model for Recommending Position of CCCL	110
V. WAVE HEIGHT DECAY CALCULATIONS	115
5.1 Introduction	115
5.2 Methodology	115
Wave Height Decay Due to Shoaling Water	116
Wave Height Decay Due to Vegetation	116
Wave Height Decay Due to Buildings	117
Combined Effects of Topography, Vegetation and Buildings	117
VI. LONG-TERM EROSIONAL CONSIDERATIONS	118
6.1 Introduction	118
6.2 Methodology	118
VII. OVERALL VERIFICATIONS OF CCCL METHODOLOGY	120
7.1 Hurricane Agnes, St. George Island, Franklin County	120
7.2 Hurricane Eloise Damage in Walton and Bay Counties	123
REFERENCES	128
APPENDIX A	130
APPENDIX B	153
APPENDIX C	159

LIST OF FIGURES

<u>Figure</u>	<u>Page</u>
II-1 General Location of the Study Area	4
II-2 Directional Distribution of Historical Hurricanes, Crystal River to East Cape, Florida	5
II-3 A Definition Sketch of Three Types of Hurricanes	6
II-4 Designation of Alongshore, Landfalling and Exiting Hurricanes Depending on Track Directions Relative to Shoreline Orientation	8
II-5 Cumulative Probability Distribution of Hurricane Track Direction	9
II-6 Cumulative Probability Distribution of Radius to Maximum Winds for Landfalling and Exiting Hurricanes	10
II-7 Cumulative Probability Distribution of Radius to Maximum Winds for Alongshore Hurricanes	11
II-8 Cumulative Probability Distribution of Central Pressure Deficity, Δp , for Landfalling and Alongshore Hurricanes	12
II-9 Cumulative Probability Distribution of Central Pressure Deficity, Δp , for Exiting Hurricanes	13
II-10 Interdependence of Central Pressure Deficity, Δp , and Radius to Maximum Winds, R	14
II-11 Cumulative Probability Distribution of Storm Translation Speed V_T , for Landfalling, Alongshore and Exiting Hurricanes	15
II-12 Cumulative Probability Distribution of Landfalling Distance, Y_F , for Landfalling and Exiting Hurricanes	17
II-13 Cumulative Probability Distribution of Offshore Distance of Passage, L, for Alongshore Hurricanes	18
II-14 Flow Chart of Methodology	19
II-15 Grid System Layout for Charlotte County	21

LIST OF FIGURES (CONT'D)

<u>Figure</u>		<u>Page</u>
II-16	Bottom Friction Coefficients for Various Bottom Conditions	25
II-17	Schematic of Implicit Method of Solving Momentum and Continuity Equations	27
II-18	Region of Interest in Description of Sub-Grid Features	29
II-19	Profile of the North Transect Line and its One-Dimensional Grid Representation	43
II-20	Profile of the Middle Transect Line and its One-Dimensional Grid Representation	44
II-21	Profile of the South Transect Line and its One-Dimensional Grid Representation	45
II-22	Flow Chart for Storm Tide Simulations (After Calibration to Determine $(AMP)_{LF}$, $(AMP)_{ALONG}$ and $(AMP)_{EXIT}$)	49
III-1	Comparison between Measured and Computed Storm Tide at Manasota Bridge, Florida for the September 1947 Hurricane	52
III-2	Comparison between Measured and Computed Storm Tide at Venice, Florida for the September 1947 Hurricane	53
III-3	Comparison between Measured and Computed Storm Tide at Ft. Myers, Florida for the September 1947 Hurricane	54
III-4	Comparison between Measured and Computed Storm Tide at St. Marks, Florida for Hurricane Agnes of 1972	57
III-5	Comparison between Measured and Computed Storm Tide at St. Marks, Florida for Hurricane Eloise of 1975	58
III-6	Comparison between Measured and Computed Storm Tide at Fernandina Beach, Florida for Hurricane Dora of 1964	60
III-7	Comparison between Measured and Computed Storm Tide at Mayport, Florida for Hurricane Dora of 1964	61
III-8	Comparison between Measured and Computed Storm Tide at Fernandina Beach, Florida for Hurricane David of 1979	62

LIST OF FIGURES (CONT'D)

<u>Figure</u>		<u>Page</u>
III-9	Comparison between Measured and Computed High Water Mayport, Florida for Hurricane David of 1979	63
III-10a	Calibration Relationship between the One-Dimensional and the Two-Dimensional Calculations of Peak Surges at the North and Middle Transect Lines of Charlotte County for Landfalling Hurricanes	69
III-10b	Calibration Relationship between the One-Dimensional and the Two-Dimensional Calculations of Peak Surge at the South Transect Line of Charlotte County for Landfalling Hurricanes	70
III-11a	Calibration Relationship between the One-Dimensional and the Two-Dimensional Calculations of Peak Surges at the North and Middle Transect Lines of Charlotte County for Alongshore Hurricanes	71
III-11b	Calibration Relationship between the One-Dimensional and the Two-Dimensional Calculations of Peak Surges at the South Transect Line of Charlotte County for Alongshore Hurricanes	72
III-12a	Calibration Relationship between the One-Dimensional and the Two-Dimensional Calculations of Peak Surges at North and Middle Transect Lines of Charlotte County for Exiting Hurricanes	73
III-12b	Calibration Relationship between the One-Dimensional and the Two-Dimensional Calculations of Peak Surges at the South Transect Line of Charlotte County for Exiting Hurricanes	74
III-13	Combined Total Storm Tide Elevation Versus Return Period for Three Representative Transect Lines in Charlotte County	76
IV-1	Location map of the 502 profiles used in the analysis (from Hayden, et al., (10))	79
IV-2	Characteristics of dimensionless beach profile $\frac{h}{h_b} = \left(\frac{x}{W}\right)^m$ for various m values (from Dean, (11))	80

LIST OF FIGURES (CONT'D)

<u>Figure</u>		<u>Page</u>
IV-3	Equilibrium beach profiles for sand sizes of 0.2mm and 0.6 mm $A(D = 0.2\text{mm}) = 0.1\text{m}^{1/3}$, $A(D = 0.6 \text{ mm}) = 0.20\text{m}^{1/3}$	81
IV-4	Histogram of exponent m in equation $h = Ax^m$ for 502 United States East Coast and Gulf of Mexico profiles (from Dean, (11))	82
IV-5	Beach profile factor, A, vs sediment diameter, D, in relationship $h = Ax^{2/3}$ (modified from Moore, (12))	84
IV-6	Profile P4 from Zenkovich (1967). A boulder coast in Eastern Kamchatka. Sand diameter: 150mm - 300mm. Least squares value of $A = 0.82\text{m}^{1/3}$ (from Moore, (12))	85
IV-7	Profile P10 from Zenkovich (1967). Near the end of a spit in Western Balck Sea. Whole and broken shells. $A = 0.24\text{m}^{1/3}$ (from Moore, (12))	85
IV-8	Profile from Zenkovich (1967). Eastern Kamchatka. Mean sand diameter: 0.25 mm. Least squares value of $A = 0.07\text{m}^{1/3}$ (from Moore, (12))	86
IV-9	Model simulation of a 0.5 meter sea level rise and beach profile response with a relatively mild sloping beach (from Moore, (12))	88
IV-10	Effect of varying the sediment transport rate coefficient on cumulative erosion during the simulation of Saville's (1957) laboratory investigation of beach profile evolution for a 0.2mm sand size (from Moore, (12))	90
IV-11	Model representation of beach profile, showing depth and transport relation to grid definitions (from Kriebel, (14))	91
IV-12	Characteristic form of berm recession versus time for increased static water level (from Kriebel, (14))	94
IV-13	Comparison of asymptotic berm recession from model (—) and as calculated by Eq. (IV.12) (••)	96

LIST OF FIGURES (CONT'D)

<u>Figure</u>		<u>Page</u>
IV-14	Effect of breaking wave height on berm recession (from Kriebel, (14))	97
IV-15	Effect of static storm surge level on berm recession (from Kriebel, (14))	98
IV-16	Effect of sediment size berm recession (from Kriebel, (14))	100
IV-17	Comparison of the effects of 12, 24, and 36 hrs. storm surge on volumetric erosion (from Kriebel, (14))	101
IV-18	Flow diagram of N-year simulation of hurricane storm surge and resulting beach erosion (from Kriebel, (14))	105
IV-19	Average frequency curve for dune recession, developed by Monte Carlo simulation, Bay-Walton Counties, Florida (from Kriebel, (14))	106
IV-20	Probability or risk of dune recession of given magnitude occurring at least once in N-years, Bay-Walton Counties, Florida (from Kriebel, (14))	107
IV-21	Features of simplified beach erosion model	109
IV-22	Results of applying erosion model to Range R-1, Martin County (Hutchinson Island), 100 year storm tide, average erosion	111
IV-23	Results of applying erosion model to Range R-89, Martin County (Jupiter Island), 100 years storm tide, average erosion	112
IV-24	Calibration of Simplified Erosion Model By Comparison with Erosion Occurring at Various Elevation Due to Hurricane Eloise	113
VI-1	General erosion conditions in Florida (Bruun, Chiu, Gerritsen and Morgan, (20))	119
VI-1a	Beach profile at Range R-105 on St. George Island. A location of severe overwash and damaged roadway due to Hurricane Agnes, 1972 (see Figure VII.1b for extension of this profile)	121

LIST OF FIGURES (CONT'D)

<u>Figure</u>	<u>Page</u>
VII-1b Continuation of profile across St. George Island, Range R-105, showing location of damaged road, due to Hurricane Agnes, 1972	122
VII-2 Landfall location of Hurricane Eloise, September 23, 1975 and some resulting tide and uprush characteristics (from Chiu, (16))	124
VII-3 Relation of erosional characteristics and pre-Eloise vegetation line to set-back line, Bay County, Florida (from Chiu, (16))	125
VII-4 Relation of erosional characteristics and pre-Eloise vegetation line to set-back line, Walton County, Florida (from Chiu, (16))	125
VII-5 Damage to structures in relation to location of set-back control line (based on study of 540 structures in Bay County after Hurricane Eloise, by Shows, (21))	126

LIST OF TABLES

<u>Table</u>	<u>Page</u>
III-1 Input Parameters for Calibration Hurricane (Hurricane of September 1947)	51
III-2 Input Parameters for Calibration Hurricanes (Hurricane Agnes of June 1972)	56
III-3 Hurricane Eloise of September 1975	56
III-4 Input Parameters for Calibration Hurricanes (Hurricane Dora of September 1964)	59
III-5 Hurricane David of September 1975	59
III-6 Parameters Defining 11 Landfalling Storms Used In Calibrating The One-Dimensional Model With The Two-Dimensional Model And The Results	64
III-7 Parameters Defining 11 Alongshore Storms Used In Calibrating The One-Dimensional Model With The Two-Dimensional Model And The Results	65
III-8 Parameters Defining 11 Exiting Storms Used In Calibrating The One-Dimensional Model With The Two-Dimensional Model And The Results	66
III-9 Values of 1-D/2-D Peak Storm Surge Correlation Coefficients For Counties Completed to Date	75
III-10 Combined Total Storm Tide Values for Various Return Periods	77

METHODOLOGY
ON
"COASTAL CONSTRUCTION CONTROL LINE ESTABLISHMENT"

I. INTRODUCTION

The coastal engineering phenomena leading to the rationale for the Coastal Construction Control Line (CCCL) are:

Shoreline Erosional Trend
Shoreline Fluctuations (Both Seasonal and Storms) and,
Storm Surges and Associated Waves.

The general objective of the CCCL program is to define the zone of impact of a one hundred year storm event along the sandy outer coastline segments of the State of Florida. This program is implemented on a county-by-county basis. The DNR permitting program applies seaward of the CCCL with the two-fold purpose of ensuring: (1) the protection of the adjacent shoreline, and (2) the integrity of structures.

Due to the scarcity of specific data which would identify directly the appropriate location for the CCCL, a series of numerical models and calculation procedures is employed and combined with historical hurricane and erosion data to establish the recommended CCCL position.

II. METHODOLOGY

The establishment of the recommended location of the CCCL requires calculation of the 100 year storm surge and accompanying waves and shoreline erosion. These models and their implementation are based on the best data generally available and on data collected specifically for the purpose of the program. In particular an extensive set of nearshore and beach profiles is taken at intervals of approximately 1,000 ft with all profiles extending out to the limit of wading and every third profile extending out to approximately the thirty foot contour. The field data are valuable input to the computer models; however, the field program will

be described elsewhere.

2.1 Introduction

As noted previously, because storm surge data are quite sparse (especially long-term storm surge data) and because most tide gages and high water marks collected are in locations which are not representative of open coast conditions, it is necessary to use numerical models with long-term historical hurricane characteristics which are relatively insensitive geographically, although there are, for example, trends in the hurricane parameters.

2.2 Parameterized Hurricane

Each hurricane is unique in its structure, shape, size, translational characteristics, etc. However, it is generally agreed that when considering many hurricanes, it is valid to employ the concept of an idealized or parameterized hurricane. In this approach, a hurricane is represented by five parameters:

Δp = the central (lowest) barometric pressure relative to the ambient pressure usually reported in inches of mercury (in. Hg) or millibars of mercury, Δp is a measure of the intensity of the hurricane,

R = radius to the band of maximum winds, usually reported in nautical miles. R is a measure of the size of the hurricane,

V_F = forward translational speed of the hurricane, usually reported in knots,

θ = forward translational direction, defined as the direction from which a hurricane originates,

L = landfall location or some other parameter positioning the hurricane at some time during the hurricane's close proximity to the area of primary concern.

2.3 Classification by Path Relative to Shoreline

Hurricanes causing appreciable storm tides in the vicinity of a county shoreline are classified as either "landfalling", "alongshore" or "exiting" storms, depending on their paths relative to the shoreline orientation. Reasonably good data are available describing the characteristics of such storms, from approximately 1900 to 1978. For purposes of establishing the statistical characteristics, the frequency and direction data contained in References (1) and (2) are merged for a segment of the coast usually extending from 100 n.mi. to 150 n.mi. up and down coast, i.e., a total length of 200-300 n.mi.

The hurricane direction is defined here as the azimuth of hurricane translation direction at the time of landfall, or, if an alongshore storm, when in close proximity to the site.

The designation of a storm as "landfalling", "exiting", or "alongshore" is somewhat arbitrary as storms travel over a continuous range of directions and there is not a particular direction relative to the shoreline for which the storm tide-generating characteristics change markedly. Moreover, one directional distribution is applied for all three types of storms. Figure II-1 presents an example of the directional distribution for Charlotte County, FL, and Figure II-2 shows the location of Charlotte County. It is important to note that the manner in which the track of a hurricane is characterized for the purposes of this study is different for landfalling, exiting and alongshore hurricanes. For landfalling and exiting hurricanes, the track is specified by a location of landfall (or exit) and direction, whereas for the alongshore storms, the track is specified by an offshore distance and a track direction. Figure II-3 presents a definition sketch of the three types of hurricanes.

For purposes of this study, landfalling and exiting hurricanes are considered to be of possible significance if they made landfall within a 250 nautical mile segment of the coast comprising the study area. Generally, this segment is

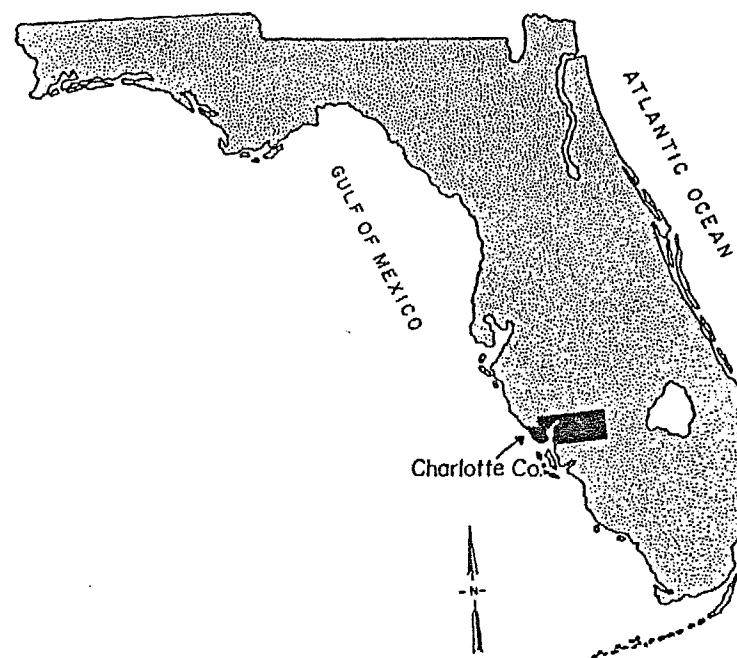


Figure II-1. General Location of the Study Area

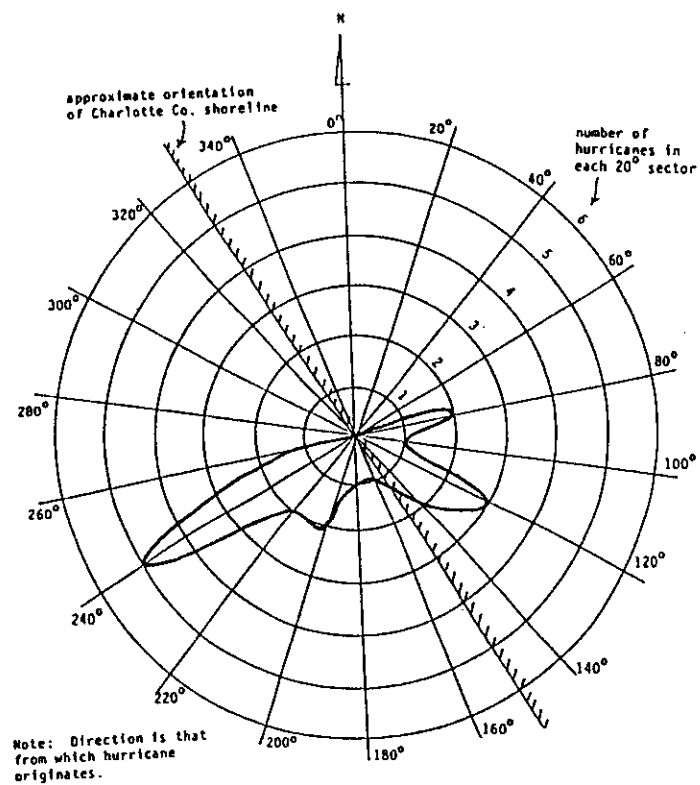


Figure II-2. Directional Distribution of Historical Hurricanes, Crystal River to East Cape, Florida

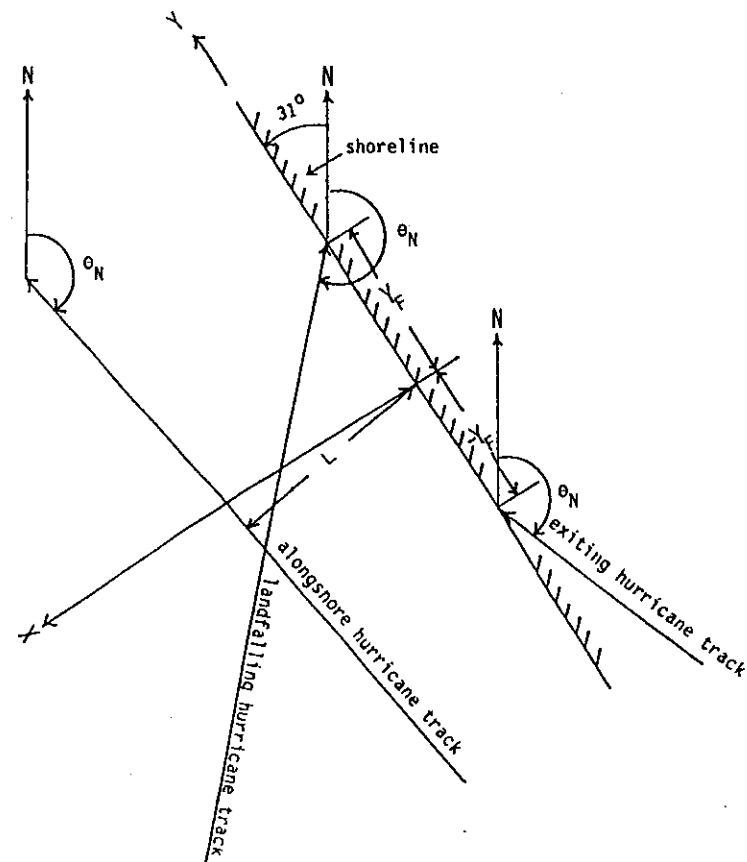


Figure II-3. A Definition Sketch of Three Types of Hurricanes

centered approximately near the mid-point of the county of interest. Usually an offshore limit of alongshore storms is on the order of 50 to 100 nautical miles. Figure II-4 shows the sectors of propagation paths for landfalling, exiting and alongshore hurricanes for Charlotte County.

For purposes of computer use, the cumulative probability distribution is developed from Figure II-2 and is presented in Figure II-5.

In the following discussion of the remaining parameters defining the idealized hurricane, Charlotte County will be used as an illustrative example. Figure II-6 presents the cumulative probability distribution of radius to maximum winds for landfalling and exiting hurricanes, and Figure II-7 presents the same for alongshore hurricanes.

The cumulative probability distribution of central pressure deficit for landfalling and alongshore hurricanes is presented in Figure II-8 and Figure II-9 presents the same information for exiting hurricanes.

Examination of historical hurricane data has demonstrated that for landfalling storms the distributions for radius to maximum winds and central pressure deficit are not independent. The correlation is such that the hurricanes with the more extreme central pressures tend to be smaller. Figure II-10 presents the interdependence ranges of R and Δp for a wider segment of the coast comprising the area of interest. For purposes of computer application, the joint cumulative probability distribution of R is modified to conform to the limited range shown on Figure II-10 for any specific Δp selected within the range of -0.9 to -2.6 in. Hg.

The cumulative probability distribution of the forward speed of translation for landfalling, exiting and alongshore hurricanes is presented in Figure II-11.

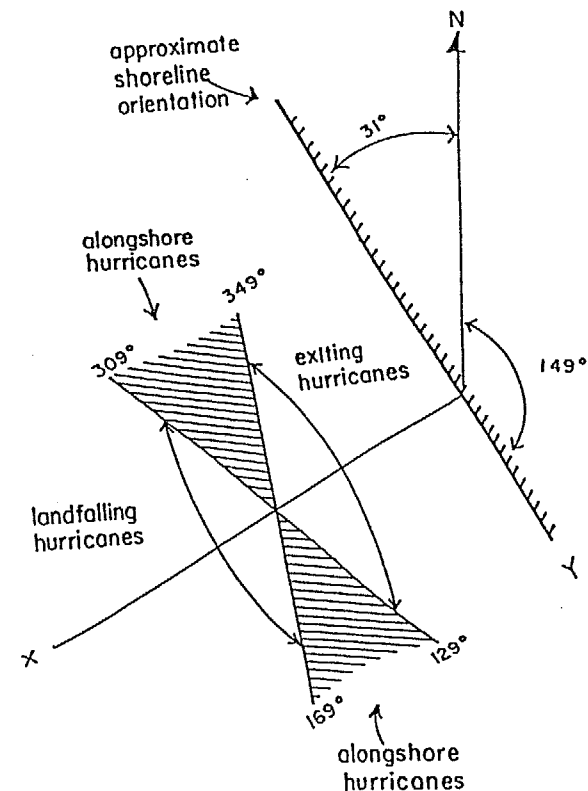


Figure II-4. Designation of Alongshore, Landfalling and Exiting Hurricanes Depending on Track Directions Relative to Shoreline Orientation

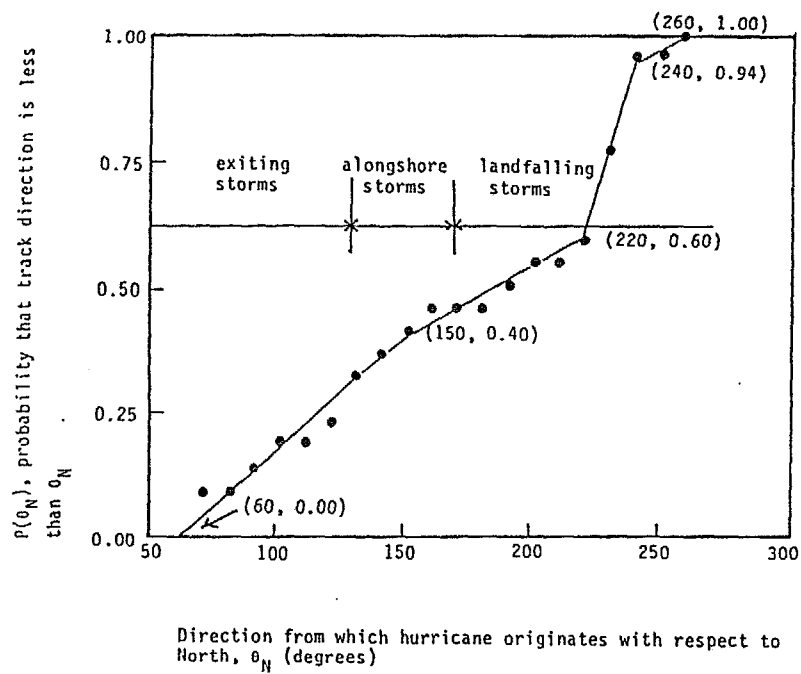


Figure II-5. Cumulative Probability Distribution of Hurricane Track Direction

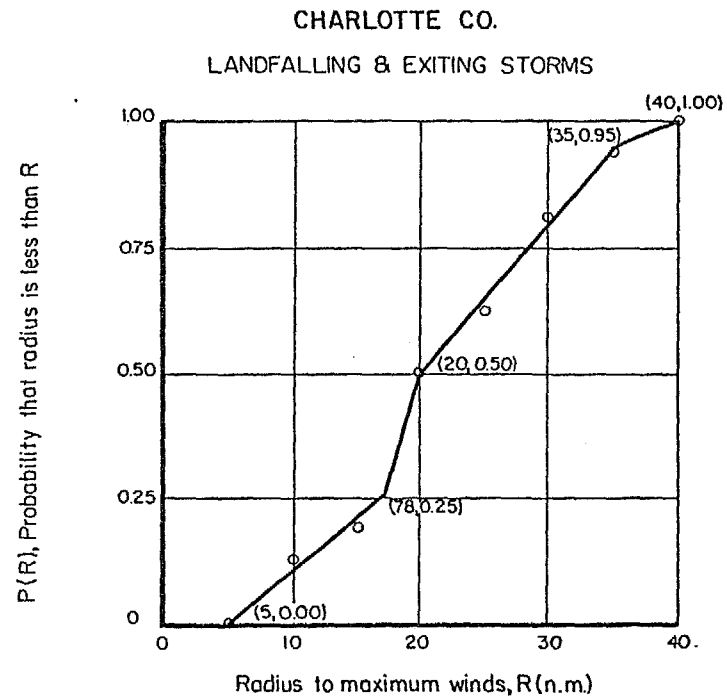


Figure II-6. Cumulative Probability Distribution of Radius to Maximum Winds for Landfalling and Exiting Hurricanes

CHARLOTTE CO.
ALONGSHORE STORMS

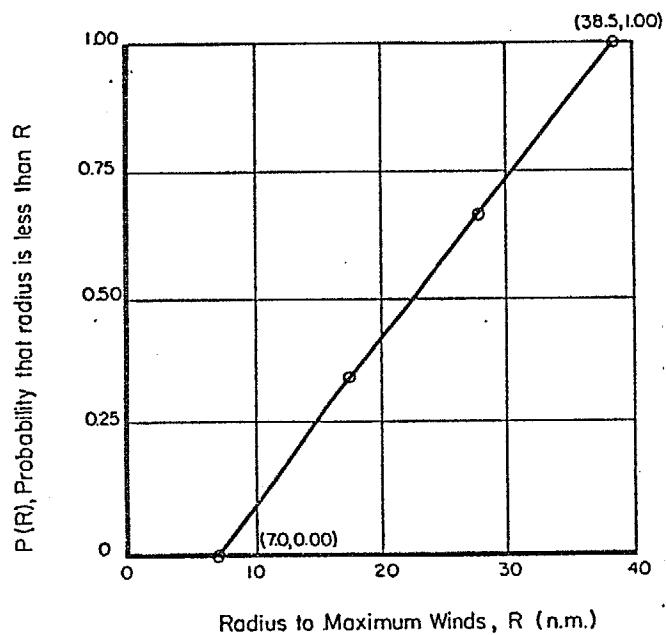


Figure II-7. Cumulative Probability Distribution of Radius to Maximum Winds for Alongshore Hurricanes

CHARLOTTE CO.
LANDFALLING & ALONGSHORE STORMS

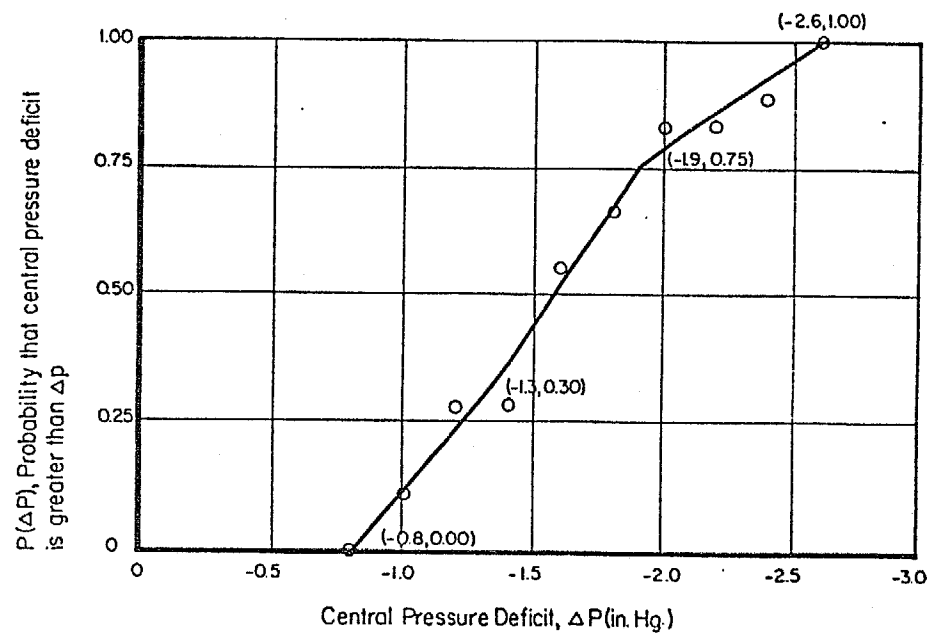


Figure II-8. Cumulative Probability Distribution of Central Pressure Deficit, Δp, for Landfalling and Alongshore Hurricanes

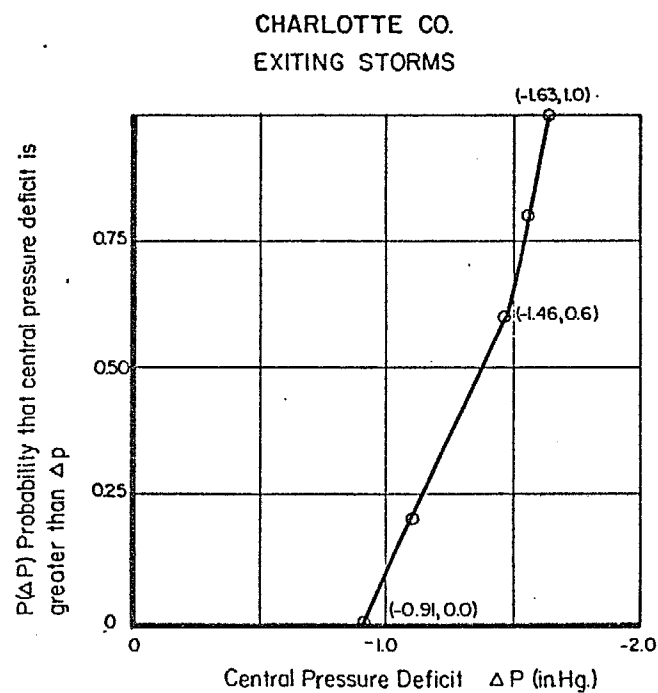


Figure II-9. Cumulative Probability Distribution of Central Pressure Deficit, ΔP , for Exiting Hurricanes

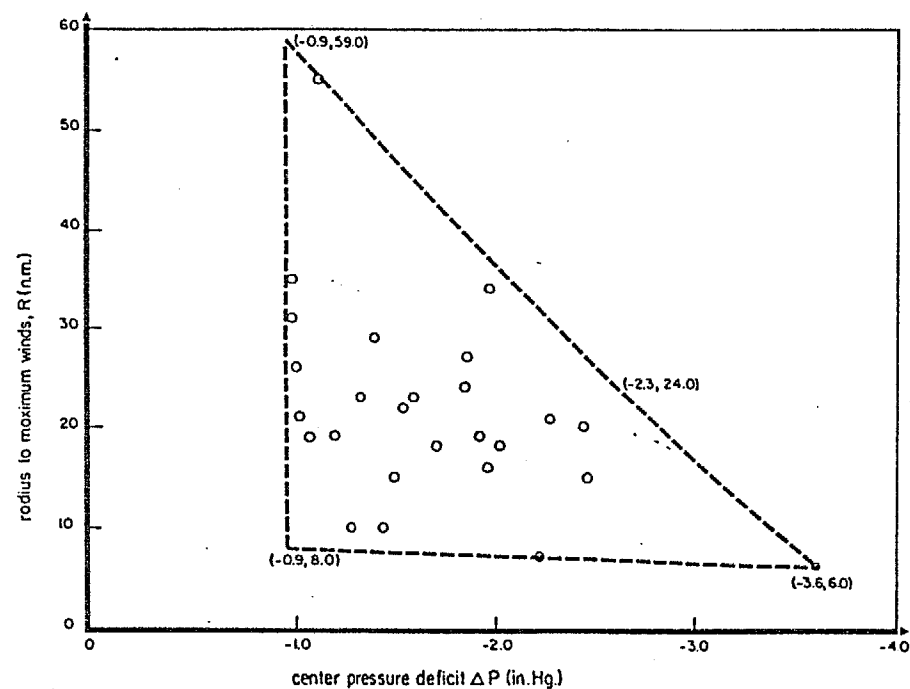


Figure II-10. Interdependence of Central Pressure Deficit, ΔP , and Radius to Maximum Winds, R

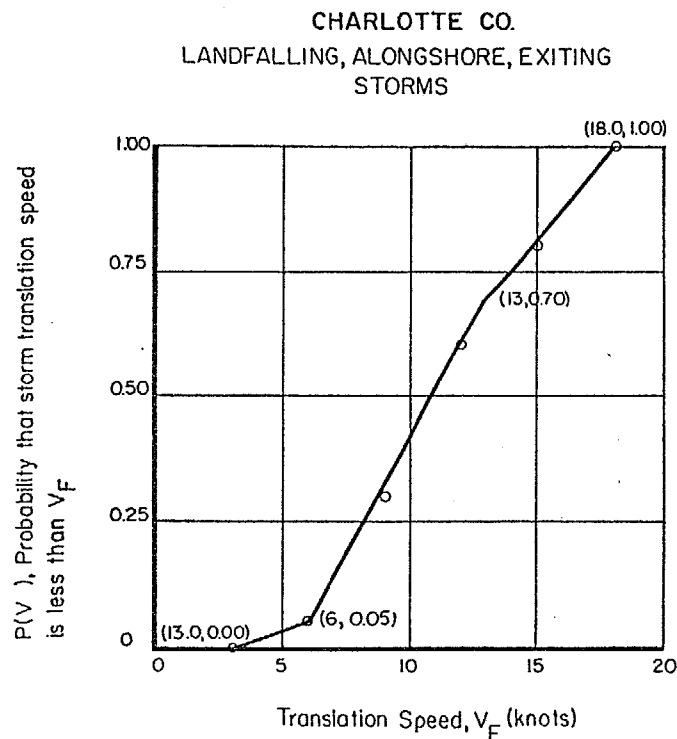


Figure II-11. Cumulative Probability Distribution of Storm Translation Speed V_F , for Landfalling, Alongshore and Exiting Hurrica

For the landfalling and exiting hurricanes, the track position is determined by y coordinate, Y_F , representing the landfall or exit point (Figure II-3). Figure II-12 presents the actual landfalling position defined by Y_F and the associated cumulative probability distribution. Figure II-13 presents the cumulative probability distribution of offshore distance of passage, L , for along-shore hurricanes.

To generate a parameter (say R) in accordance with the statistical distribution, a random number is generated between 0 and 1 and the associated R value interpolated from the cumulative probability distribution. Since the cumulative probability distribution (cdf) is the integral of the probability density function (pdf), the slope of the cdf is proportional to the probability of occurrence and thus the method above yields the correct population of the parameter (in this case, R).

2.4 General Overview of Storm Surge Numerical Models and Procedures

In the establishment of the return period vs storm surge relationship, two numerical models were employed to obtain the best combination of accuracy, detail and economy. The first model employed is a two-dimensional (2-D) variable grid numerical model and may extend over a shoreline length of 100-200 n.mi. The purpose of the 2-D model is two-fold: (1) to verify and develop confidence in the 2-D model by comparing predicted storm surges with those caused by storms of record, and (2) to provide a data base of storm tides for calibration of the faster and more economical one-dimensional (1-D) model. As inferred, the 2-D model is much more expensive to run than the 1-D model. The ratio of run times is approximately 200:1 to 400:1.

The flow chart presented in Figure II-14 describes the general methodology and relationship of the two numerical models to the overall computational process.

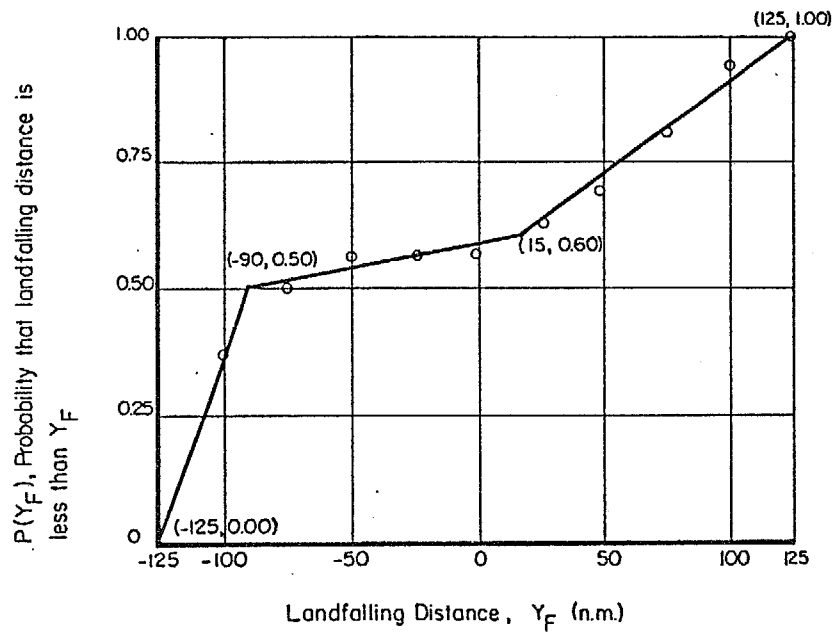


Figure II-12. Cumulative Probability Distribution of Landfalling Distance, Y_F , for Landfalling and Exiting Hurricanes

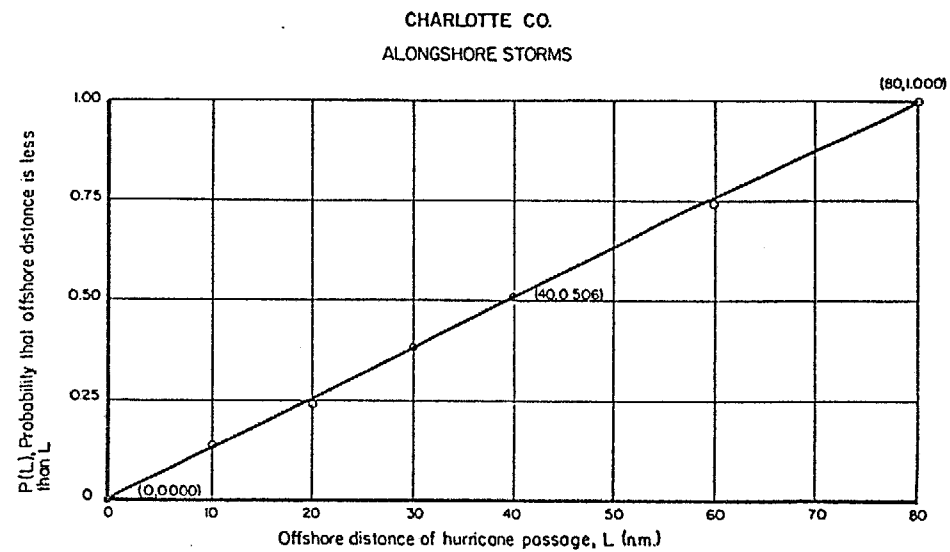


Figure II-13. Cumulative Probability Distribution of Offshore Distance of Passage, L , for Alongshore Hurricanes

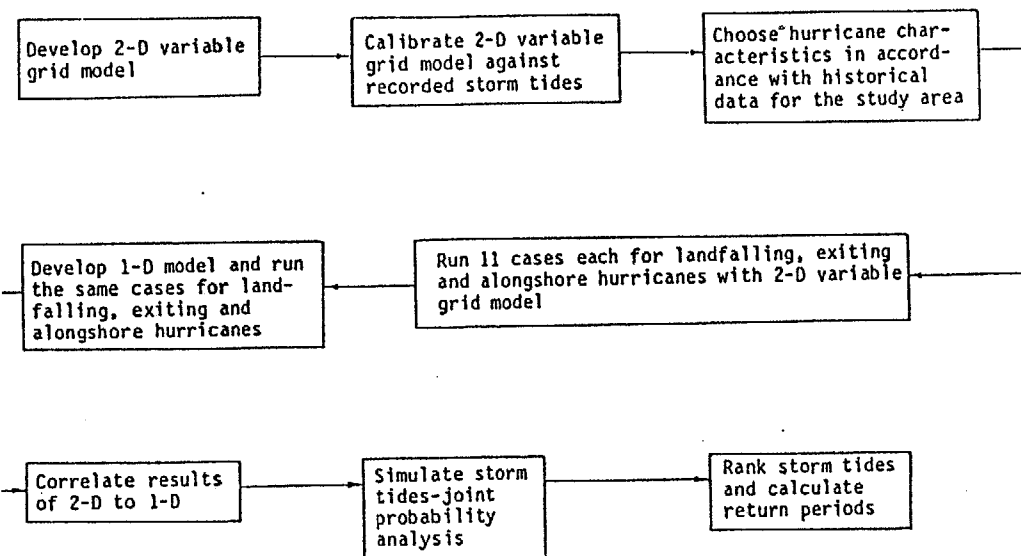


Figure II-14. Flow Chart of Methodology

The following sections describe each of the two numerical models, with illustrative examples from Charlotte County.

2.5 Features and Solution of the Two-Dimensional Numerical Model

As noted previously, this is a variable grid two-dimensional model for the offshore and coastal areas which affects the generation of storm tide for the particular county of interest. For Charlotte County, the grids of the model are arranged in such a way that

1) The finest grids cover the coastal areas of Charlotte County to yield detailed information for the study. Fine grids are also used in locations where calibration of the model results against measured storm tides is going to take place.

2) The coarsest grids cover the north, south and seaward model boundary areas where detailed information is not needed.

3) A number of grids varying gradually in size are used for the transition from the coarsest to the finest grids.

This arrangement of the varying grid system of the two-dimensional model gives good efficiency of computing time utilization.

The size of the finest grid is 1,000 ft. x 5,000 ft. and the coarsest 50,000 ft. x 35,500 ft. The two-dimensional model covers an area of 188.3 n.mi. x 167.0 n.mi. with the eastern side in approximate orientation with the shoreline of Charlotte County. Figure II-15 shows the grid system layout.

The two-dimensional hurricane model is an implicit finite difference system in which the three governing differential equations are the two vertically averaged equations of momentum and the equation of continuity. The solution to the equations is carried out by a fractional time step procedure. The advantage of this fractional time step procedure is that it is time and space centered to first order. The finite difference equations appropriate for implicit solution

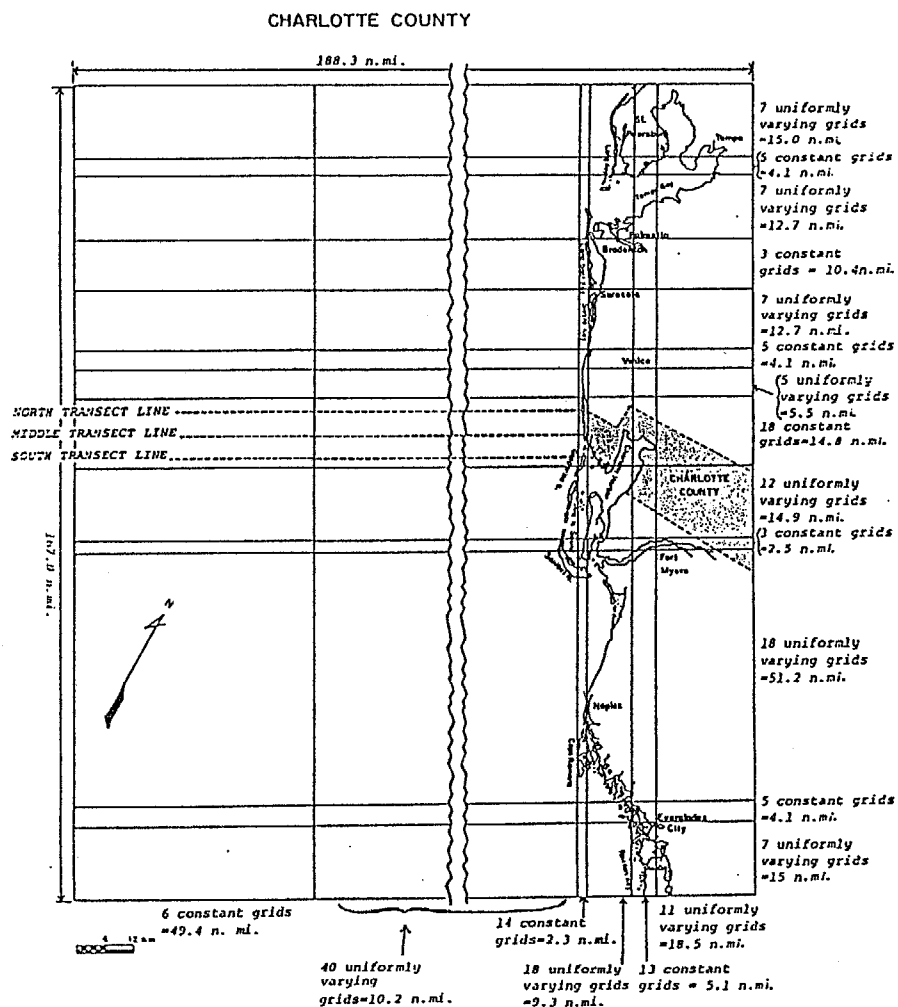


Figure II-15. Grid System Layout for Charlotte County

are solved by the "double sweep" method, and will be described later in this section. The surface (wind) and bottom (friction) shear stresses, the barometric pressure, the Coriolis effect, the components of slope of the water surface and the boundary conditions are all incorporated into the solution processes.

Inlets and barrier islands which are too small to be resolved by the normal grid sizes are represented in the model by a special treatment. The boundary conditions specified on the two-dimensional model are that the water surface displacement on the boundaries where water is present are equal to the barometric head, due to atmospheric pressure variations. The normal discharge at these boundaries is that necessary to satisfy the volume requirement by the rising and falling water surface encompassed by the boundaries. Although this is an approximation, if the boundaries are sufficiently distant from the site of interest, any extraneous effects of this approximation should be small. The second type of boundary condition is the no-flow requirement which ensures that the flows are zero normal to grid lines where land elevations exist that are higher than the adjacent water elevations. At times when the elevation of a rising water surface exceeds the land elevation of an adjacent grid block, that block is flooded by a simple algorithm and vice versa for the "deflooding" from grid blocks at times that the falling water surface leaves a block exposed. The effects of vegetation on bottom and surface friction factors are accounted for in an approximate manner.

Governing Differential Equations For Two-Dimensional Numerical Model

The governing differential equations for the two-dimensional model are the two vertically averaged equations of momentum and the equation of continuity, given by:

$$\text{Momentum Equations} \left\{ \begin{aligned} \frac{\partial q_x}{\partial t} + \frac{q_x}{D} \frac{\partial q_x}{\partial x} + \frac{q_y}{D} \frac{\partial q_x}{\partial y} &= -gD \frac{\partial \eta}{\partial x} - \frac{D}{\rho} \frac{\partial p}{\partial x} + \frac{\tau_{wx}}{\rho} - \frac{\tau_{bx}}{\rho} - \beta q_y \quad (II.1) \\ \frac{\partial q_y}{\partial t} + \frac{q_x}{D} \frac{\partial q_y}{\partial x} + \frac{q_y}{D} \frac{\partial q_y}{\partial y} &= -gD \frac{\partial \eta}{\partial y} - \frac{D}{\rho} \frac{\partial p}{\partial y} + \frac{\tau_{wy}}{\rho} - \frac{\tau_{by}}{\rho} + \beta q_x \quad (II.2) \end{aligned} \right.$$

$$\text{Continuity Equation} \quad \frac{\partial \eta}{\partial t} + \frac{\partial q_x}{\partial x} + \frac{\partial q_y}{\partial y} = 0 \quad (II.3)$$

in which

- $\begin{Bmatrix} q_x \\ q_y \end{Bmatrix}$ = volumetric transport components per unit width in the $\begin{Bmatrix} x \\ y \end{Bmatrix}$ directions
 t = time
 D = total water depth ($h+\eta$) including the still water depth, h_s and the storm surge,
 η = storm surge above mean water level
 x = horizontal coordinate, directed offshore
 y = horizontal coordinate direction according to the left-hand coordinate system
 g = gravitational constant
 ρ = mass density of water
 p = barometric pressure

$$\begin{Bmatrix} \tau_{wx} \\ \tau_{wy} \end{Bmatrix} = \text{wind shear stress components in the } \begin{Bmatrix} x \\ y \end{Bmatrix} \text{ directions}$$

$$\begin{Bmatrix} \tau_{bx} \\ \tau_{by} \end{Bmatrix} = \text{bottom shear stress components in the } \begin{Bmatrix} x \\ y \end{Bmatrix} \text{ directions}$$

- f = Darcy Weisbach friction coefficient
 β = Coriolis parameter = $2\Omega \sin \psi$
 Ω = angular speed of earth rotation = 7.27×10^{-5} rad/sec
 ψ = latitude of site of interest

The surface and bottom shear stress components are related to the wind speed W and discharge components by

$$\begin{Bmatrix} \tau_{wx} \\ \tau_{wy} \end{Bmatrix} = \rho K W \begin{Bmatrix} W_x \\ W_y \end{Bmatrix} \quad (II.4)$$

$$\begin{Bmatrix} \tau_{bx} \\ \tau_{by} \end{Bmatrix} = \frac{\rho f |q|}{8D^2} \begin{Bmatrix} q_x \\ q_y \end{Bmatrix} \quad |q| = \sqrt{q_x^2 + q_y^2} \quad (II.5)$$

in which K is an air-sea friction coefficient developed by Van Dorn (3); and depends on the wind speed as follows:

$$K = \begin{cases} 1.1 \times 10^{-6} & \text{for } W < W_{cr} \\ 1.1 \times 10^{-6} + 2.5 \times 10^{-6} \left(1 - \frac{W_{cr}}{W}\right)^2 & \text{for } W \geq W_{cr} \end{cases} \quad (II.6)$$

where $W_{cr} = 23.6$ ft/sec.

The quantity, f , is the Darcy-Weisbach bottom friction coefficient and varies with depth, bottom roughness and vegetation, if present. For purposes of this study, f was developed by Christensen and Walton (4) of the University of Florida and is presented in Figure II-16.

Finite Difference Forms of Governing Differential Equations

The finite difference representations of Equations (II.1), (II.2) and (II.3)

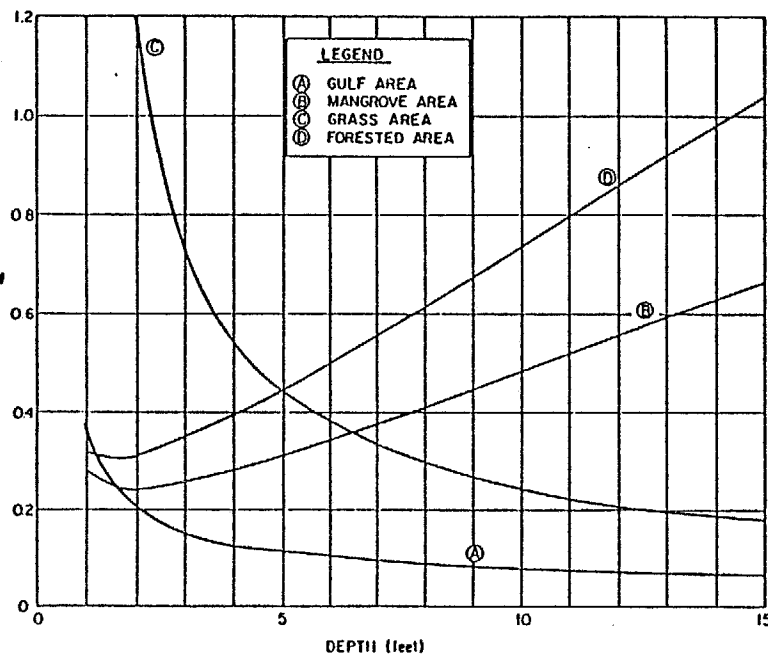


Figure II-16. Bottom Friction Coefficients for Various Bottom Conditions.

are expressed as follows with the convective terms (i.e., $\frac{\eta_x}{D} \frac{\delta q_x}{\delta x}$, etc.) omitted in preparation for an implicit type of solution. The solution to the equations will be carried out in a fractional time step procedure. This procedure is schematized in Figure II-17. The advantage of this fractional time step procedure is that it is time and space centered to first order.

The finite difference equations for the first portion of the fractional time step that are appropriate for the implicit method of solution are:

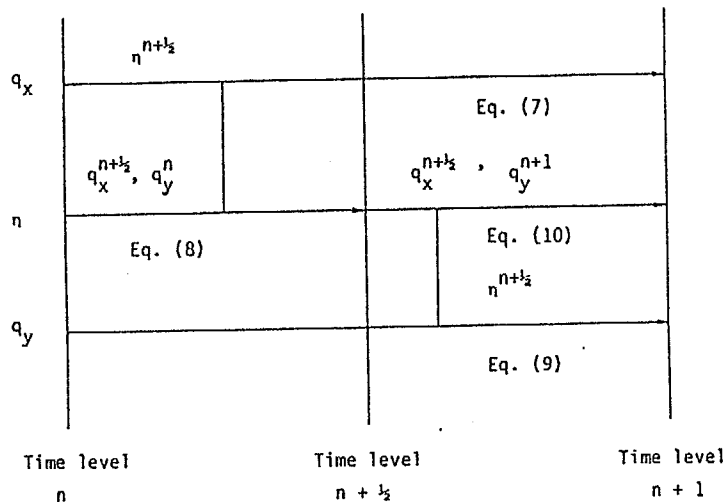
$$A_i^{n+\frac{1}{2}} n_{i,j} + B_i^{n+1} q_{x,i,j}^{n+1} + C_i^{n+\frac{1}{2}} n_{i-1,j}^{n+\frac{1}{2}} = D_i \quad (II.7)$$

$$A_i^* q_{x,i+1,j}^{n+1} + B_i^* n_{i,j}^{n+\frac{1}{2}} + C_i^* q_{x,i,j}^{n+1} = D_i^* \quad (II.8)$$

where Eq. (II.7) represents the momentum equation in the x-direction and Eq. (II.8) represents the continuity equation; these two equations are to be solved simultaneously. The second set of simultaneous equations which is solved subsequent to the solution of the first set is

$$A_j^{n+\frac{1}{2}} n_{i,j}^{n+\frac{1}{2}} + B_j^{n+1} q_{y,i,j}^{n+1} + C_j^{n+1} n_{i,j-1}^{n+1} = D_j \quad (II.9)$$

$$A_j^* q_{y,i,j+1}^{n+1} + B_j^* n_{i,j}^{n+\frac{1}{2}} + C_j^* q_{y,i,j}^{n+1} = D_j^* \quad (II.10)$$



- Notes: (1) Vertical links denote equations which are solved simultaneously.
- (2) Values adjacent to the horizontal bars indicate the time level of the different variables entering into the computations.

Figure II-17. Schematic of Implicit Method of Solving Momentum and Continuity Equations

Inlet and Barrier Island Representation as Hydraulic Elements

Inlets and barrier islands represent features which are too small to be resolved by the normal grid sizes (= miles) of the numerical model. Thus, these features are termed "sub-grid" features and must be represented by a special treatment.

The domain of interest here is the two adjacent half grid blocks with a sub-grid feature imbedded in the grid line common to the grid blocks, see Figure II-18. The grid line can be oriented in either the x or y-direction and here is indicated generically as in the x -direction with the direction of flow occurring in the s -direction. The sub-grid feature can consist of the following combinations:

- a barrier of a prescribed height, and frictional characteristics, extending over the full length, DL of grid line,
- a barrier of prescribed height, width, W_B , and frictional characteristics. The remaining width, $(DL - W_B)$, of the grid line is considered too high for flow to occur over the top,
- a barrier of prescribed height, width and frictional characteristics with an inlet of designated width, W_I , depth and frictional characteristics occupying a portion of the grid line length.

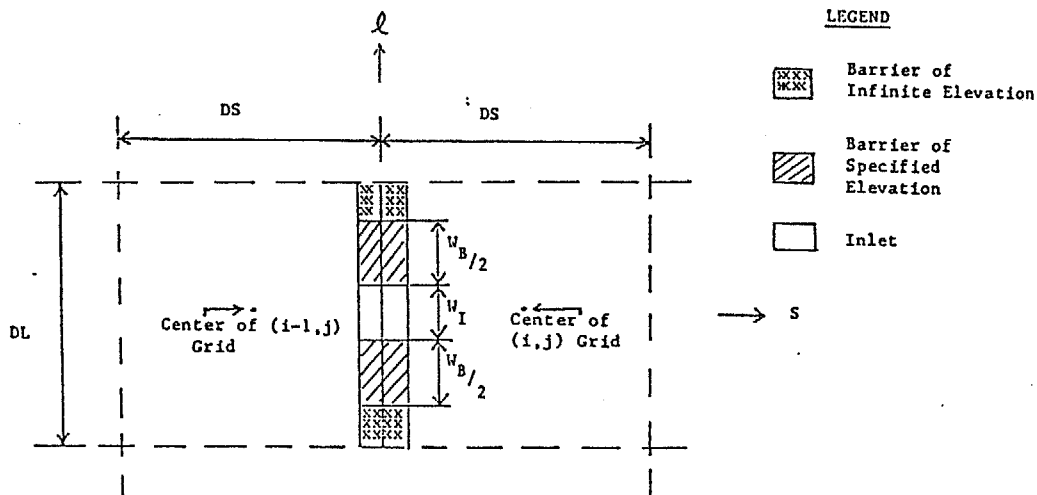


Figure II-18. Region of Interest in Description of Sub-Grid Features.

The computer program allows flow to occur over the barrier if the average water elevation as determined from the two adjacent grid blocks exceeds the barrier elevation. In addition the appropriate flow occurs through the inlet, if present.

The section below describes the methodology for representing the barrier/inlet features and of incorporating this representation into the numerical formulation.

Methodology

Consider the following simplified form of the momentum equation expanded in the s direction (direction of flow).

$$\frac{\partial q_s}{\partial t} = -g(h + \eta) \frac{\partial \eta}{\partial s} - \frac{f |q_s| q_s}{8(h + \eta)^2} \quad (\text{II-11})$$

in which q_s is the average discharge per unit width in the s -direction and $h + \eta$ represents the total water depth. The application of Eq.(II-11) is relatively straight forward to a normal grid block in which there are no sub-grid features. This results in the following finite difference form.

$$q_{s1}^{n+1} = \frac{1}{F_2} \left[q_{s1}^n - F_1 g(h + \eta) \frac{(\eta_1^n - \eta_{i-1}^n)}{DS} \right] \quad (\text{II-12})$$

in which

$$\begin{aligned} F_1 &= 1 \\ F_2 &= 1 + \frac{f|q_s|DT}{8(h+n)^2} \end{aligned} \quad (II-13)$$

In order to utilize the existing framework for solution of the finite difference equations, Equations (II-12) and (-13) are modified slightly to

$$q_{s,i}^{n+1} + \frac{1}{F_2} q_{s,i}^n - F_1 g \cdot (h+n) \frac{(\eta_i^n - \eta_{i-1}^n)}{DS} \quad (II-14)$$

The paragraphs below describe the rationale for determining the factors F_1 and F_2 .

The only invariant in the flow in the s -direction is the total discharge. Thus we first integrate Eq.(II-11) over the l -direction to obtain Q , then integrate over the s -direction between the centers of the $i-1$ and i grid cells. The result of the first integration is

$$\frac{\partial Q_s}{\partial t} = -gW(h+n) \frac{\partial \eta}{\partial s} - \sum \frac{fWq|q|}{8(h+n)^2} \quad (II-15)$$

in which W represents the local width at some locations, i.e. $W=W(s)$. The last term which represents the flow resistance involves a sum since the flow properties at various locations along the grid line differ. In order to express this flow term as a function of $Q|Q|$, we consider that the flow over the grid line will be friction-dominated, i.e., equations the head loss across the grid line and introducing entrance and exit loss terms.

$$\begin{aligned} \Delta \eta_{GL} &= \frac{f_I Q_I^2 DS_I}{8g(h+n)_I^3 W_I^2} + \frac{(K_{en}+K_{ex})_I Q_I^2}{2g(h+n)_I^2 W_I^2} = \frac{f_B Q_B^2 DS_B}{8g(h+n)_B^3 W_B^2} \\ &+ \frac{(K_{en}+K_{ex})_B Q_B^2}{2g(h+n)_B^2 W_I^2} \end{aligned} \quad (II-16)$$

or

$$\frac{Q_B}{Q_I} = \sqrt{\frac{\alpha_I}{\alpha_B}} \quad (II-17)$$

in which

$$\alpha_I = \frac{f_I DS_I}{8(h+n)_I^3 W_I^2} + \frac{(K_{en}+K_{ex})_I}{2W_I^2 (h+n)_I^2} \quad (II-18)$$

and a similar expression applies to α_B . Eq.(II-15) can now be expressed as

$$\frac{\partial Q_s}{\partial t} = -gW(h+n) \frac{\partial \eta}{\partial s} - G Q_s |Q_s| \quad (II-19)$$

where

$$G = \frac{f DS}{8(h+n)^2 W}, \text{ Normal Section}$$

$$\text{Sub-Grid Contribution} \left\{ \begin{aligned} G_I &= \alpha_I W_I (h+n)_I, \text{ Inlet Only Present and Active} \\ G_B &= \alpha_B W_B (h+n)_B, \text{ Barrier Only Present and Active} \\ G_{IB} &= \left[\frac{G_I}{\left[1 + \sqrt{\frac{\alpha_I}{\alpha_B}}\right]^2} + \frac{G_B}{\left[1 + \sqrt{\frac{\alpha_B}{\alpha_I}}\right]^2} \right], \text{ Both Barrier and Inlet Present and Active} \end{aligned} \right\} \quad (II-20)$$

To carry out the integration of Eq.(II-19) in the l -direction, it is necessary to know the approximate distribution of $\frac{\partial \eta}{\partial s}$ with s . Inspection of Eq.(II-19) reveals that

$$\frac{\partial \eta}{\partial s} \approx \frac{1}{w^m (h+\eta)^n} \quad (II-21)$$

where

$$m, n = \begin{cases} 1, 1 & \text{if inertia-dominant} \\ 2, 3 & \text{if friction-dominant} \end{cases}$$

For purposes here, we will consider that

$$\frac{\partial \eta}{\partial s} = K \frac{1}{(h+\eta)^2 w^2} \quad (II-22)$$

in which K represents a constant to be determined by equating the result from integrating Eq. (II-22) with the total (known) $\Delta \eta$ between the centers of the two adjacent grid cells. For the grid-line where both inlets and barriers are present, the right hand-side of Eq. (II-22) will be represented by the respective widths of inlets and barriers. The result is then

$$\Delta \eta = K \left[\frac{Ds_1}{(h+\eta)_1^2 w_1^2} + \frac{Ds_2}{(w_1+w_B)^2} \left(\frac{w_I}{(h+\eta)_1^2 w_1^2} + \frac{w_B}{(h+\eta)_B^2 w_B^2} \right) + \frac{Ds_3}{(h+\eta)_3^2 w_3^2} \right] \quad (II-23)$$

$$= K \mu$$

which defines μ as the bracketed term in Eq. (II-23). Eq. (II-19) can now be integrated over the total length of the domain of interest to yield

$$DS \frac{\partial Q}{\partial t} = -g \sum w_s (h+\eta)_s \left(\frac{\partial \eta}{\partial z} \right) \Delta s - Q|Q| \sum G_s \Delta s \quad (II-24)$$

which can be simplified to

$$DS \frac{\partial Q}{\partial t} = -g \sum \frac{K \Delta s}{w_s (h+\eta)_s} = Q|Q| \sum G_s \Delta s \quad (II-25)$$

in which the sub-grid term entering into the two summations should be considered as effective values and will be expressed in detailed form later. Reducing Eq. (II-25) to the form of Eq. (II-11) by dividing by $(D1 + DS)$, and inserting the expression for K

$$\frac{\partial q}{\partial t} = -\frac{g}{DLDS} \sum \frac{\Delta \eta_s \Delta s}{\rho w_s (h+\eta)_s} - \frac{DS}{DL} q|q| \sum G_s \Delta s \quad (II-26)$$

$$\frac{\partial q}{\partial t} = -g(h+\eta) \frac{\Delta \eta}{\Delta s} \frac{1}{\mu DL(h+\eta)} \sum \frac{\Delta s}{w_s (h+\eta)_s} - \frac{DL}{DS} q|q| \sum G_s \Delta s \quad (II-27)$$

Thus, by comparison with Eq. (II-14) we see that the expressions for F_1 and F_2 are

$$F_1' = \frac{1}{DL(h+\eta)} \left[\frac{Ds_1}{w_1 (h+\eta)_1} + \frac{Ds_2}{(w_B+w_I)} \left(\frac{w_I}{w_1 (h+\eta)_1} + \frac{w_B}{w_B (h+\eta)_B} \right) + \frac{Ds_3}{(h+\eta)_3} \right] \quad (II-28)$$

$$F_2' = 1.0 + \frac{DL}{DS} [G_I + G_2 + (G_I, G_B \text{ or } G_{IB})] |q|DT \quad (II-29)$$

This completes the description of the treatment of the sub-grid features.

Boundary Conditions

To complete formulation of the problem, boundary conditions must be specified at the boundaries of the grid presented in Figure II-15. On the "open" (water) boundaries, the water surface is specified to be that associated with the barometric pressure, i.e.

$$\eta_{B_{i,j}} = \left(\frac{p_{\infty} - p_{i,j}}{\rho g} \right) \quad (\text{II-30})$$

in which p_{∞} denotes the far field barometric pressure. In addition, on the open boundary grid cells, it is specified that only discharge components perpendicular to the boundaries occur and that these discharges on the exterior boundaries of the grid system are those required to satisfy the continuity equation (Eq. II-8).

On the "closed" boundaries, i.e., at the shoreline where land elevations are higher than the adjacent water elevations, a no-flow boundary condition is specified perpendicular to that boundary. However, "flooding" and "deflooding" of grid blocks adjacent to the boundaries can occur. Flooding occurs when the water level is greater by a specified small amount than the ground elevation of an adjacent grid block. When this condition exists, the grid block is activated by a simple allocation of this excess elevation on the newly activated block and in subsequent time steps the grid block is incorporated into the normal calculation scheme. Deflooding occurs when the water level on a grid block drops below a specified level leaving a very small depth on that block. The block is "deactivated" and the excess water placed on the adjacent grid.

The solution is started from an initial condition of zero water surface displacement and zero discharge components. The hurricane system is translated along a specified path at a designated speed. At each time step, the hurricane

effects (represented by the pressure and wind stress components) on each cell are calculated and the finite-difference equations (Eqs. (II-7), (II-8), (II-9) and (II-10) employed. The results are updated values of η , q_x and q_y for each cell.

Implicit Solution of the Finite Difference Equations

The solution for each time step progresses by first solving Eqs. (II-7) and (II-8) simultaneously for each j grid line sweeping over all values of i . This establishes the values of η^{n+1} and q_y^{n+1} for the entire (i,j) field. The procedure is then repeated for Eqs. (II-9) and (II-10) in which this pair of equations is solved simultaneously for η^{n+1} and q_x^{n+1} for the entire (i,j) field. This latter pair of equations is expressed sequentially for each value of i , then solved for all values of j , for that particular i grid line. The expressions for the various coefficients are presented as follows:

$$A_i = g(\overline{h+n}) \frac{\Delta t}{\Delta x}$$

$$B_i = 1 + \frac{f|q_{i,j}^n| \Delta t}{8(\overline{h+n})^2}$$

$$C_i = -A_i$$

$$D_i = q_{x_{i,j}}^n + \Delta t \left[\frac{(\overline{h+n})}{\rho} \frac{\partial p}{\partial x} + \frac{\tau_{wx_{i,j}}}{\rho} - \beta(\overline{q_y})^n \right]$$

$$A_i^* = \frac{\Delta t}{4\Delta x}$$

$$B_i^* = 1.0$$

$$C_i^* = -\frac{\Delta t}{4\Delta x}$$

$$D_j^* = n_{i,j}^n - \frac{1}{4} \frac{\Delta t}{\Delta x} \left(q_{x_{i+1}}^n - q_{x_i}^n \right) - \frac{\Delta t}{2\Delta y} \left(q_{y_{i,j+1}}^n - q_{y_{i,j}}^n \right)$$

$$\bar{q}_{y_{i,j}}^n = \frac{1}{4} \left[q_{y_{i-1,j}}^n + q_{y_{i,j}}^n + q_{y_{i-1,j+1}}^n + q_{y_{i,j+1}}^n \right]$$

$$\left| q_{y_{i,j}}^n \right| = \sqrt{\left(q_{x_{i,j}}^n \right)^2 + \left(\bar{q}_{y_{i,j}}^n \right)^2}$$

$$A_j = \frac{g(h+n)}{2} \frac{\Delta t}{\Delta x}$$

$$B_j = 1 + \frac{f|q_{i,j}^n| \Delta t}{8(h+n)^2}$$

$$C_j = -A_j$$

$$D_j = q_{y_{i,j}}^n + \Delta t \left[-\frac{g(h+n)}{2\Delta x} \Delta t \left(n_{i,j}^n - n_{i,j-1}^n \right) - \frac{(h+n)}{\rho} \frac{\partial p}{\partial y} + \frac{\tau_{wy_{i,j}}}{\rho} + \beta(\bar{q}_x)^n \right]$$

$$\bar{q}_{x_{i,j}}^n = \frac{1}{4} \left[q_{x_{i,j}}^n + q_{x_{i,j-1}}^n + q_{x_{i+1,j}}^n + q_{x_{i+1,j-1}}^n \right]$$

$$\left| q_{x_{i,j}}^n \right| = \sqrt{\left(\bar{q}_{x_{i,j}}^n \right)^2 + \left(q_{y_{i,j}}^n \right)^2}$$

$$A_j^* = \frac{\Delta t}{2\Delta y}$$

$$B_j^* = 1.0$$

$$C_j^* = -A_j^*$$

$$D_j^* = n_{i,j}^{n+1/2} - \frac{\Delta t}{4\Delta x} \left(q_{x_{i+1,j}}^n - q_{x_{i,j}}^n \right) - \frac{\Delta t}{4\Delta x} \left(q_{x_{i+1,j}}^{n+1} - q_{x_{i,j}}^{n+1} \right)$$

With the coefficients specified as detailed in Section II.1.5.2, the method of solving the sets of simultaneous equations will be described. The method is termed the "double sweep" method in which the first sweep involves "conditioning" two sets of auxiliary coefficients (E_i, F_i, E_i^*, F_i^*). The second sweep determines the values of n and q and, in the process, incorporates the required boundary conditions. The procedure will be illustrated for Equations (II-7) and (II-8) and it is noted that the same exact procedure is applicable to solving Equations (II-9) and (II-10). The procedure commences by establishing two auxiliary equations with four variables (E_i, F_i, E_i^*, F_i^*) which are initially unknown,

$$n_{i,j}^{n+1/2} = E_i q_{x_{i,j}}^{n+1} + F_i \quad (II-31a)$$

$$q_{x_{i+1,j}}^{n+1} = E_i^* n_{i,j}^{n+1/2} + F_i^* \quad (II-31b)$$

Eqs. (II-31) and (II-32) are substituted in Eqs. (II-7) and (II-8) and the results simplified to yield

$$q_{x_{i,j}}^{n+1} = -\frac{C_i}{A_i E_i + B_i} n_{i-1,j}^{n+1/2} + \frac{D_i - A_i F_i}{A_i E_i + B_i} \quad (II-32a)$$

$$n_{i,j}^{n+1/2} = -\frac{C_i^*}{A_i^* E_i^* + B_i^*} q_{x_{i,j}}^{n+1} + \frac{D_i^* - A_i^* F_i^*}{A_i^* E_i^* + B_i^*} \quad (II-32b)$$

Comparison of Eqs (II-31) and (II-32) establishes the values of the unknown coefficients (E, F, E^*, F^*) in terms of the known coefficients ($A, B, \dots, A^*, B^*, \dots$).

The expressions are

$$E_i = -\frac{C_i^*}{A_i^* E_i^* + B_i^*}, \quad F_i = \frac{D_i^* - A_i^* F_i^*}{A_i^* E_i^* + B_i^*} \quad (II-33)$$

$$E_{i-1}^* = -\frac{C_i}{A_i E_i + B_i}, \quad F_{i-1}^* = \frac{D_i - A_i F_i}{A_i E_i + B_i} \quad (II-34)$$

To illustrate the manner in which boundary condition information is incorporated into the procedure, suppose that water surface level, n , is specified at $i = \text{IMAX}$ and that q_x is specified as zero at $i = 2^5$. The first sweep commences by noting (from Eq. (II-31a))

$$\begin{aligned} E_{\text{IMAX}} &= 0.0 \\ F_{\text{IMAX}} &= n_{\text{IMAX},j}^{n+1} \end{aligned} \quad (\text{II-35})$$

With the values of E_{IMAX} and F_{IMAX} known, $E_{\text{IMAX}-1}^*$ and $F_{\text{IMAX}-1}^*$ can be calculated from Eq. (II-34), then values of $E_{\text{IMAX}-1}$ and $F_{\text{IMAX}-1}$ computed from Eq. (II-33) and so on. E_i^* and F_i^* are set equal to

$$E_i^* = F_i^* = 0.0 \quad (\text{II-36})$$

in accordance with the boundary condition and Eq. (II-31b). This completes the first sweep and establishes all the coefficients over the grid line.

The second sweep simply consists of applying Eqs. (II-32) from small i to large i (IMAX). In summary, the "double sweep" procedure as presented here, progresses from large i to small i for the first sweep (conditioning the E , F , E^* , F^* coefficients), and then progresses back from small i to large i for the second sweep (determining the n , q_x values from the coefficients).

It can be shown that this procedure results in an exact solution of the tri-diagonal set of simultaneous equations represented by Eqs. (II-31). As noted previously, the same procedure is then applied to solve Eqs. (II-9) and (II-10) which completes establishing n , q_x and q_y at the $(n+1)^{\text{th}}$ time step.

³ It is noted that other combinations of boundary conditions at the two ends of the grid line could be accommodated. Also, internal boundary conditions of the type $q_{x,i,j}^{n+1} = 0$ are satisfied by the choice of coefficients: $E_{i-1}^* = F_{i-1}^* = 0$.

Dynamic Wave Set-Up

When waves break, a shoreward directed force in addition to the wind stress, is exerted on the water in the surf zone. This causes an additional rise in water level termed "wave set-up". This effect has been studied extensively in the laboratory (Saville (5), Bowen et.al., (6)), and tide gage measurements during severe storms have confirmed its importance in nature. Most of the information relative to wave set-up has been developed for "regular" waves, that is for a wave train in which each wave is the same as the preceding wave. Waves in nature, however, are not regular and tend to occur in groups. A recent analytical study by Lo (7) has shown that for natural wave trains there is a dynamic wave set-up that is approximately 50% larger than would be predicted by a static treatment. In order to evaluate this result, model studies were conducted in the large University of Florida wave tank. It was found that the experimental and analytical results by Lo were in approximate agreement.

The maximum dynamic wave set-up, n'_{max} , across the surf zone can be shown to be approximately

$$n'_{\text{max}} = 0.285 \left[1 - 2.82 \left(\frac{H_b}{gT^2} \right)^{1/2} \right] H_b \quad (\text{II-37})$$

which includes the dynamic factor of 50% and in which T is the wave period and H_b is the breaking wave height based on the deep water significant wave height, H_0 , taken approximately as

$$H_b = 0.94 H_0 \quad (\text{II-38})$$

The deep water significant wave height is determined from an extension of a method recommended for hurricane generated waves as summarized in the Shore Protection Manual (8),

$$(H_o)_{\max} = 16.5 e^{R(\Delta p/100)} \left(1 + \frac{0.208 V_F}{\sqrt{U_R}}\right) \quad (\text{II-39})$$

where R = radius of maximum winds in nautical miles, Δp = central pressure deficit in inches of mercury, V_F = translation speed of hurricane in knots, and U_R = maximum sustained wind speed in knots. For purposes here the local effective deep water significant wave height is based on the local winds, U , at the surf zone area of interest and the maximum winds in the hurricane, U_{\max} as

$$H_o = (H_o)_{\max} \left(\frac{U}{U_{\max}}\right)^2 \quad (\text{II-40})$$

Equations 22, 23, 24 and 25 provide the basis for determining the maximum dynamic wave set-up within the surf zone. The computed value of η'_{\max} was added to the nearshore storm surge. It is stressed that η'_{\max} represents the maximum dynamic wave set-up across the surf zone and that this value varies with time (since the wind speed varies with time). The value of η'_{\max} was computed at each time step for the shoreward grid, and added to the corresponding surge value resulting from wind stress, barometric pressure and the effect of astronomical tide to yield the combined total storm tide history.

With this combined total storm tide history thus determined, it is a simple matter to search in the computer to obtain the maximum of the combined total storm tide at the site of interest.

2.6 Features of the One-Dimensional Numerical Model

As noted earlier, a simple one-dimensional numerical model was developed and calibrated to allow the statistics to be generated based on simulation (calculations) of many storms and associated storm tides.

The one-dimensional numerical model is described as follows. A transect line is established along a line which is approximately perpendicular to the bottom contours. The characteristics (Δp , R , θ , V_F and track) of the hurricane are defined and the hurricane is advanced along the track line. The water surface displacement (boundary condition) at the seaward end of the transect line is taken as the static response of the water surface to the barometric pressure deviation at that point. The locations of the three transect lines for Charlotte County are shown in Figure II-15. Figures II-19, II-20 and II-21 present the profiles of the three transect lines and their one-dimensional grid representations.

Governing Differential Equations For One-Dimensional Numerical Model

The one-dimensional numerical model is significantly less expensive and simpler to run and is used in the long-term simulation phase, in order to generate the required data within budgetary constraints. The justification for using the one-dimensional model is that it can be adequately calibrated with the rather complete two-dimensional model.

The one-dimensional numerical model is the Bathystropic Storm Tide model by Freeman, Baer and Jung (9) and is static in the x-direction model. The governing differential equations in the x and y directions are:

$$\frac{\delta \eta}{\delta x} = \frac{1}{gD} \left(\frac{\tau_{wx}}{\rho} - \beta q_y \right) - \frac{1}{\rho g} \frac{\delta p}{\delta x} \quad (\text{II-41})$$

$$\frac{dq_y}{dt} = \frac{1}{\rho D} (\tau_{wy} - \tau_{by}) \quad (\text{II-42})$$

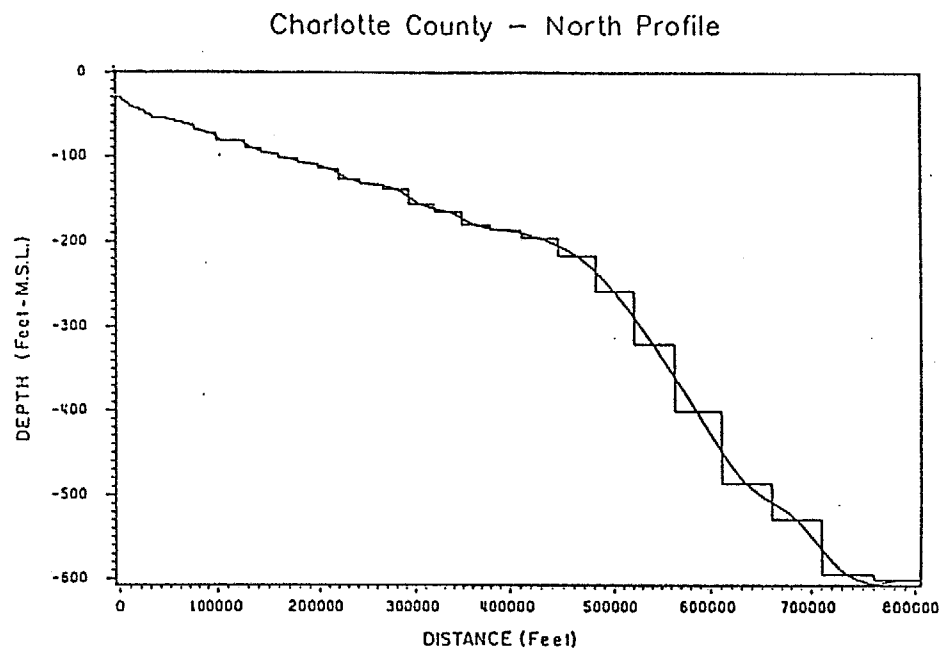


Figure II-19. Profile of the North Transect Line and its One-Dimensional Grid Representation

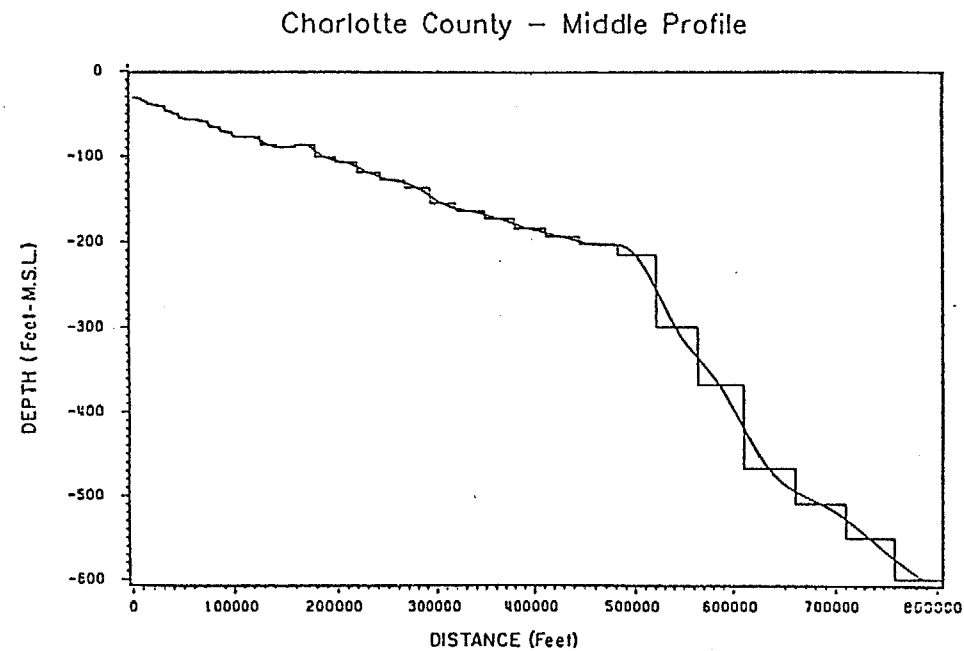


Figure II-20. Profile of the Middle Transect Line and its One-Dimensional Grid Representation

in which all variables are evaluated along the transect line perpendicular to shore and passing through the site.

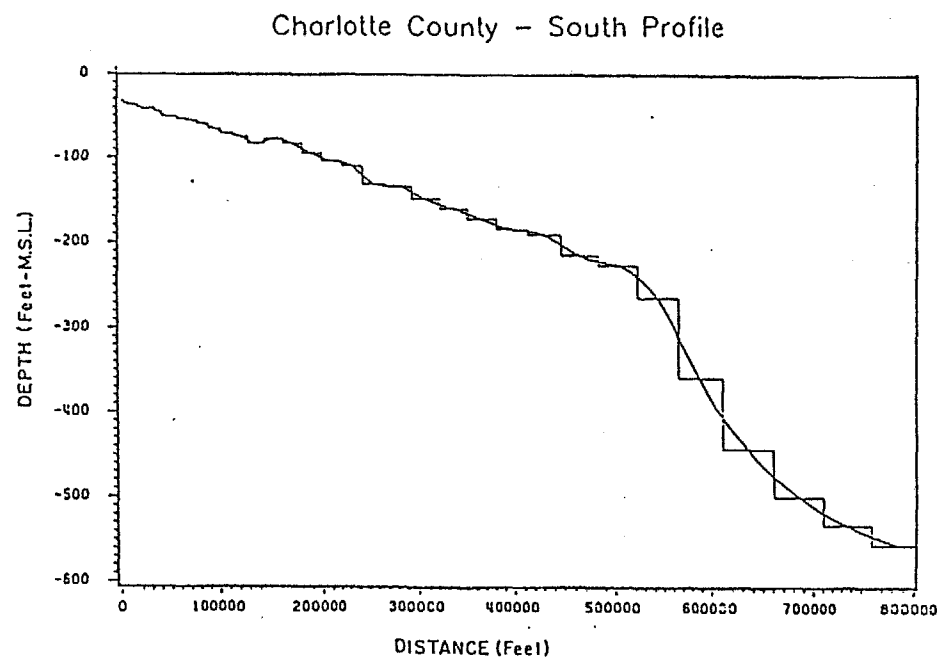


Figure II-21. Profile of the South Transect Line and its One-Dimensional Grid Representation

Finite Difference Forms of Governing Differential Equations

The finite difference forms of the governing one-dimensional differential equations (Eqs. II-1) and (II-2) are:

$$q_{y_i}^{n+1} = \frac{1}{BB} \left[q_{y_i}^n + \frac{\Delta t}{\rho} \tau_{wy_i} \right] \quad (II-43)$$

$$\eta_{i+1}^{n+1} = \eta_i^{n+1} + \frac{\Delta x}{gD_i} \left[-\frac{\tau_{wx_i}}{\rho} - \beta q_{G_i}^{n+1} \right] + \frac{p_i^{n+1} - p_{i+1}^{n+1}}{\rho g} \quad (II-44)$$

where

$$BB = 1.0 + \frac{f \cdot \Delta t |q_{y_i}^n|}{D_i} \quad (II-45)$$

where the variables are as defined previously for the two-dimensional model.

Initial and Boundary Conditions For the One-Dimensional Model

The one-dimensional model is initiated from a condition of rest ($q_y \equiv 0$) and zero water surface displacement ($\eta \equiv 0$). The only boundary condition required is that at the seaward end ($i = 1$) of each transect where the "barometric tide" is imposed as

$$\eta = \frac{p_\infty - p_1}{\rho g} \quad (II-46)$$

Explicit Solution of the Finite Difference Equations

Eqs. (II-41) and (II-42) are solved sequentially for each time step with the hurricane advanced along its specified track with the initial position of the hurricane at a sufficient distance to allow the longshore transport q_y to be free of any artificial transients. The solutions of these equations are straight forward and free of any potential instabilities. At the landward grid the wave set-up is superposed as described previously for the two-dimensional model (Section 2.5).

2.7 Long-Term Simulation

With the statistical characteristics of historical hurricanes available and the simple one-dimensional model calibrated as described previously, the long-term simulation (500 years, generally) is carried out. The first phase of the simulation comprises the selection of the hurricane characteristics in accordance with the historical data. In each storm, this involves the following (also, see Figures II-14 and II-22).

- 1) Quantifying Δp , R , V_F , θ and hurricane track in accordance with the historical probabilities (Section 2.2).
- 2) For these characteristics, a random astronomical tide from the hurricane season is generated as a boundary condition to the one-dimensional numerical model and the model is run to determine the storm surge at the site of interest. This storm surge is then adjusted in accordance with the factors obtained from the two-dimensional model calibration runs.
- 3) For the landward grid and each time step, the contribution due to dynamic wave set-up is included to yield the combined total storm tide.
- 4) Determine whether enough storms have been simulated for the n -year simulation.
- 5) After the required number of storms and associated storm tides have been simulated, the peak water levels for each storm are ranked and the return period, TR , is calculated, according to

$$TR = \frac{500}{M} \quad (II-47)$$

where M is the rank of the combined total tide level. (For example, if the simulation was carried out for a 500 year period, the highest combined total tide level would have a return period of 500 years, etc.) Finally, by presenting these results on semilog paper, it is possible to interpolate for the return periods of interest, i.e., $TR = 10, 50, 100$ and 500 years.

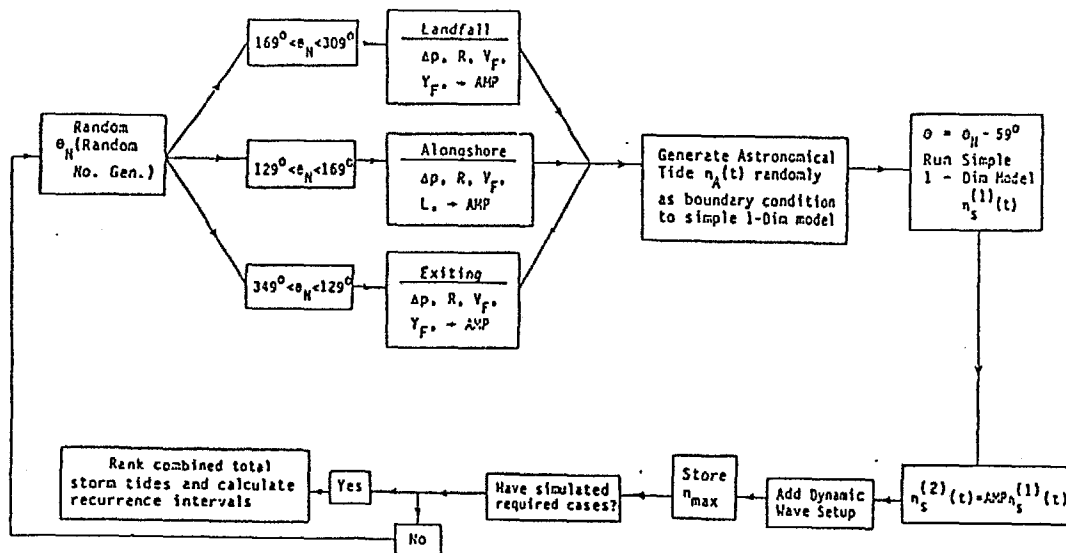


Figure II-22. Flow Chart for Storm Tide Simulations (After Calibration to Determine $(AMP)_{LF}$, $(AMP)_{ALONG}$ and $(AMP)_{EXIT}$)

III. APPLICATIONS OF STORM SURGE METHODOLOGY WITH SPECIFIC ILLUSTRATION BY EXAMPLE TO CHARLOTTE COUNTY

3.1 Two-Dimensional Model (Appendix A)

As noted previously, the two-dimensional model is first verified using storms of record and then employed to generate a data base for calibration of the one-dimensional model.

Verification With Storms of Record

Several examples will be presented comparing measured and calculated storm tides for storms of record. In these comparisons, an attempt was made to extract the astronomical tide and only tide measurements were generally used for comparison since the more abundant high water marks can be shown to contain significant extraneous effects. The calculated storm tides were based on a parameterized hurricane which is undoubtedly responsible for some of the differences between the measured and compiled tides. The parameters were allowed to change along the hurricane path in accordance with measurements of these parameters.

The only appropriate storm tide located for calibration for Charlotte County was the September, 1947 hurricane. The parameters for the 1947 hurricane used for input into the program are presented in Table III-1. Water level measurements were available at three locations: Manasota Bridge, Venice and Fort Meyers and the comparisons are presented in Figures III-1, III-2 and III-3, respectively. It is seen that although the peak surges due to this hurricane were not large (≈ 4.0 ft), there is generally reasonable agreement between the peak measured and measured storm surges, with the maximum deviation being approximately 0.5 ft for the Manasota Bridge (Figure III-1).

Comparisons conducted for Franklin County included Hurricanes Agnes (1972) and Eloise (1975) with measurements available from the St. Marks tide gage. These

TABLE III-1

Input Parameters for Calibration Hurricane
Hurricane of September 1947

date	time (EST)	Δp (in.Hg)	V_F (knots)	R (n.mi.)	θ_H (degrees)
9/17	1900	-1.95	5.4	34.0	90.0
9/18	0100	-1.95	6.6	34.0	107.7
	0700	-1.95	13.1	34.0	117.3
	1300	-1.95	17.9	34.0	116.5
	1900	-1.95	22.3	34.0	122.6
9/19	0100	-1.40	21.0	34.0	121.6

Starting coordinates:

 $X_S = 43.8$ n.mi. $Y_S = -60.5$ n.mi.

Landfalling coordinates:

 $X_F = -4.2$ n.mi. $Y_F = 78.71$ n.mi.

SEPTEMBER 1947 HURRICANE - Manasota Bridge

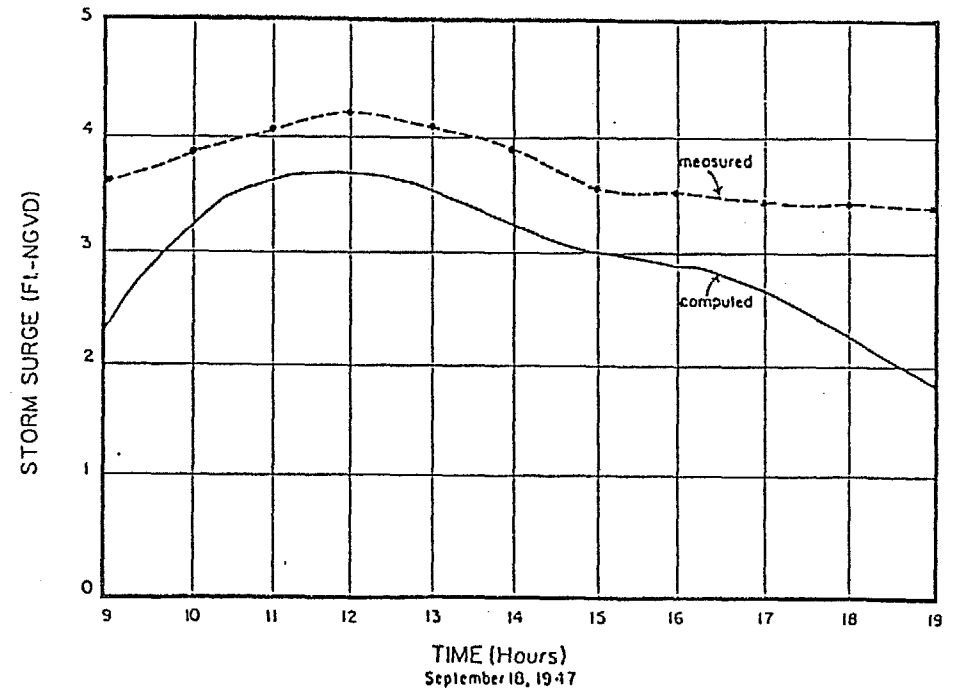


Figure III-1. Comparison between Measured and Computed Storm Tide at Manasota Bridge, Florida for the September 1947 Hurricane

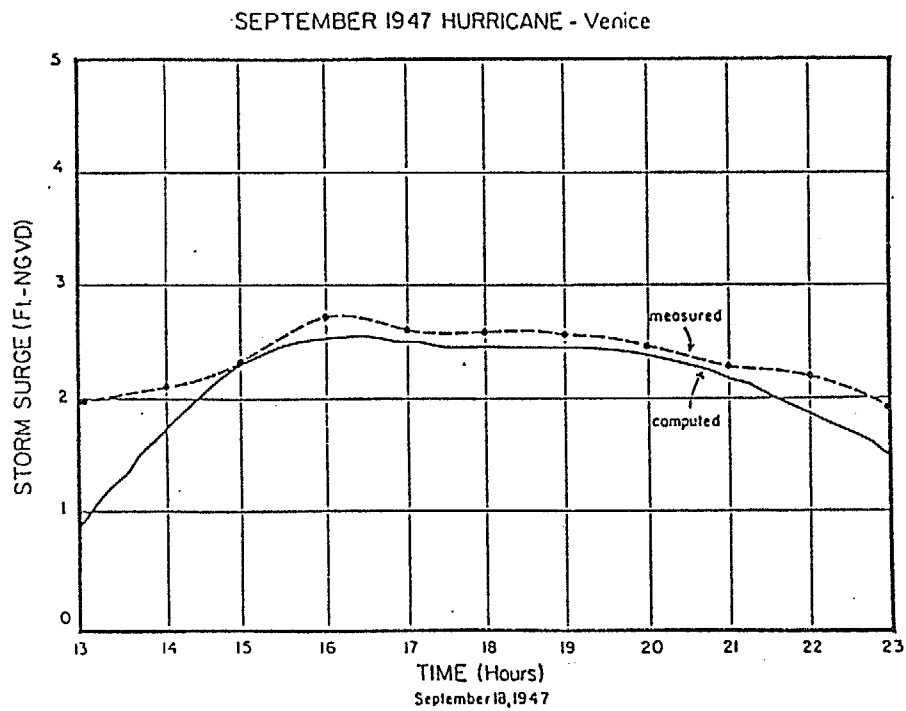


Figure III-2. Comparison between Measured and Computed Storm Tide at Venice, Florida for the September 1947 Hurricane

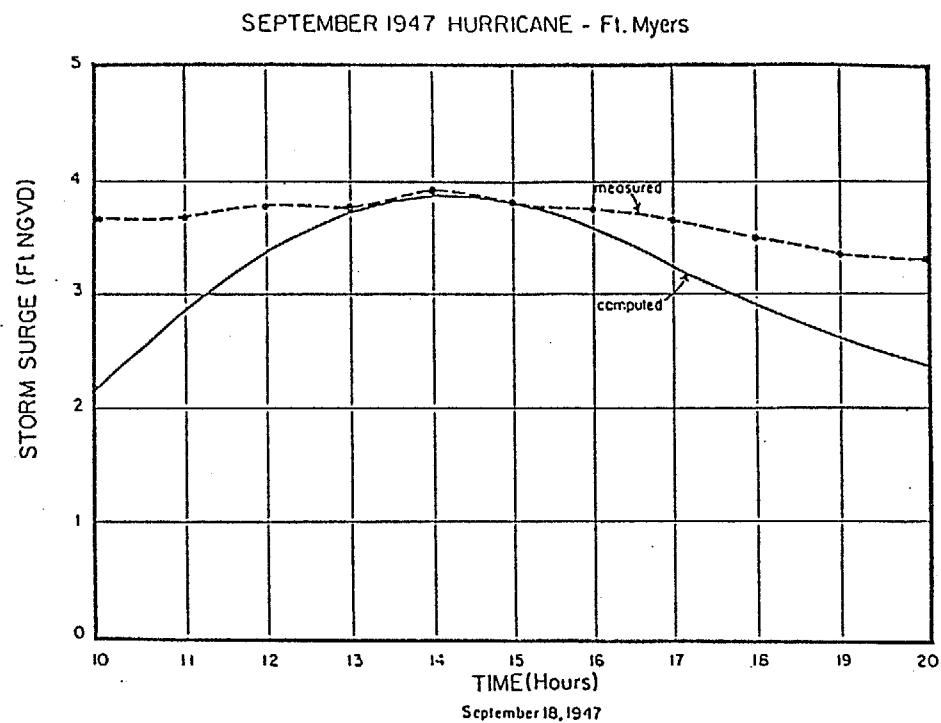


Figure III-3. Comparison between Measured and Computed Storm Tide at Ft. Myers, Florida for the September 1947 Hurricane

input data for these hurricanes are presented in Tables III-2 and III-3 and the comparisons are presented in Figures III-4 and III-5 for Hurricane Agnes and Hurricane Eloise, respectively. For Hurricane Agnes, the peak measured tide exceeds the computed by approximately 0.8 ft, whereas for Hurricane Eloise, the peak computed tide exceeds the measured by approximately 0.5 ft; on the average this is considered reasonable agreement.

In the CCCL study for Nassau County, comparisons were carried out for Hurricane Dora (1964) and Hurricane David (1979), using the input parameters presented in Tables III-4 and III-5, respectively. Measurements were available at Fernandina Beach and Mayport. The comparisons are presented in Figures III-6, III-7, III-8 and III-9. In general the average agreement is considered good.

In summary of the comparisons shown (and others available but not shown for Dade, Broward and Walton Counties), the agreement between measured and computed storm surges is considered good. We regard this comparison/validation phase as useful in demonstrating the validity of the model and ensuring that the nearshore bathymetry/topography is represented adequately. Differences that exist in the peak surges are believed to be due to the wind field structure of the specific hurricanes, i.e., a measure of the deviation from the idealized hurricane used as input and other factors such as the difference in air-sea temperature which influences the wind surface stress coefficient.

Generation of Data Base for Calibration of One-Dimensional Model

With the two-dimensional model validated, a data base is generated spanning the hurricane parameters of interest. This data base is subsequently employed for calibration of the one-dimensional model which includes more severe approximations to the physics of the hurricane problem.

To illustrate the range of hurricane parameters included in the data base, Tables III-6, III-7 and III-8 present the cases selected for Landfalling,

TABLE III-2

Input Parameters for Calibration Hurricanes
Hurricane Agnes (June, 1972)

date	time (EST)	Δp (in. Hg)	V_F (n. mi.)	R (n. mi.)	θ_N (degrees)
6/18	1900	-0.92	12.0	20	180.0
6/19	0100	-1.04	13.0	20	180.0
	0700	-1.04	11.0	20	184.5
	1300	-0.89	9.7	20	201.11
	1900	-0.79	10.0	20	205.8
6/20	0100	-0.68	11.2	20	224.4

Starting coordinates:	Landfalling coordinates:
$X_S = 220.2$ n. mi.	$X_F = 4.2$ n. mi.
$Y_S = 45.4$ n. mi.	$Y_F = 40.2$ n. mi.

TABLE III-3

Hurricane Eloise (September, 1975)

date	time (EST)	Δp (in. Hg)	V_F (n. mi.)	R (n. mi.)	θ_N (degrees)
9/22	0100	-0.59	10.0	18	175.0
	0700	-0.80	7.1	18	187.1
	1300	-0.98	11.2	18	224.3
	1900	-1.33	15.2	18	223.5
9/23	0100	-1.63	20.0	18	205.8
	0700	-1.72	28.5	18	190.5
	1300	-0.91	27.8	18	205.9

Starting coordinates:	Landfalling coordinates:
$X_S = 292.2$ n. mi.	$X_F = -31.8$ n. mi.
$Y_S = 238.3$ n. mi.	$Y_F = 76.6$ n. mi.

HURRICANE AGNES - St. Marks

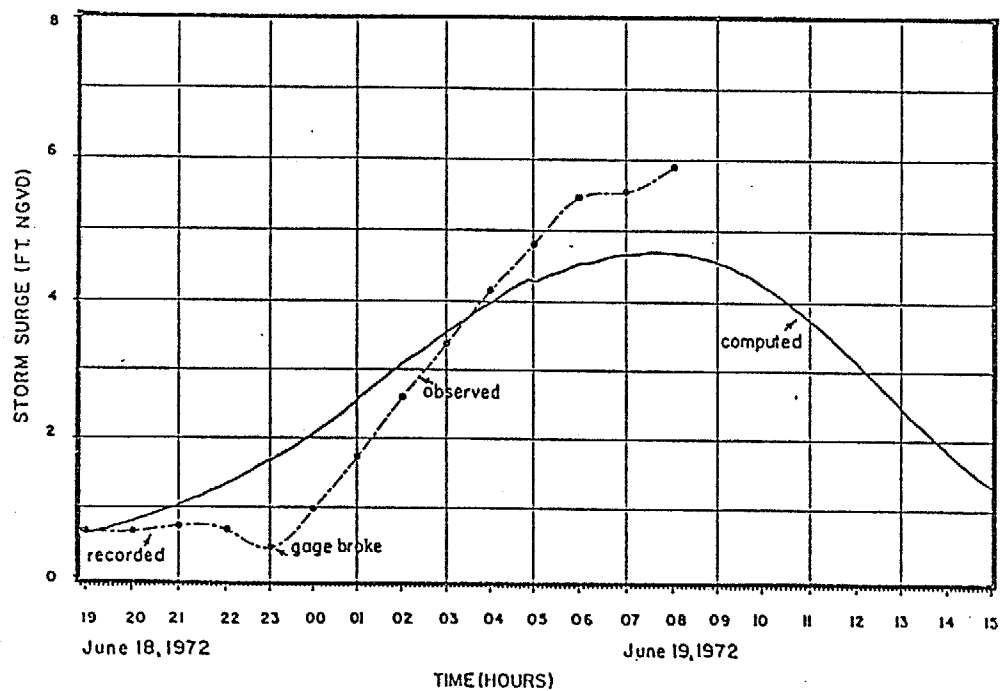


Figure III-4. Comparison between Measured and Computed Storm Tide at St. Marks, Florida for Hurricane Agnes (1972)

HURRICANE ELOISE - St. Marks

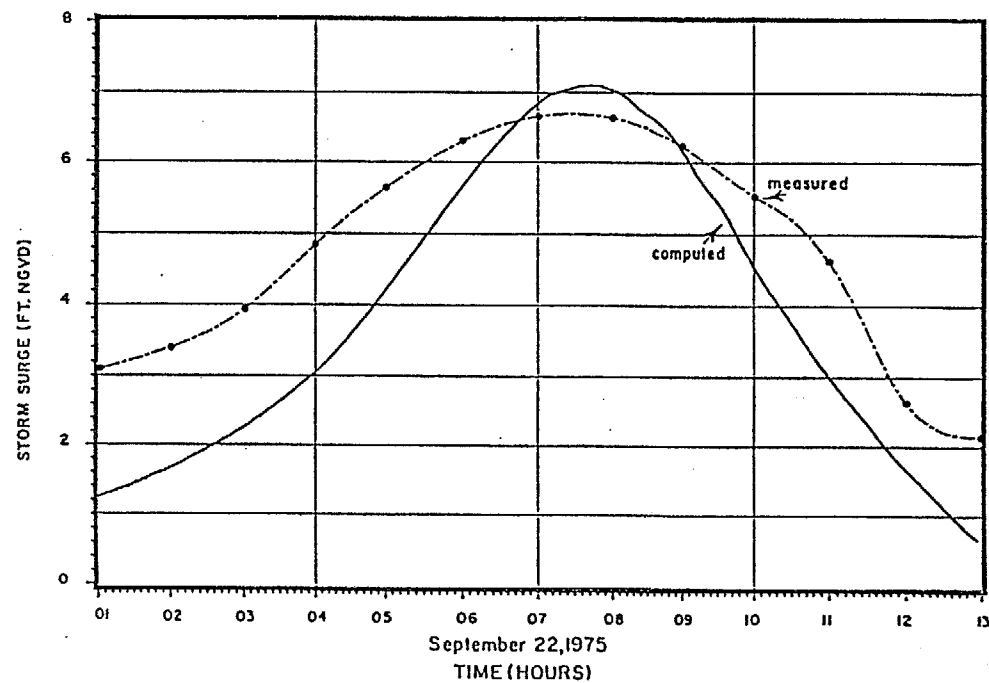


Figure III-5. Comparison between Measured and Computed Storm Tide at St. Marks, Florida for Hurricane Eloise (1975)

TABLE III-4

Input Parameters for Calibration Hurricanes

Hurricane Dora (September, 1964)

date	time* (GMT)	Δp (in. Hg)	V_F (n. mi.)	R (n. mi.)	θ_N (degrees)
9/8	1800	-1.48	13.1	20	98.80
	0000	-1.35	8.0	20	104.60
	0600	-1.21	10.3	20	112.88
	1200	-1.27	6.0	20	120.13
	1800	-1.51	6.0	20	99.41
9/10	0000	-1.45	6.1	20	99.41
	0600	-1.39	8.7	20	96.62
	1200	-1.30	6.1	20	96.62
	1800	-1.25	3.5	20	90.00

Starting coordinates:

 $X_S = 165.43$ n.mi. $Y_S = 90.00$ n.mi.

Landfalling coordinates:

 $X_F = 5.17$ n.mi. $Y_F = 36.00$ n.mi.

TABLE III-5

Hurricane David (September, 1979)

date	time* (GMT)	Δp (in. Hg)	V_F (n. mi.)	R (n. mi.)	θ_N (degrees)
9/3	1200	-1.14	10.4	10	150.14
	1800	-1.17	8.4	10	162.07
9/4	0000	-1.20	11.3	10	166.07
	0600	-1.23	11.0	10	175.52
	1200	-1.23	13.3	10	168.75
9/5	1800	-1.23	10.0	10	184.92
	0000	-1.17	10.2	10	189.78
	0600	-1.05	14.2	10	190.46
	1200	-0.98	14.2	10	190.46

Starting coordinates:

 $X_S = 51.70$ n.mi. $Y_S = 150.00$ n.mi.

Offshore coordinates:

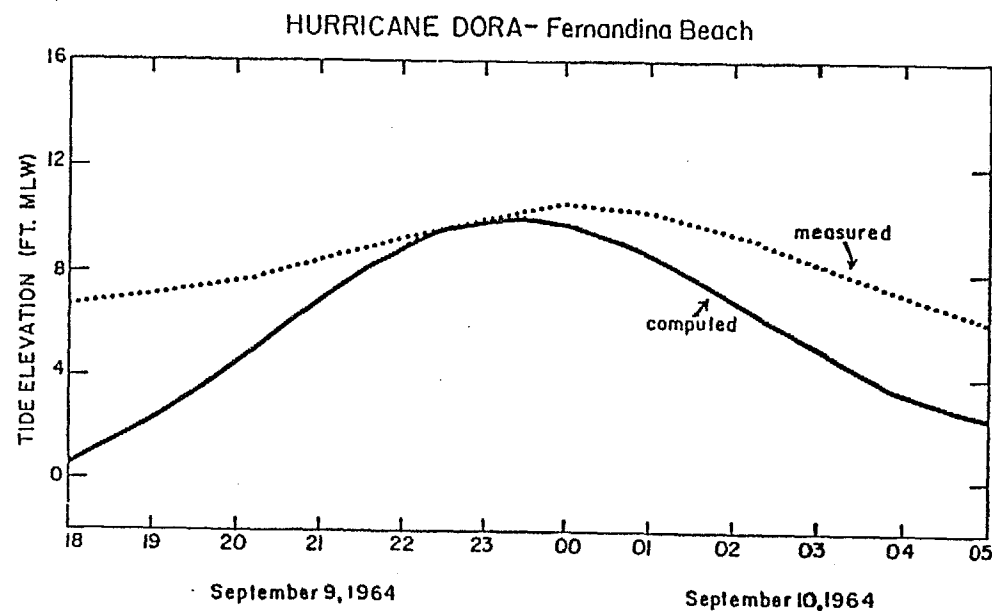
 $X_L = 15.51$ n.mi. $Y_L = -60.00$ n.mi.

Figure III-6. Comparison between Measured and Computed Storm Tide at Fernandina Beach, Florida for Hurricane Dora (1964)

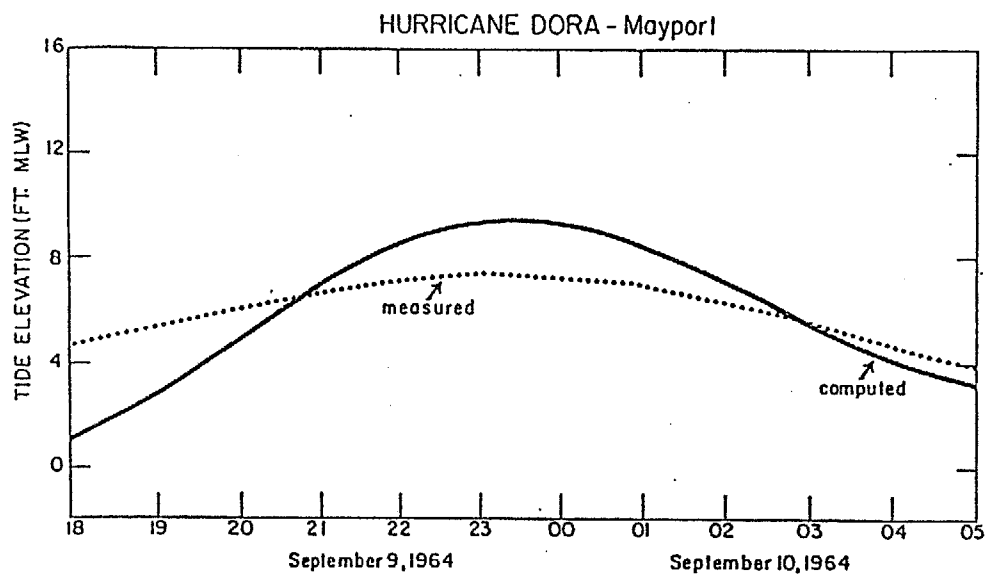


Figure III-7. Comparison between Measured and Computed Storm Tide at Mayport, Florida for Hurricane Dora (1964).

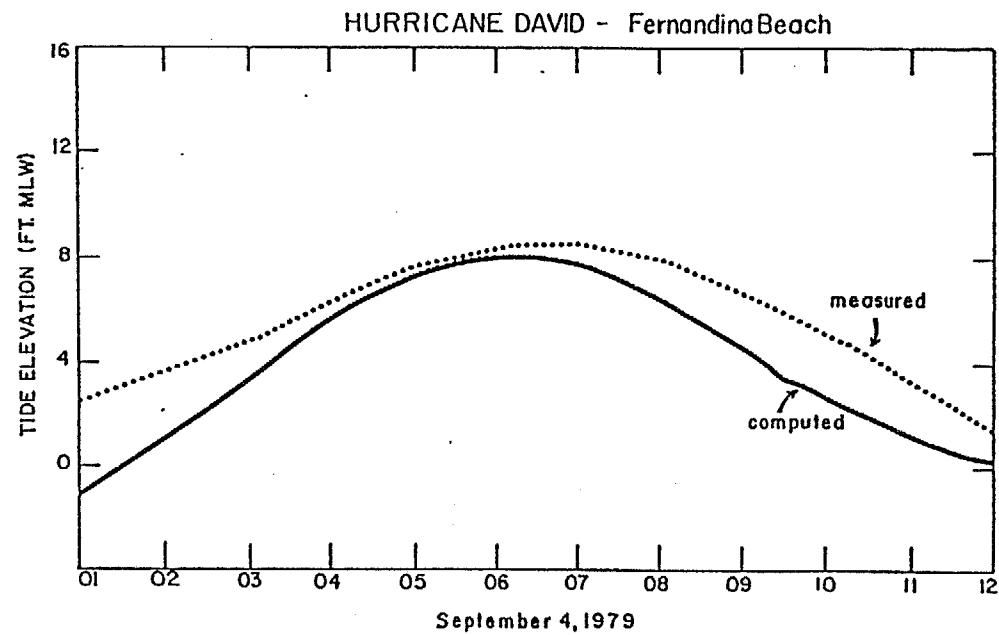


Figure III-8. Comparison between Measured and Computed Storm Tide at Fernandina Beach, Florida for Hurricane David (1979)

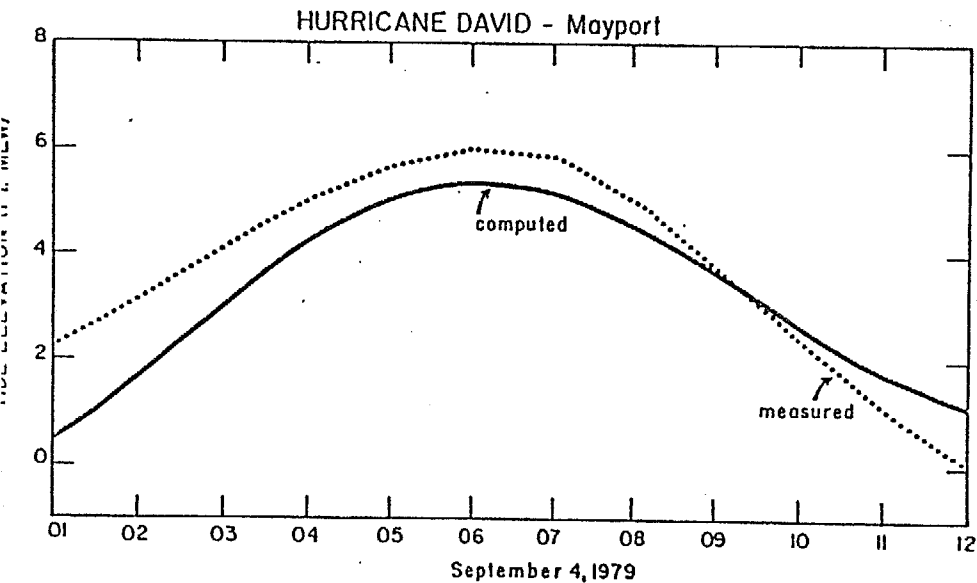


Figure III-9. Comparison between Measured and Computed High Water Mayport, Florida for Hurricane David (1979)

Table III-6.
Parameters Defining 11 Landfalling Storms Used
In Calibrating The One-Dimensional Model With
The Two-Dimensional Model And The Results

MODEL STORM	ΔP (in.-Hg)	R (n. mi.)	V_F (n. mi.)	θ_H (degrees)	Landfalling Coordinates (n. mi.)		Starting Coordinates (n. mi.)		$\eta_{max.}$ (ft. M.S.L.)					
									North Profile		Middle Profile		South Profile	
					X_F	Y_F	X_S	Y_S	1-D	2-D	1-D	2-D	1-D	2-D
1	-1.6	20	12	225	-2.5	12.0	102.29	-14.13	9.28	10.64	11.03	12.15	11.54	12.50
2	-2.2	20	12	225	-2.5	12.0	102.29	-14.13	11.57	13.37	13.68	15.03	14.33	15.53
3	-1.2	20	12	225	-2.5	12.0	102.29	-14.13	7.81	8.86	9.33	10.27	9.75	10.66
4	-1.6	12	12	225	-2.5	12.0	102.29	-14.13	9.47	10.30	9.95	10.24	9.34	9.49
5	-1.6	30	12	225	-2.5	12.0	102.29	-14.13	9.27	10.81	11.13	12.51	12.43	13.63
6	-1.6	20	8	225	-2.5	12.0	98.41	-13.16	8.88	9.78	10.43	11.20	10.88	11.54
7	-1.6	20	15	225	-2.5	12.0	99.38	-13.40	9.57	10.70	11.46	12.32	12.03	12.77
8	-1.6	20	12	170	-2.5	12.0	36.20	-88.83	10.03	10.68	10.31	10.73	10.38	10.50
9	-1.6	20	12	240	-2.5	12.0	105.48	13.88	8.59	10.43	11.03	12.64	11.73	13.33
10	-1.6	20	12	225	-2.5	32.0	102.29	5.87	10.58	12.49	10.16	11.95	9.58	11.37
11	-1.6	20	12	225	-2.5	-8.0	102.29	-34.13	2.34	2.99	3.30	4.11	4.81	5.65

Table III-7.

Parameters Defining 11 Alongshore Storms Used
In Calibrating The One-Dimensional Model With
The Two-Dimensional Model And The Results

MODEL STORM	ΔP (in.-Hg)	R (n. mi.)	V_F (n. mi.)	θ_N (degrees)	Offshore Coordinates (n. mi.)		Starting Coordinates (n. mi.)		$\eta_{max.}$ (ft. M.S.L.)					
					X_L	Y_L	X_S	Y_S	North Profile		Middle Profile		South Profile	
									1-D	2-D	1-D	2-D	1-D	2-D
1	-1.6	20	12	150	40	12	41.88	-95.98	4.83	4.81	4.95	4.81	5.02	4.65
2	-2.2	20	12	150	40	12	41.88	-95.98	6.54	6.38	6.71	6.36	6.82	6.22
3	-1.2	20	12	150	40	12	41.88	-95.98	3.73	3.77	3.81	3.77	3.86	3.65
4	-1.6	20	12	150	40	12	41.88	-95.98	4.83	4.81	4.95	4.81	5.02	4.65
5	-1.6	12	12	150	40	12	41.88	-95.98	3.10	2.99	3.18	2.99	3.24	2.88
6	-1.6	30	12	150	40	12	41.88	-95.98	6.69	6.75	6.84	6.77	6.92	6.57
7	-1.6	20	8	150	40	12	41.81	-91.98	4.68	4.38	4.80	4.37	4.87	4.20
8	-1.6	20	15	140	40	12	23.57	-91.71	4.35	4.08	4.53	4.14	4.68	4.02
9	-1.6	20	12	160	40	12	60.61	-94.02	5.46	5.71	5.51	5.65	5.50	5.43
10	-1.6	20	12	150	18	12	19.88	-95.98	7.33	7.47	7.49	7.44	7.59	7.18
11	-1.6	20	12	150	62	12	63.88	-95.98	3.28	3.50	3.37	3.53	3.42	3.43

Table III-8.

Parameters Defining 11 Exiting Storms Used
In Calibrating The One-Dimensional Model With
The Two-Dimensional Model And The Results

MODEL STORM	ΔP (in.-Hg)	R (n. mi.)	V_F (n. mi.)	θ_N (degrees)	Exiting Coordinates (n. mi.)		Starting Coordinates (n. mi.)		$\eta_{max.}$ (ft. M.S.L.)					
					X_F	Y_F	X_S	Y_S	North Profile		Middle Profile		South Profile	
									1-D	2-D	1-D	2-D	1-D	2-D
1	-1.4	20	12	100	-2.5	12.0	- 84.01	-58.85	7.14	6.53	7.94	7.37	8.23	7.53
2	-1.6	20	12	100	-2.5	12.0	- 84.01	-58.85	7.93	7.19	8.80	8.10	9.11	8.25
3	-1.1	20	12	100	-2.5	12.0	- 84.01	-58.85	5.97	5.56	6.66	6.29	6.92	6.45
4	-1.4	12	12	100	-2.5	12.0	- 84.01	-58.85	6.89	6.46	7.24	6.87	6.82	6.49
5	-1.4	30	12	100	-2.5	12.0	- 84.01	-58.85	7.43	6.71	8.29	7.53	8.88	7.91
6	-1.4	20	8	100	-2.5	12.0	- 80.99	-56.23	7.22	6.53	8.07	7.37	8.40	7.57
7	-1.4	20	15	100	-2.5	12.0	- 81.74	-56.89	7.07	6.56	7.81	7.31	8.07	7.36
8	-1.4	20	12	80	-2.5	12.0	-103.33	-26.70	6.12	5.50	7.63	7.00	8.14	7.46
9	-1.4	20	12	120	-2.5	12.0	- 54.86	-82.46	8.00	7.71	8.35	8.07	8.47	8.02
10	-1.4	20	12	100	-2.5	32.0	- 84.01	-38.85	7.70	7.54	7.41	7.27	6.95	6.85
11	-1.4	20	12	100	-2.5	-8.0	- 84.01	-62.85	6.35	5.66	7.43	6.77	8.06	7.21

Alongshore and Exiting Storms in the Charlotte County vicinity. Note that eleven storms are selected for each hurricane path category. The last columns in these tables contain the maximum storm surges for the coastal terminus of the three transects shown in Figures II-19, II-20 and II-21 and will be discussed in the next section.

3.2 One-Dimensional Model (Appendix B)

In the following, the results will be presented of calibrating the one-dimensional model with the data base generated by the two-dimensional model. In addition, the results of the long-term simulation will be illustrated.

Calibration With Two-Dimensional Model Results

The one-dimensional numerical model represents the physics of storm surges in a much greater simplified manner than does the two-dimensional model. Simplifications in the 1-D model include, but are not limited to:

- a) The onshore dynamics of the storm surge are not represented,
- b) Only the hurricane pressure and wind stresses along the transect selected are taken into account, and
- c) Convergences and divergences of flow are not represented.

Because of the omission of these and other realistic features from the one-dimensional model and the comprehensive nature of the validated two-dimensional model, the latter is considered as a reliable basis for calibrating the one-dimensional model.

Comparisons of the one-dimensional and two-dimensional peak surges along the three transect lines for Charlotte County are shown in Figures II-19, II-20 and II-21 and for each of the hurricane categories are presented in Tables III-6, III-7

and III-8 and in Figures III-10 through III-12. In each of these nine graphs, best fit least squares curves are shown of the form

$$(\eta_{\max})_{2-D} = K (\eta_{\max})_{1-D} \quad (III-1)$$

where for perfect agreement, a value of unity would be obtained for K. For landfalling storms, the range of K is 1.09 to 1.14, and the associated ranges for alongshore and exiting storms are 0.93 to 1.00 and 0.93 to 0.94, respectively. These values are reasonably close to unity and are employed in the subsequent long-term simulation which uses the one-dimensional model.

Table III-9 presents the ranges of K values for the three categories of storms and all Counties completed to date.

3.3 Long-Term Simulations

As noted previously, long-term simulations are carried out using the one-dimensional numerical model, usually for a duration of at least 500 years. The study of historical occurrence ensures along with the directional distribution (presented for Charlotte County in Figure II-5) that the correct number and category of hurricanes are selected.

The long-term simulation is carried out for each transect selected, the peak total storm surges ranked and their return periods calculated in accordance with Eq. (II-47).

For Charlotte County, five 500 year simulations were carried out and averaged for each of the three transect lines. The return period vs peak total storm tide relationships for these transects are presented in Figure III-13 and are summarized for selected specific return periods in Table III-10. It is seen that the 100 year peak storm tide ranges from 12.7 ft (above MSL) for the southern profile to 13.1 ft for the northern profile.

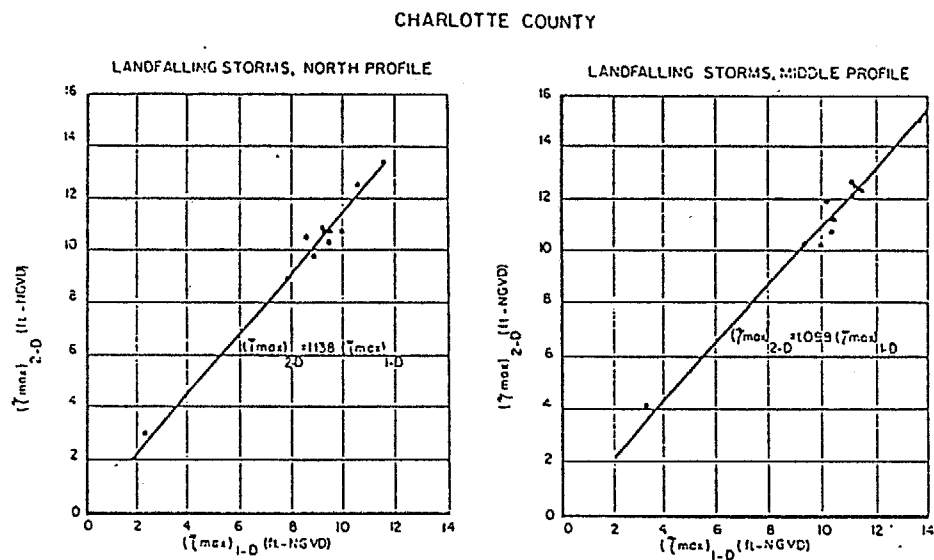


Figure III-10a. Calibration Relationship between the One-Dimensional and the Two-Dimensional Calculations of Peak Surges at the North and Middle Transect lines of Charlotte County for Landfalling Hurricanes

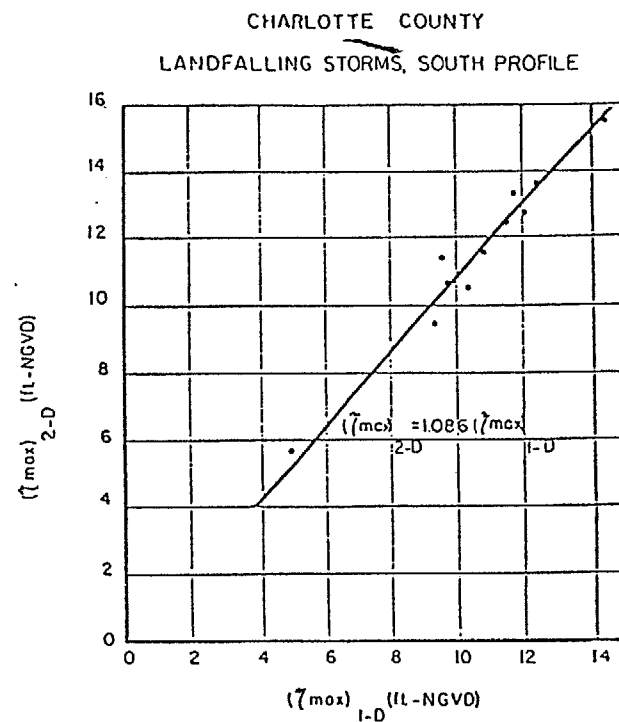


Figure III-10b. Calibration Relationship between the One-Dimensional and the Two-Dimensional Calculations of Peak Surges at the South Transect Line of Charlotte County for Landfalling Hurricanes

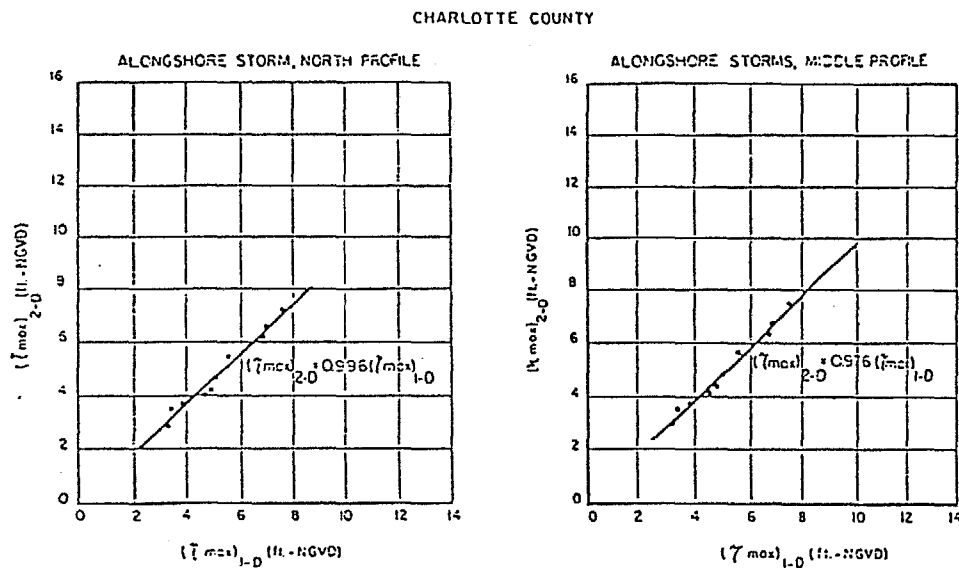


Figure III-11a. Calibration Relationship between the One-Dimensional and the Two-Dimensional Calculations of Peak Surges at the North and Middle Transect Lines of Charlotte County for Alongshore Hurricanes

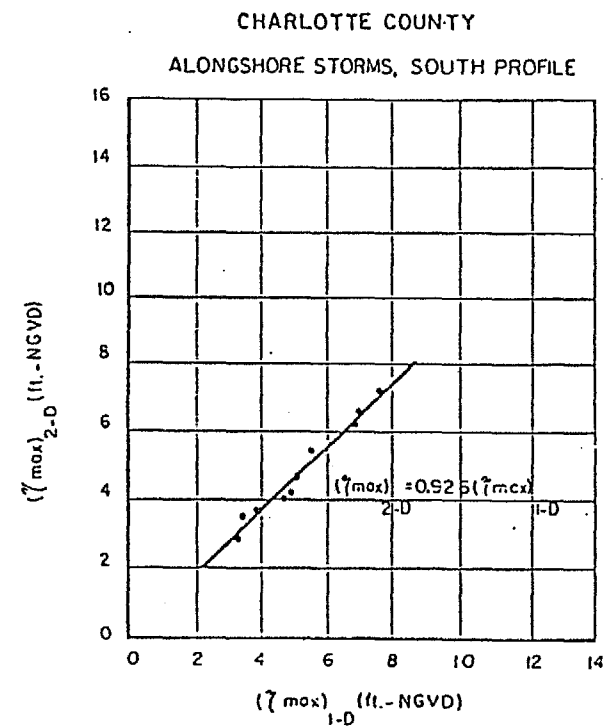


Figure III-11b. Calibration Relationship between the One-Dimensional and the Two-Dimensional Calculations of Peak Surges at the South Transect Line of Charlotte County for Alongshore Hurricanes

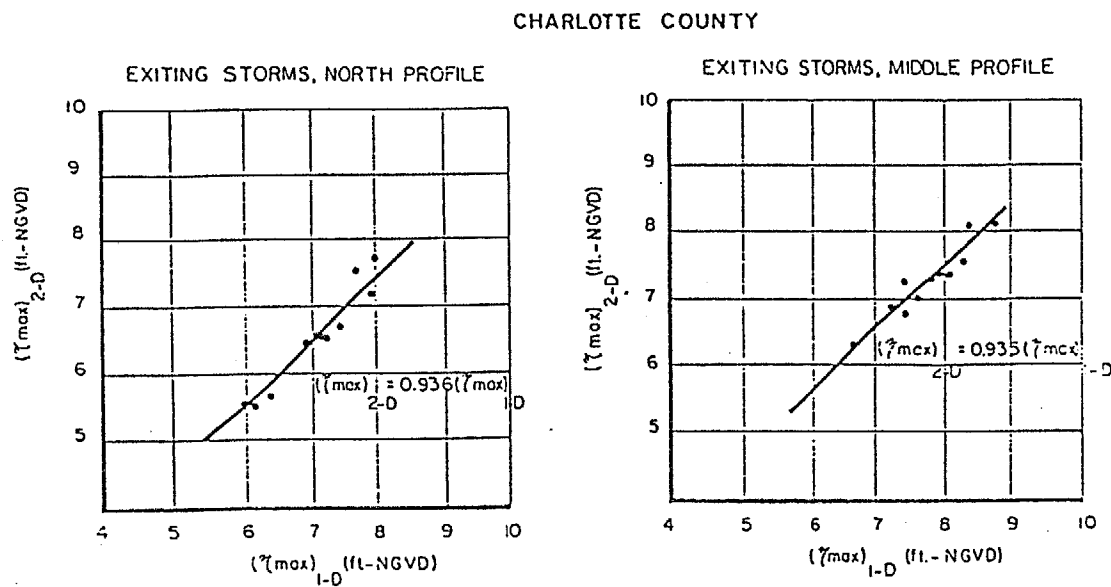


Figure III-12a. Calibration relationship between the One-Dimensional and the Two-Dimensional Calculations of Peak Surges at North and Middle Transect lines of Charlotte County for Exiting Hurricanes

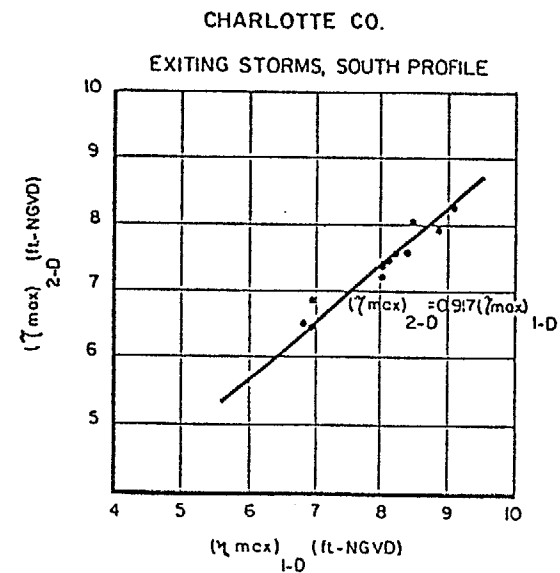


Figure III-12b. Calibration Relationship between the One-Dimensional and the Two-Dimensional Calculations of Peak Surges at the South Transect line of Charlotte County for Exiting Hurricanes

TABLE III-9

Values of 1-D/2-D Peak Storm Surge
Correlation Coefficients For Counties Completed to Date

County	Date of Study	Range of K For		
		Landfalling Hurricanes	Alongshore Hurricanes	Exiting Hurricanes
Broward	1981	1.07*	1.07*	***
Charlotte	1984	1.09-1.14	0.93-1.00	0.93-0.94
Dade	1981	1.03	1.34	1.13
Franklin	1983	0.95-1.18	***	***
Nassau	1982	0.93-0.99	0.84-0.90**	0.84-0.90**
Walton	1982	0.99-1.05	***	***

*The calibration of the landfalling and alongshore hurricanes was combined.

**The calibration of the alongshore and exiting hurricanes was combined.

***Due to their very small relative frequency of occurrence, alongshore and exiting hurricanes were not included.

CHARLOTTE COUNTY

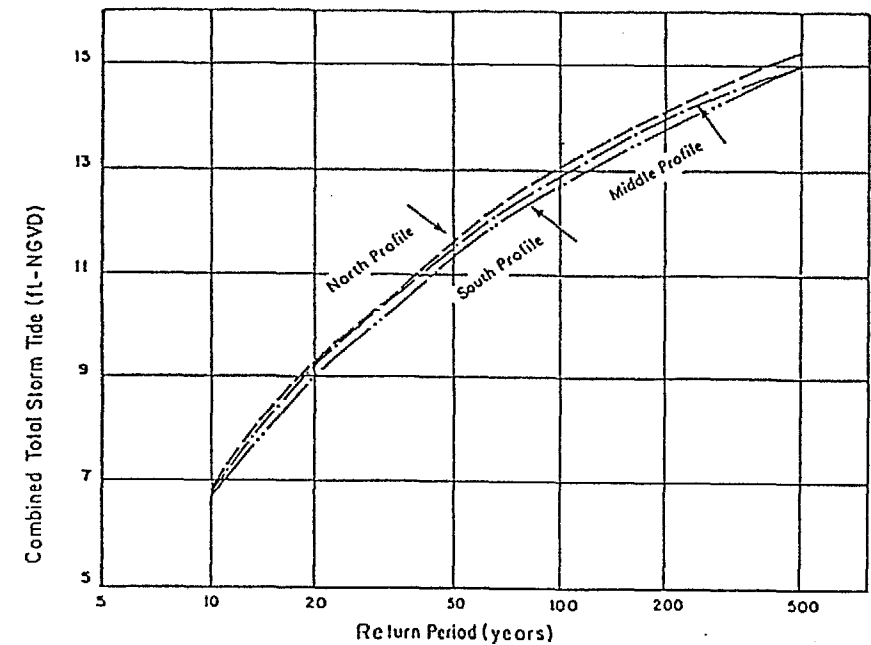


Figure III-13. Combined Total Storm Tide Elevation Versus Return Period for Three Representative Transect lines in Charlotte County

TABLE III-10

Combined Total Storm Tide Values for Various Return Periods

Return Period, TR (years)	Combined Total Storm Tide Level* above MSL (ft)		
	North	Middle	South
500	15.3	15.0	15.0
200	14.1	14.0	13.8
100	13.1	12.9	12.7
50	11.7	11.5	11.4
20	9.3	9.3	9.0
10	6.8	6.8	6.7

*Includes contributions of: wind stress, barometric pressure, dynamic wave setup and astronomical tides.

IV EROSION CALCULATION METHODOLOGY

4.1 Introduction

The erosion calculation methodology is based on measurements of beach profiles, both in an equilibrium and post-storm state and reasonable approximations to the physics, where necessary. These methods have been under development for approximately seven years and the numerical models are continually being upgraded, both as new and improved information becomes available and in our continuing attempt to include as much realism (for example, overwash) in the numerical model as possible.

4.2 Equilibrium Beach Profiles

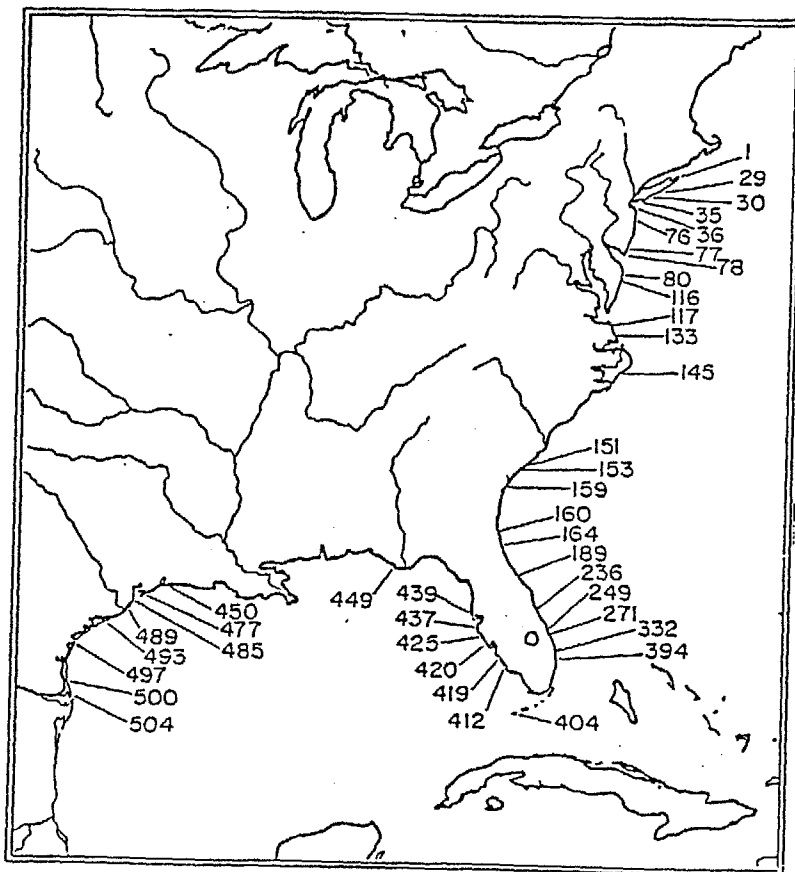
A number of theories have been advanced attempting to describe the properties of and mechanisms associated with equilibrium beach profiles.

Based on a data set comprising more than 500 beach profiles ranging from the eastern tip of Long Island to the Texas-Mexico border, see Figure IV.1, the following form for an equilibrium beach profile was identified

$$h(x) = Ax^m \quad (IV.1)$$

in which A and m are scale and shape parameters, respectively. Figure IV.2 presents normalized beach profiles for various m values. It is seen that for $m < 1$, the profile is concave upward as commonly found in nature. Figure IV.3 demonstrates the effect of the scale parameter, A.

The data from the 502 wave profiles were evaluated employing a least squares procedure to determine the A and m values for each of the profiles. The results of this analysis strongly supported a value of $m = 0.667$, (see Figure IV.4). It can be shown that a value of $m = 2/3$ corresponds to uniform wave energy dissipation per unit water volume in



IV.1 Location map of the 502 profiles used in the analysis (from Hayden, et al., (10)).

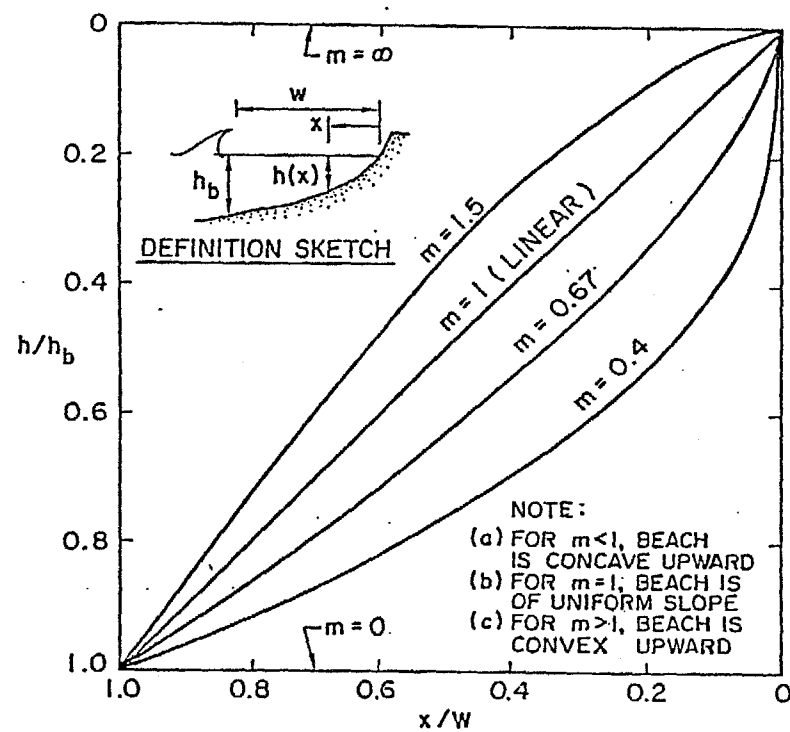


Figure IV.2 Characteristics of dimensionless beach profile $\frac{h}{h_b} = \left(\frac{x}{W}\right)^m$ for various m values. (from Dean, (11)).

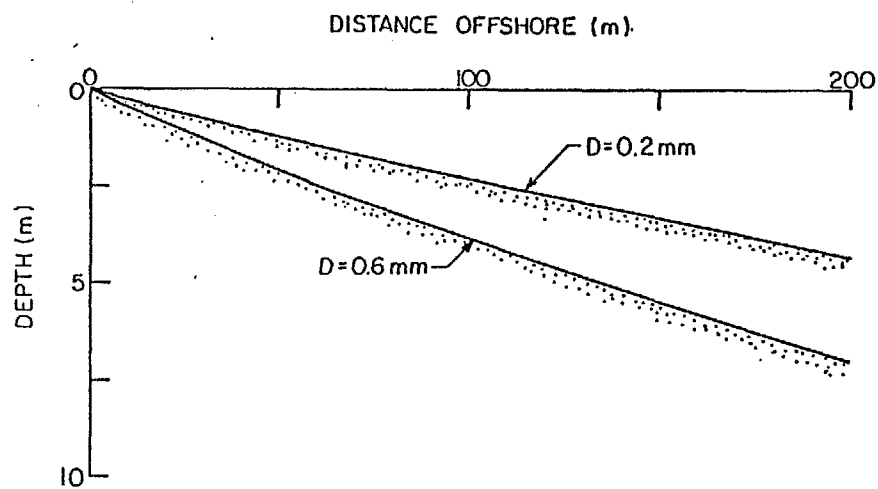


Figure IV.3 Equilibrium beach profiles for sand sizes of 0.2 mm and 0.6 mm
 $A(D = 0.2 \text{ mm}) = 0.1 \text{ m}^{1/3}$, $A(D = 0.6 \text{ mm}) = 0.20 \text{ m}^{1/3}$.

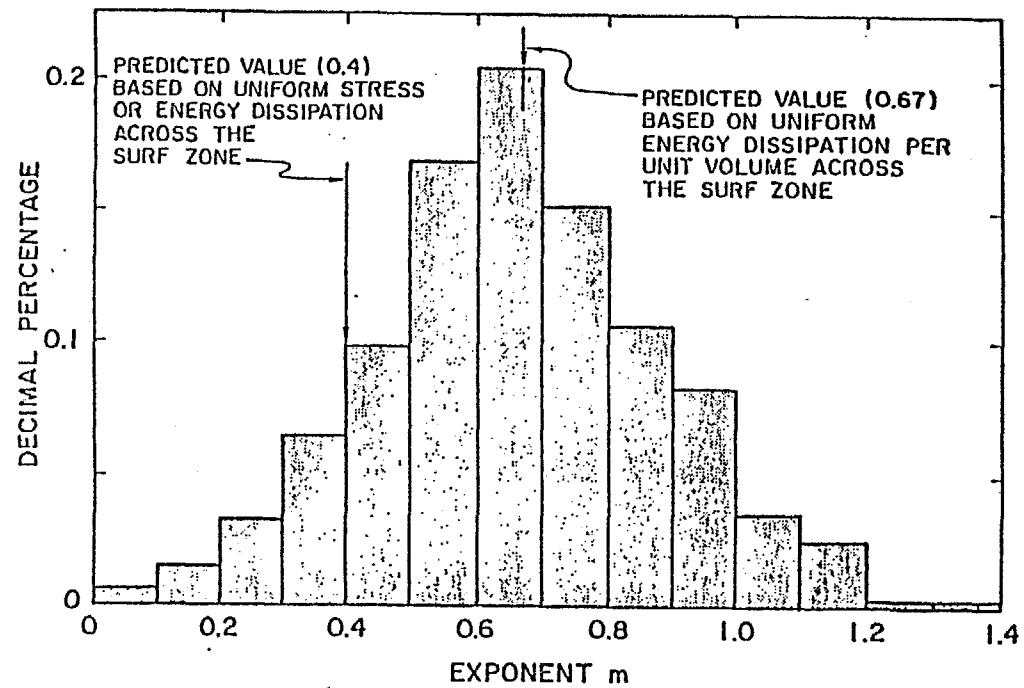


Figure IV.4 Histogram of exponent m in equation $h = Ax^m$ for 502 United States East Coast and Gulf of Mexico profiles (from Dean, (11)).

the surf zone. The physical explanation associated with this mechanism is as follows. As the wave propagates through the surf zone, coherent wave energy is converted to turbulent energy by the breaking process. This turbulent energy is manifested as eddy motions of the water particles, thus affecting the stability of the bed material. Any model must acknowledge that a particular sand particle is acted on by constructive and destructive forces. The model here addresses directly only the destructive (destabilizing) forces. It was reasoned that the parameter A depends primarily on sediment properties, and secondarily on wave characteristics, i.e.

$$A = F(\text{Sediment Properties, Wave Characteristics}) \quad (\text{IV.2})$$

where "F()" denotes "function of" and it would be desirable to combine wave and sediment characteristics to form a single dimensionless parameter.

A portion of Mr. Brett Moore's M.S. Thesis (12) was directed toward an improved definition of the scale parameter, A. Moore combined available laboratory and field data to obtain the results presented in Figure IV.5, thereby extending considerably the previous definition of A. Some of the individual beach profiles used in the development of Figure IV.5 are interesting. For example, Figure IV.6 presents the actual and best least squares fit to a beach consisting of "sand particles" 15-30 cm in diameter (approximately the size of a bowling ball). Figure IV.7 presents the same information for a beach reported to be composed almost entirely of whole and broken shells. Figure IV.8 shows a profile with a bar present resulting in one of the poorer fits to the data. It is emphasized that the analytical form (Eq. (IV.2)) describes a monotonic profile.

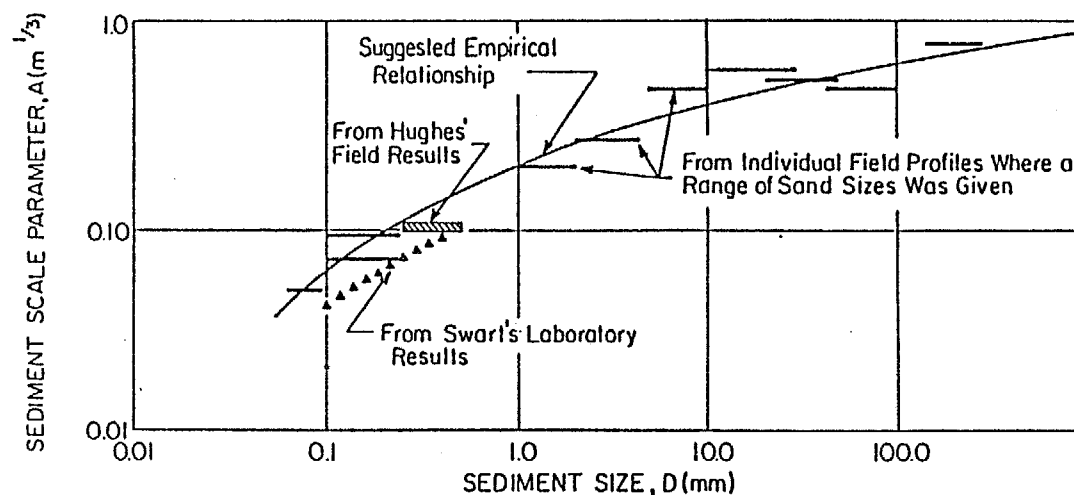


Figure IV.5 Beach profile factor, A, vs sediment diameter, D, in relationship $h = Ax^{2/3}$ (modified from Moore, (12))

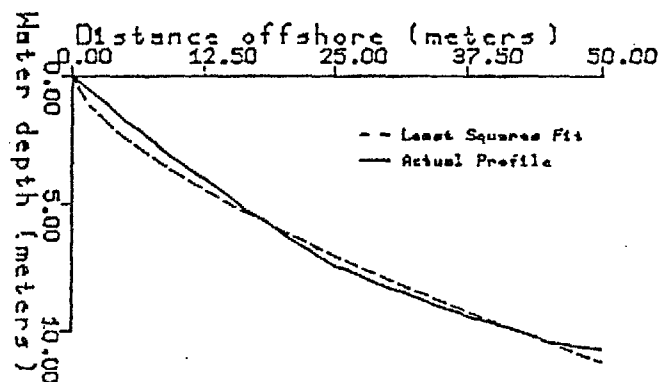


Figure IV.6 Profile P4 from Zenkovich (1967). A boulder coast in Eastern Kamchatka. Sand diameter: 150 mm - 300 mm. Least squares value of $A = 0.82 \text{ m}^{1/3}$ (from Moore, (12))

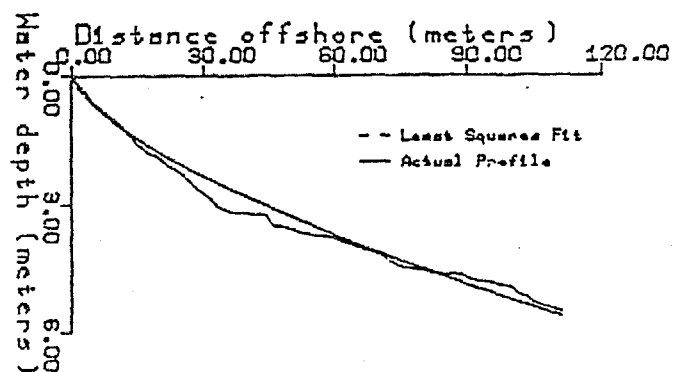


Figure IV.7 Profile P10 from Zenkovich (1967). Near the end of a spit in Western Black Sea. Whole and broken shells. $A = 0.25 \text{ m}^{1/3}$ (from Moore, (12))

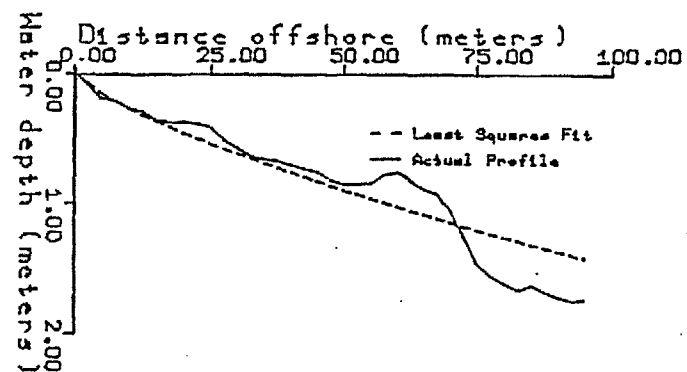


Figure IV.8 Profile from Zenkovich (1967). Eastern Kamchatka. Mean sand diameter: 0.25 mm. Least squares value of $A = 0.07 \text{ m}^{1/3}$ (from Moore, (12)).

4.3 Cross-shore Transport Models

It has been noted that most equilibrium profiles correspond to uniform energy dissipation per unit volume with the scale of the profile represented by the parameter A which depends primarily on sediment characteristics and secondarily on wave characteristics, i.e.

$$h(x) = Ax^{2/3} \quad (IV.3)$$

The parameter, A , and the uniform energy dissipation per unit volume, \bar{p}_* , are related for linear spilling waves by

$$A = \left[\frac{24}{5} \frac{\bar{p}_*}{\rho g^{3/2} \kappa^2} \right]^{2/3} \quad (IV.4)$$

It can be shown that for the spilling breaker assumption and linear waves, the energy dissipation per unit volume, \bar{p} , is proportional to the product of the square root of the water depth and the gradient in depth,

$$\bar{p} = \frac{5}{16} \rho g^{3/2} \kappa^2 h^{1/2} \frac{\partial h}{\partial x} \quad (IV.5)$$

Thus it is clear that an increase in water level such as due to a storm surge will cause wave energy dissipation to increase beyond the equilibrium value. It is also known that the beach responds by erosion of sediment in shallow water and deposition of this sediment in deeper water (Figure IV.9). It therefore appears reasonable to propose as a hypothesis that the offshore sediment transport, Q_s , per unit width is given by

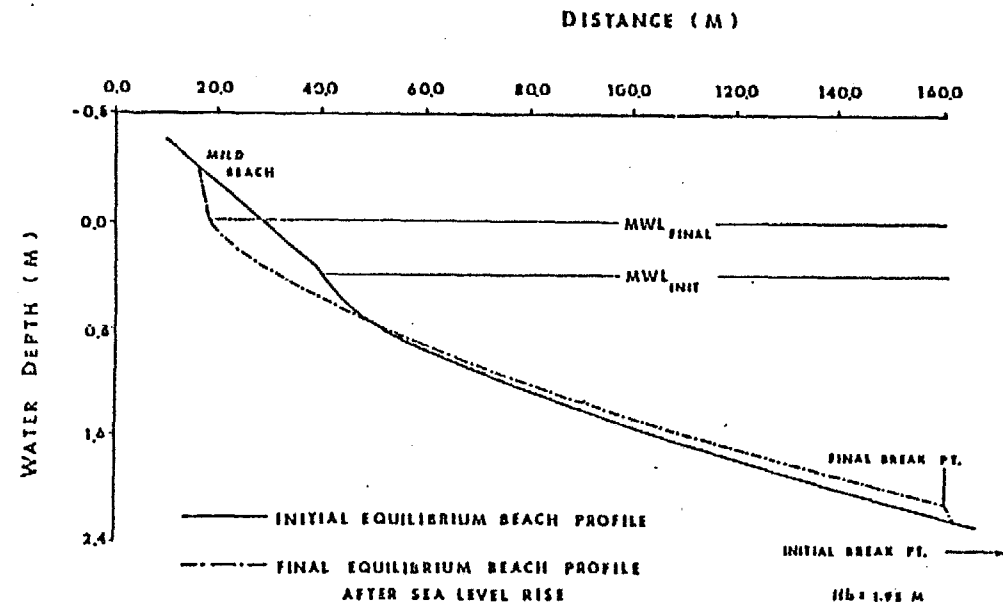


Figure IV.9 Model simulation of a 0.5 meter sea level rise and beach profile response with a relatively mild sloping beach (from Moore, (12))

$$Q_s = K(D - D_*) \quad (IV.6)$$

where K is a rate constant that hopefully does not vary too greatly with scale. Moore (12) evaluated this relationship using large scale wave tank data of Saville (13) and found

$$K = 2.2 \times 10^{-6} m^4/N \quad (IV.7)$$

Figure IV.10 presents comparisons of predicted cumulative erosion for various values of K with the measured values obtained from Saville's wave tank tests.

4.4 Prediction of Beach and Dune Erosion Due to Severe Storms by Kriebel's Model

Mr. David Kriebel carried out a Master's thesis on this subject. He incorporated previous work and developed considerable original contributions to this problem, including the capability to model single storm events and long-term scenarios in which many storms occur.

Profile Schematization

The profile was schematized as a series of depth contours, h_n , the locations of which are specified by coordinates, x_n , measured from an arbitrary baseline, see Figure IV.11. The profile is thus inherently monotonic and at each time step, the x_n values of each of the active contours is updated.

Governing Equations

As in most transport problems, there are two governing equations. One is an equation describing the transport in terms of a gradient or some other feature. The second is a continuity or conservation equation which accounts for the net fluxes into a cell.

As discussed previously, the offshore transport is defined by Eq. (IV.6) in terms of the excess energy dissipation per unit volume. Specifically, in finite difference form

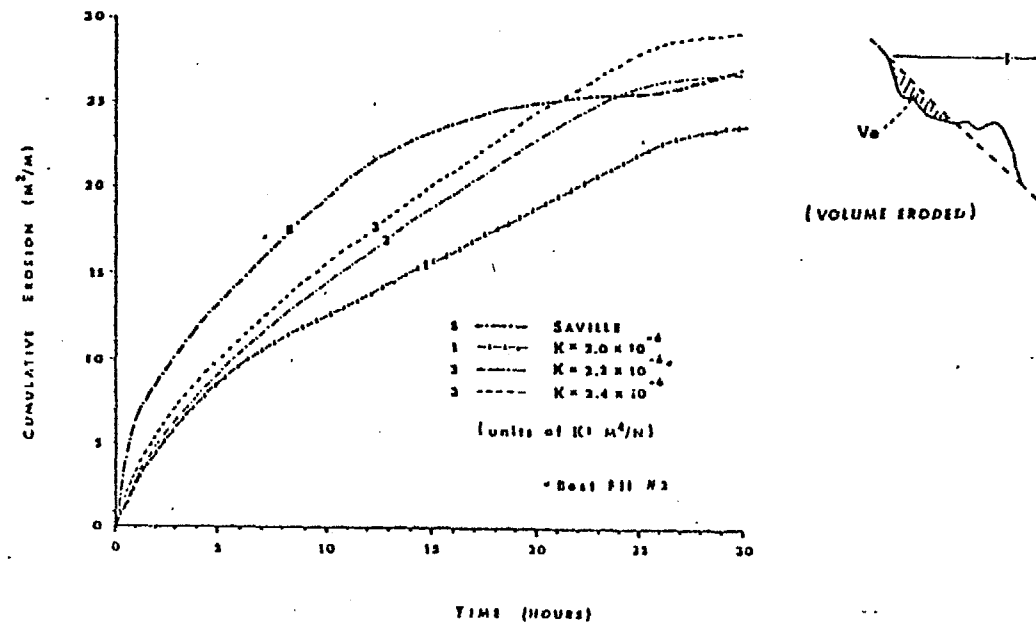


Figure IV.10 Effect of varying the sediment transport rate coefficient on cumulative erosion during the simulation of Saville's (1957) laboratory investigation of beach profile evolution for a 0.2 mm sand size (from Moore, (12))

$$D_{n+1} = k_D \frac{h_{n+1}^{5/2} - h_n^{5/2}}{(h_{n+1}' + h_n')(x_{n+1} - x_n)} \quad (IV.8)$$

where

$$k_D = \frac{\gamma}{4} \kappa^2 \sqrt{g} \quad (IV.9)$$

The sand conservation equation is

$$\Delta x_n = \frac{\kappa \Delta t}{\Delta h} (D_n - D_{n+1}) \quad (IV.10)$$

Method of Solution of Finite Difference Equations

A number of methods could be employed for solving Eqs. (IV.6) and (IV.10). For example, explicit methods would be fairly direct and simple to program; however, the maximum time increment would be relatively small resulting in a program which is quite expensive to run. Implicit methods are somewhat more difficult to program, but have the desirable feature of remaining stable with a much greater time step. Because of the planned application to long-term simulation in which for a 500 year time period and on the order of three hundred storms would be modeled, each with an erosional phase of six to twelve hours, an implicit method was adopted. This method will not be described in detail here except to note that a double sweep approach is used in which the Q_{s_n} values and the x_n values are updated simultaneously at each time step. For Δh values of 1 ft, and a time step of thirty minutes, the system of equations was stable.

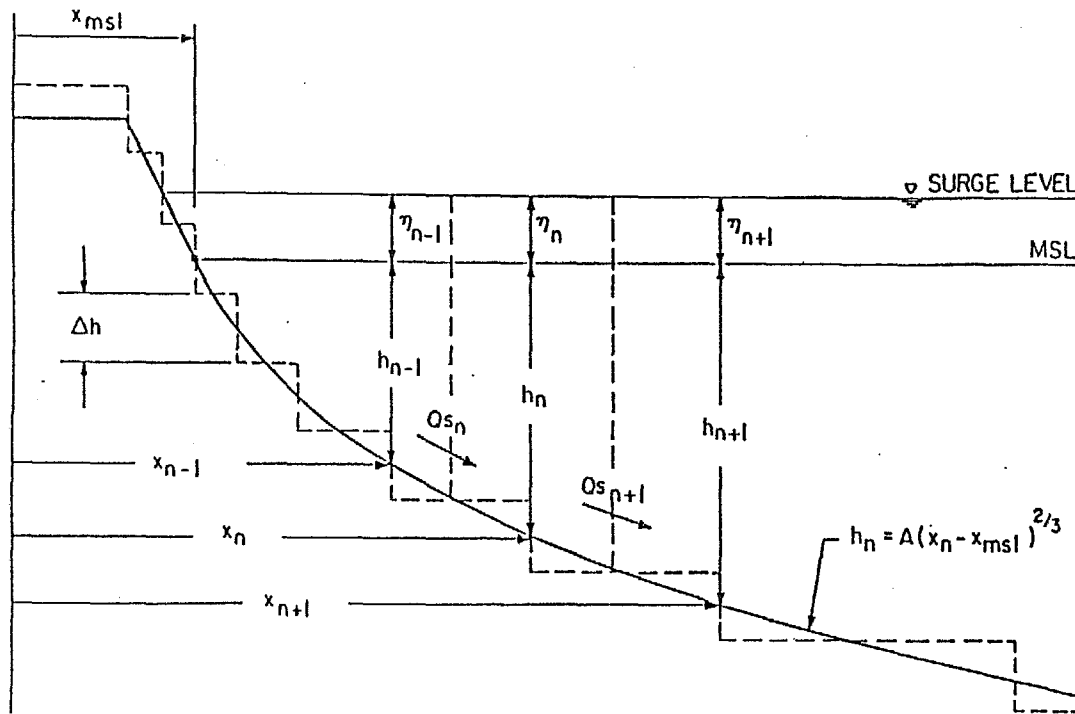


Figure IV.11 Model representation of beach profile, showing depth and transport relation to grid definitions (from Kriebel, (14))

The boundary conditions used were somewhat intuitive. At the shoreward end of the system, erosion proceeded with a specified slope above a particular depth, h_* . The depth, h_* , is the depth that the equilibrium slope and the slope corresponding to the beach face are the same. Thus a unit of recession of the uppermost active contour causes an erosion of the profile above the active contour that is "swept" by this specified slope. This material is then placed as a source into the uppermost active contour. The offshore boundary condition is that the active contours are those within which wave breaking occurs. If an active contour extends seaward, thereby encroaching over the contour below to an extent that the angle of repose is reached, the lower contour (and additional lower contours if necessary) are displaced seaward to limit the slope to that of the angle of repose.

Application of Method to Computation of Idealized Beach Response

Kriebel (14) carried out computations for a number of idealized cases, some of which are reviewed below. Details of the erosion model are presented in another report (Kriebel (15)).

Response to Static Increased Water Level - Figure IV.12 presents the beach recession due to a static increase in water. The beach responds as expected. In the early stages, the rate of adjustment is fairly rapid with the latter adjustments approaching the equilibrium recession in an asymptotic manner. Of special relevance is that the response time to equilibrium is long compared to the duration of most severe storm systems, such as hurricanes. The form of the response presented in Figure IV.12 is reminiscent of that for a first order process in which the time rate of change of beach recession, R , is represented as

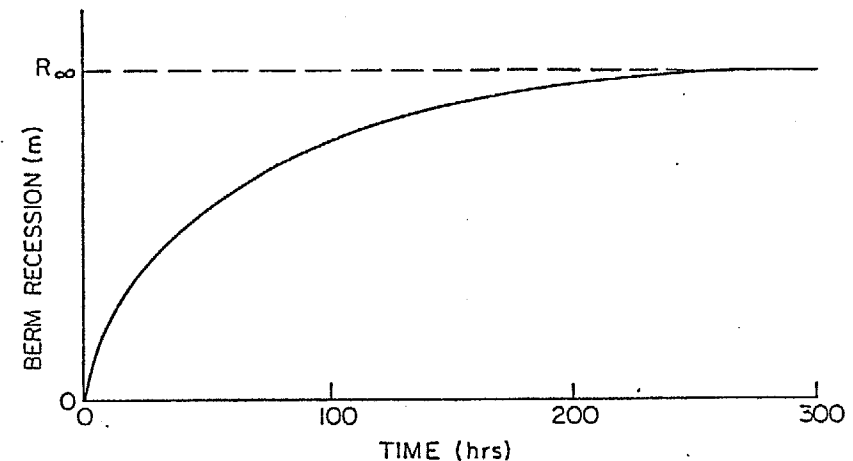


Figure IV.12 Characteristic form of berm recession versus time for increased static water level (from Kriebel, (14))

$$\frac{dR}{dt} = -KR \quad (IV.11)$$

for which the solution is

$$\frac{R(t)}{R_{\infty}} = (1 - e^{-Kt}) \quad (IV.12)$$

Figure IV.13 presents a comparison of the response from the numerical model and Eq. (IV.12). This similarity forms the basis for a very simple and approximate numerical model of beach and dune profile response. Such a model has been developed, is used currently in the CCCL program and will be described in the next section.

Effects of Various Wave Heights - Considering a common increased water level, but storms with different wave heights, the larger wave heights will break farther offshore causing profile adjustments over a greater distance and thus a greater shoreline recession. Simulations were carried out to examine evolution of the beach under different wave heights with the results presented in Figure IV.14. As expected, the greater shoreline recessions are associated with the larger wave heights. Surprisingly, however during the early phases of the evolution, the larger wave heights do not cause proportionally larger erosions. Thus, for storms of short duration, the sensitivity of the maximum erosion to breaking wave height may not be large.

Effects of Various Storm Tide Levels - The counterpart to the previous case is that of a fixed wave height and various storm water levels. The results of these simulations are presented in Figure IV.15. In contrast to the previous case, the various storm tide levels cause recession rates in the early stages of the process which are nearly proportional to the storm water level.

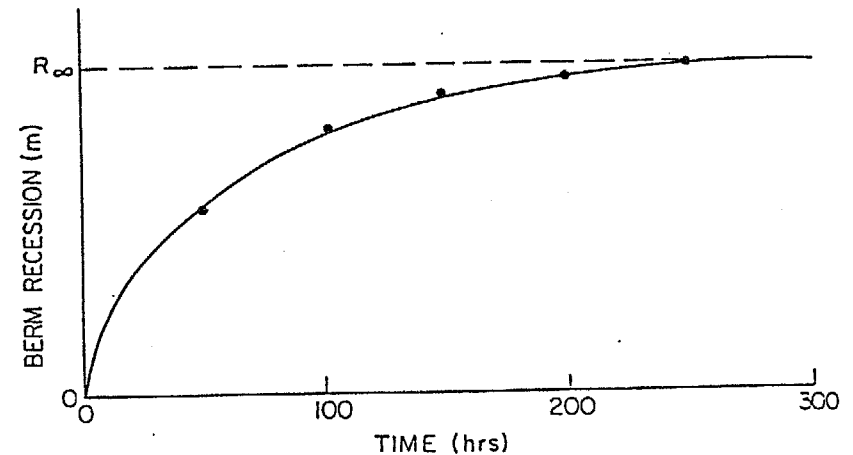


Figure IV.13 Comparison of asymptotic berm recession from model (—) and as calculated by Eq. (IV.12) (• •).

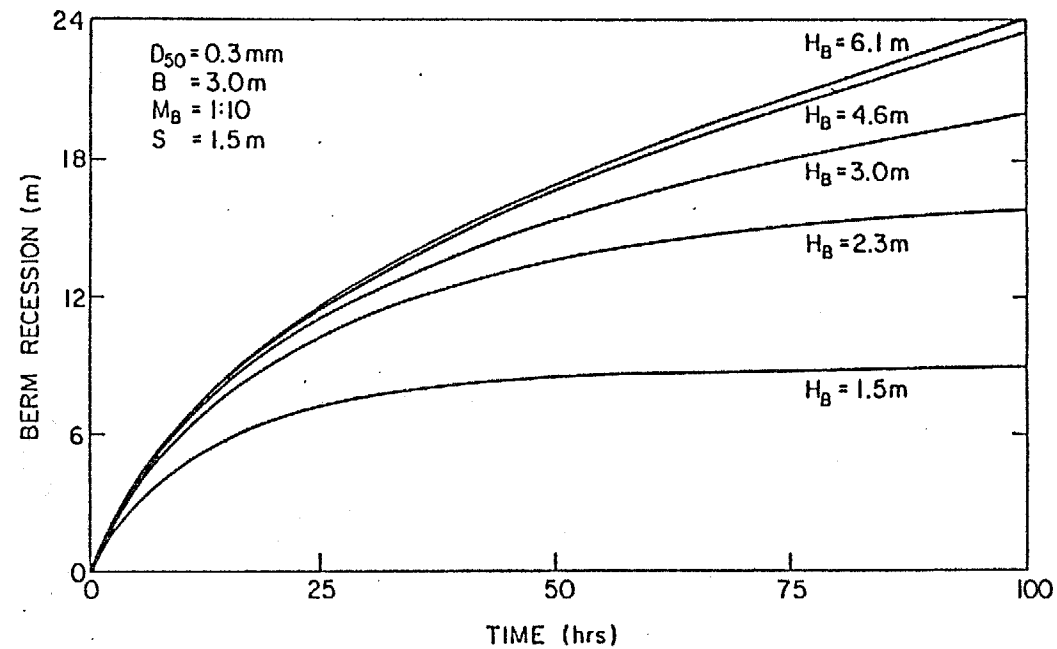


Figure IV.14 Effect of breaking wave height on berm recession (from Kriebel, (14))

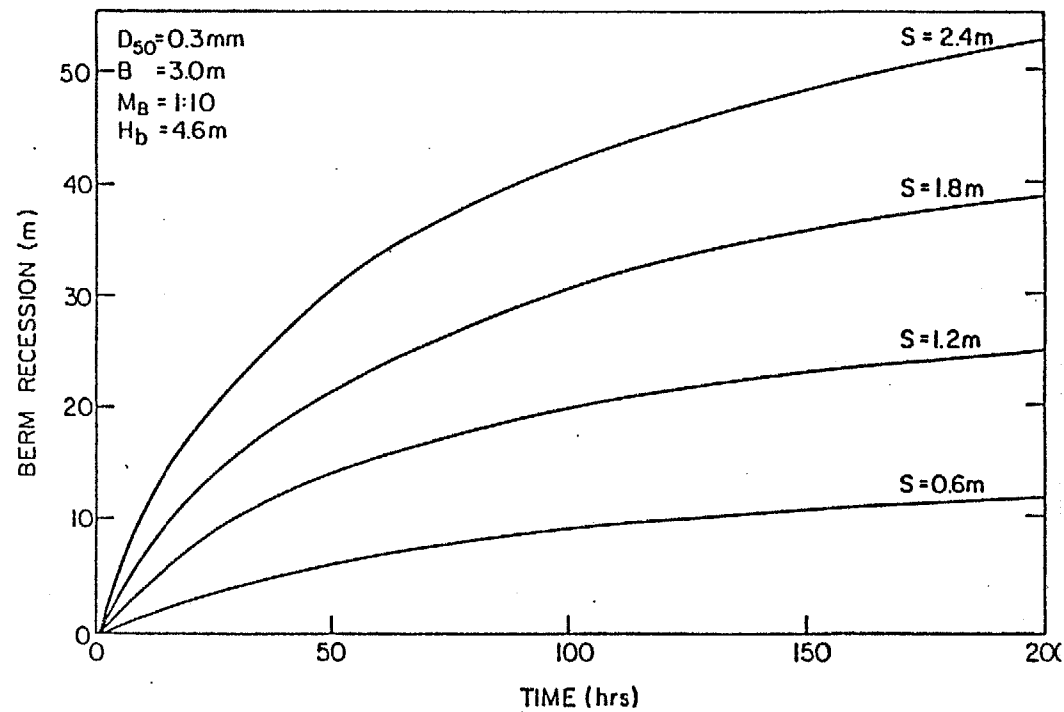


Figure IV.15 Effect of static storm surge level on berm recession (from Kriebel, (14))

Effect of Sediment Size on Berm Recession - The effect of two different sediment sizes on amount and rate of berm recession is shown in Figure IV.16. The equilibrium recession of a coarser material is much less; however, the equilibrium is achieved in a much shorter time than that for the finer sediment. The explanation for the lesser equilibrium erosion for the coarser material is that since the beach is steeper, the waves break closer to shore and thus less material is required to be transferred offshore to establish an equilibrium profile out to the breaking depth (considered to be the limit of motion). Presumably the explanation for the slower approach to equilibrium for the finer material is that, as will be shown by consideration of the initial and equilibrium profile geometries, a much greater volume of sediment must be moved a greater distance to establish equilibrium.

Effect of Storm Duration - The effect of storm duration on shoreline recession was investigated by considering a fixed wave height and an idealized storm tide variation, expressed as

$$\eta = 1.2 \cos^2\left(\frac{\sigma(t-18)}{2}\right), \quad |t-18| < \frac{T}{2} \quad (IV.13)$$

$$= 0, \quad |t-18| > T/2$$

in which $T (\cong 2\pi/\sigma)$ is the total storm duration in hours. The results are presented for three storm durations in Figure IV.17. For the shortest storm duration ($T = 12$ hours), the potential volume eroded is approximately $70 \text{ m}^3/\text{m}$ whereas the computed actual maximum volume eroded is $10 \text{ m}^3/\text{m}$. With increasing storm tide duration, the computed actual maximum volume eroded increases. Tripling the storm tide duration to

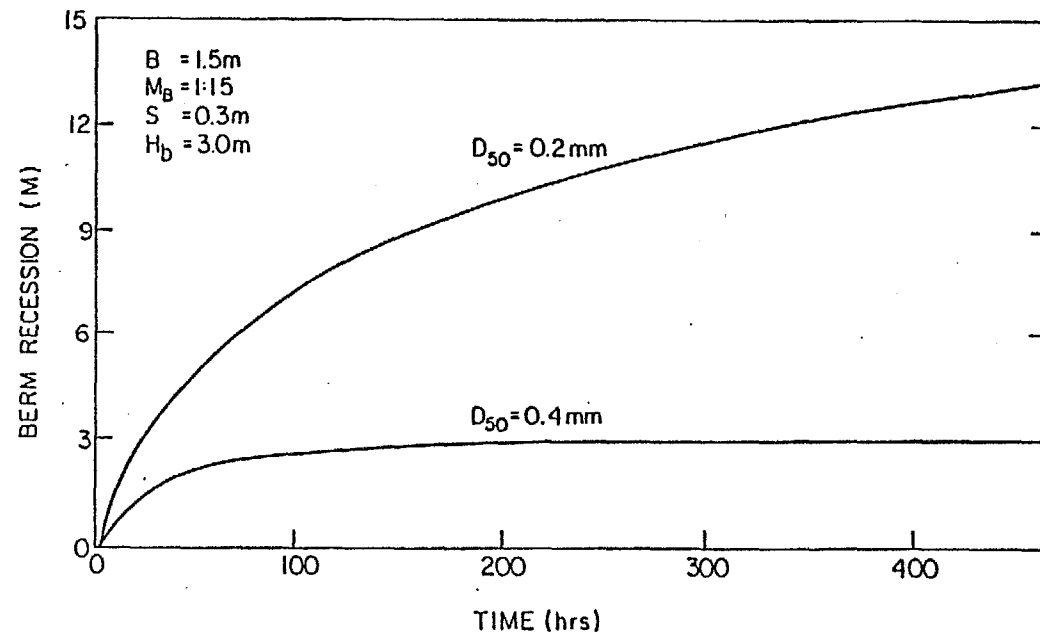


Figure IV.16 Effect of sediment size on berm recession (from Kriebel, (14))

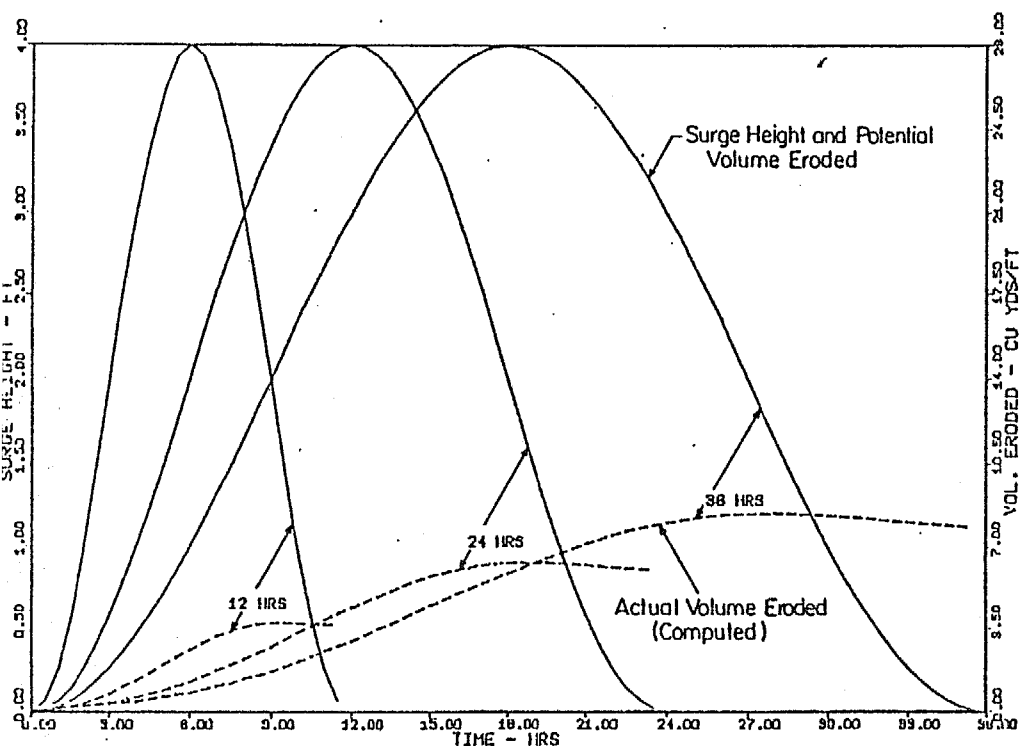


Figure IV.17 Comparison of the effects of 12, 24, and 36 hrs. storm surge on volumetric erosion (from Kriebel, (14))

36 hours doubles the maximum volume eroded to $20 \text{ m}^3/\text{m}$. It is noted that this is only approximately 28% of the potential volume eroded, again underscoring the likelihood that most storms will only reach a fraction of their potential erosion limit. This feature also highlights the significance of cumulative effects of sequential storms and of the need to better understand the recovery process (especially the rates), a portion of the cycle not addressed in this project.

Application of Method to Long-Term Beach and Dune Response Simulations

The previous section has described the application of the model to idealized examples of beach and dune response. The model can also be applied to more realistic situations in which the initial beach and dune conditions are specified along with time-varying waves and tides.

Evaluation of Method by Hurricane Eloise Erosion Data - Kriebel

carried out an evaluation of the method by comparing erosion computations for Hurricane Eloise (1975) with measurements reported by Chiu (16). Although the wave and tide conditions were not measured along the beaches of Bay and Walton Counties (Florida) of interest, some tide data were available and wave heights were estimated. Erosion was computed for twenty combinations of dune slope, wave height and peak surge. It was found that the volumetric erosion ranged from 21 to $38 \text{ m}^3/\text{m}$ compared to average measured values of 18 to $20 \text{ m}^3/\text{m}$ for Bay and Walton Counties, respectively and an average of $25 \text{ m}^3/\text{m}$ near the area of peak surge. Although the predicted values are somewhat larger than the observed, Chiu (16) states that the beaches had started to recover at the time of the post-storm surveys, with approximately $5 \text{ m}^3/\text{m}$ of sand having returned to the beach. Thus the maximum eroded volume would be $30 \text{ m}^3/\text{m}$ compared to a maximum calculated value of $38 \text{ m}^3/\text{m}$, a difference

of approximately 27%. This reasonably close agreement was considered adequate recognizing the uncertainty in the storm tide employed in the computations; therefore no further calibration of the model was considered warranted. It is of interest that the erosion potential associated with the peak tide is approximately nine times that predicted for the time-varying conditions included in the computations. This again reinforces the fact that most storms in nature cause only a fraction of the potential erosion associated with the maximum conditions in the storm.

Long-Term Simulation - With the model reasonably verified for the Bay and Walton Counties area of Florida, a long-term simulation of beach and dune erosion was carried out. The hurricane wind and pressure fields were idealized in accordance with a representation published by Wilson (17). The five idealized hurricane parameters

- Δp = Maximum Pressured Deficit
- R_{max} = Radius to Maximum Winds
- V_F = Hurricane System Translational Speed
- β = Hurricane Translational Direction
- y_F = Landfall Point

were selected by a Monte Carlo method in accordance with the historical characteristics of hurricanes in the general area. For each hurricane, the storm tide was calculated using the Bathystrophic Storm Tide Model of Freeman, Baer and Jung (9). With the time-varying storm tide and wave height calculated, the beach and dune model was applied until maximum erosion was achieved. As the recovery mechanism is not yet understood to a degree for realistic modelling and because hurricanes occur approximately on a biennial basis, the erosion for successive

hurricanes was assumed to commence from a fully recovered condition. This is clearly an approximation as the recovery process occurs at several rates of magnitude slower than the erosion process. Study of some recovery stages from severe storms has shown that up to seven years may be required to achieve approximately 90% recovery. The duration required for recovery from milder storms would, of course, be less.

Figure IV.18 presents a "flow chart" describing the elements of the long-term simulation. In the Bay-Walton Counties area, hurricanes making landfall within ± 150 n.mi. of these counties were considered requiring a total of 393 hurricanes to simulate a 500 year record. The return periods associated with various dune recessions as determined from the simulations are presented in Figure IV.19. As examples, the dune recessions for return periods of 10, 100 and 500 years are 4 m, 12 m and 18 m, respectively. Based on these results, Hurricane Eloise is judged to represent a 20 to 50 year erosional event; however based on results from a storm surge analysis, Hurricane Eloise was a 75 to 100 year coastal flooding event.

It is also possible to present the results of the erosion simulations in a manner that is of maximum relevance to individuals or agencies responsible for shoreline management. This type of presentation is demonstrated for the Bay-Walton County area in Figure IV.20. This plot includes the contributions from storms and sea level rise. As examples, without any erosion mitigation measures within the next 50 years, the erosion due to sea level rise (regarded as a certainty or probability of 100%) is expected to be approximately 15 ft. Within 50 years, the probability of dune erosion occurring to a distance of 40 ft is 85% and for distances of 60 and 80 ft, the

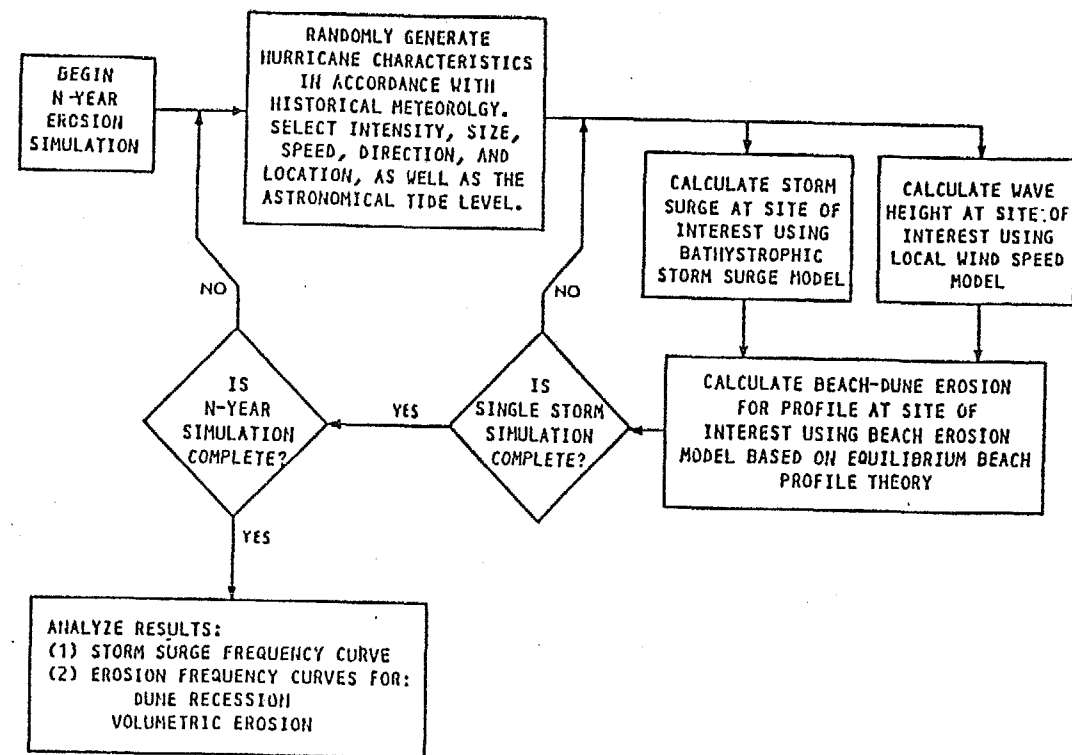


Figure IV.18 Flow diagram of N-year simulation of hurricane storm surge and resulting beach erosion (from Kriebel, (14)).

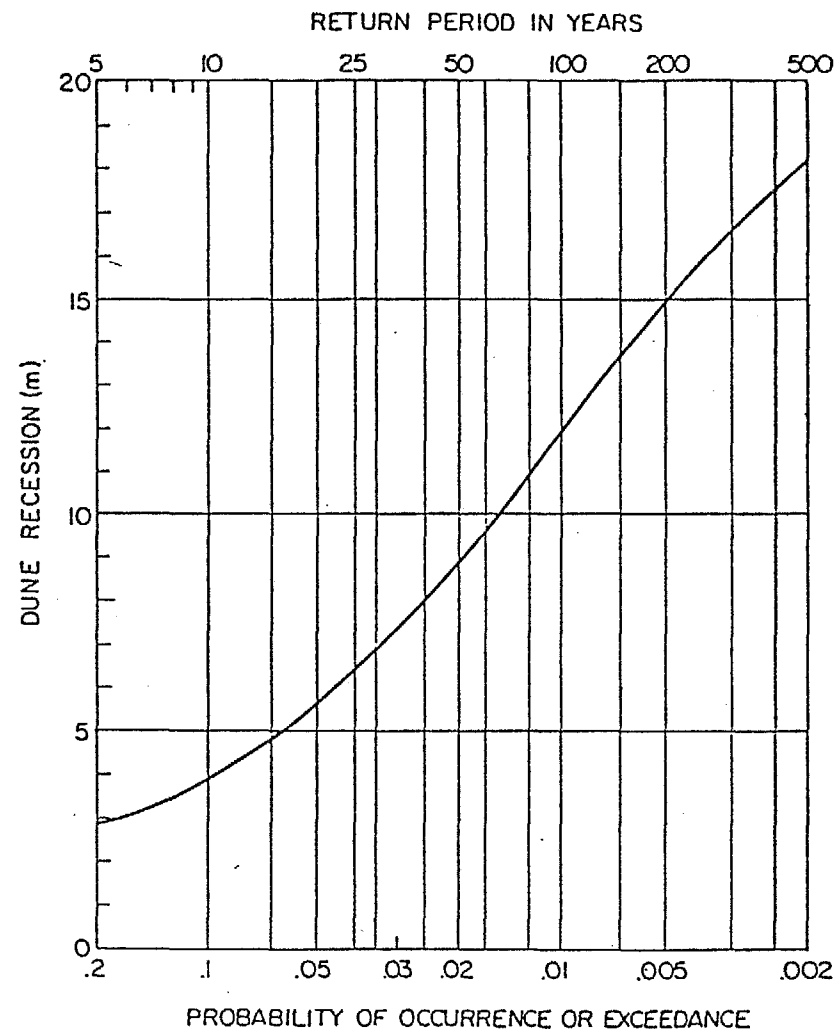


Figure IV.19 Average frequency curve for dune recession, developed by Monte Carlo simulation, Bay-Walton Counties, Florida (from Kriebel, (14)).

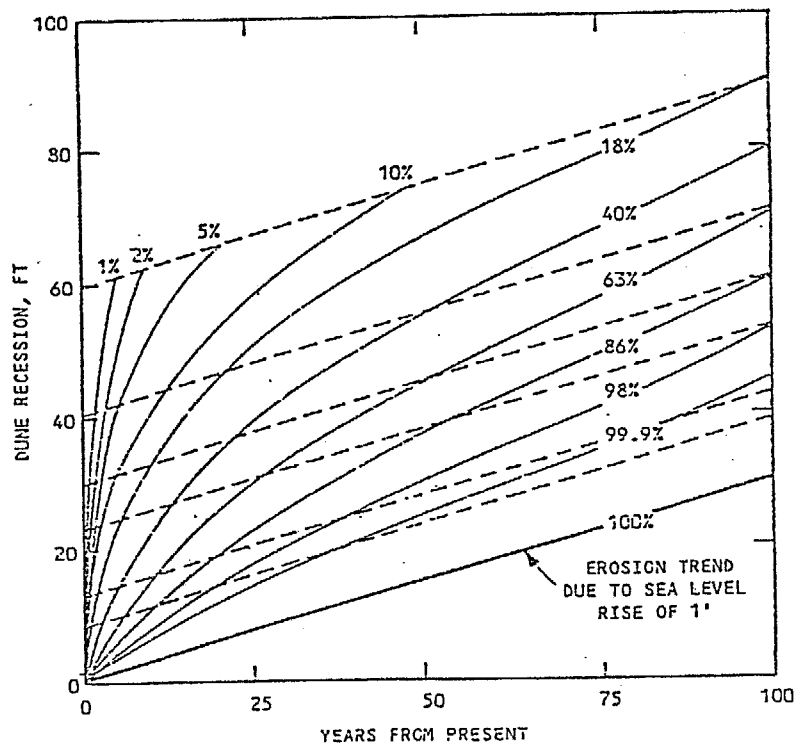


Figure IV.20 Probability or risk of dune recession of given magnitude occurring at least once in N-years, Bay-Walton Co., Florida (from Kriebel, (14))

corresponding probabilities are 32% and 9%, respectively. Through the use of figures such as these it would be possible to weigh the costs of certain erosion control measures against the potential of damage if those measures are not carried out.

These procedures provide, for the first time, a basis for conducting the necessary technical studies to implement the erosion component calculations of the Flood Insurance Act of 1973 which provides for the application of methodology to provide the basis for insurance rates for flooding and erosion coastal hazards. Although the flooding component of this act has been implemented, the erosion component has not.

4.5 Prediction of Beach and Dune Erosion Due to Severe Storms by Simple Model

For computational ease and economy, a much simpler erosion model was developed and is applied in the CCCL process (Appendix C). This model is not physically-based, yet retains the overall characteristic response described previously in the Kriebel model.

The model is based on the characteristic response exhibited in Figure IV.13 and Eq. (IV.12) rewritten for reference purposes as

$$\frac{R(t)}{R_{\infty}} = (1 - e^{-Kt}) \quad (IV.14)$$

At each time step, for the instantaneous value of the time-varying water level $S(t)$ and the selected breaking wave height, H_b , the equilibrium profile and the associated equilibrium recession, R_{∞} , from the existing profile is established, see Figure IV.21. The characteristics of the equilibrium profile are:

- (1) the eroded volume above the "hinge point" equals the deposited volume below the hinge point,

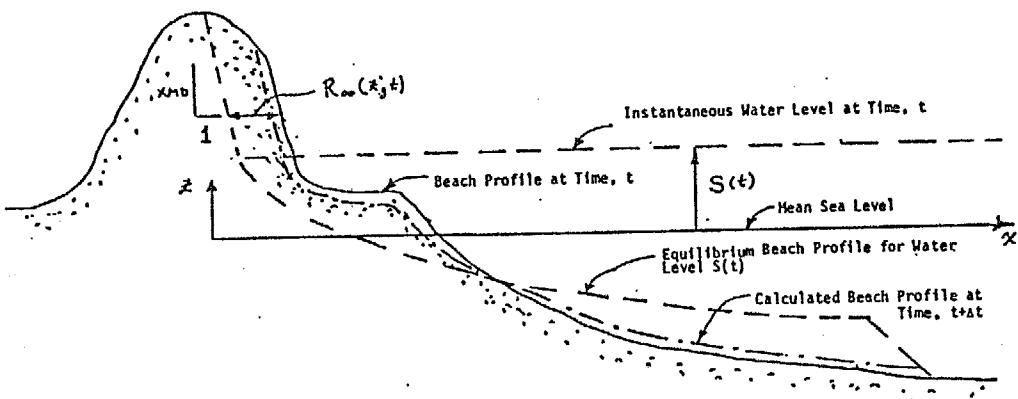


Figure IV.21 Features of simplified beach erosion model

- (2) The equilibrium profile is in accordance with Eq. (IV.1) with the scale parameter either specified by the user, or determined as a best-least squares fit to the measured profile during the field program, and
- (3) the equilibrium profile above the instantaneous water level is characterized by a uniform slope, X_{MD} , on the order of 2 or 3 as determined by post-storm profile measurements following Hurricane Eloise (1975) and other storms.

With the equilibrium profile established, the erosion occurring from time t to time $t+\Delta t$, Δx is given by

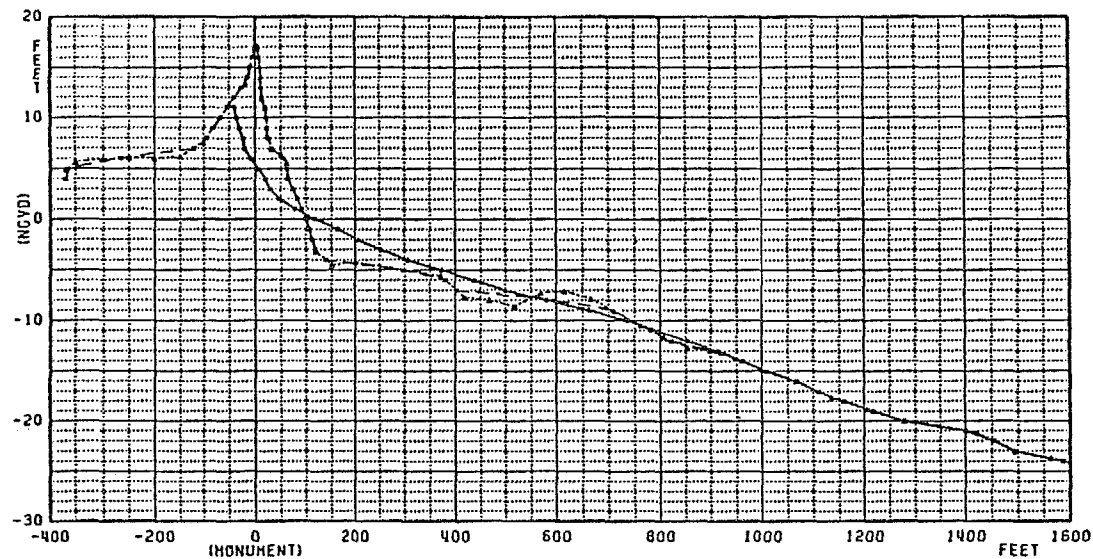
$$\Delta x = x(t+\Delta t) - x(t) = -R_{\infty}(1-e^{-K\Delta t}) \quad (IV.15)$$

where, through calibration with Kriebel's model, a K value of 0.075 sec^{-1} has been found.

Figures IV.22 and IV.23 present examples of application of the erosion model to two ranges in Martin County.

4.6 Augmentation of the Erosion Predicted by the Model for Recommending Position of CCCL

As noted previously, the erosion model accounts only for cross-shore sediment transport and has been verified against the average erosion occurring in Hurricane Eloise, see Figure IV.24. As documented by Chiu, there are a number of factors which result in considerable variability about the mean value. Probably the greatest causes of this variability are the gradients in longshore sediment transport as a result of the relatively small scale of the hurricane system, and natural variability due to inhomogeneities in the system (sand size, consolidation, offshore bay system, etc.). Regardless, the variability



OFFSHORE PROFILE

--- SURVEY
— INITIAL-SMOOTHED
— ERODED-FROM SHO.

COUNTY: MARTIN

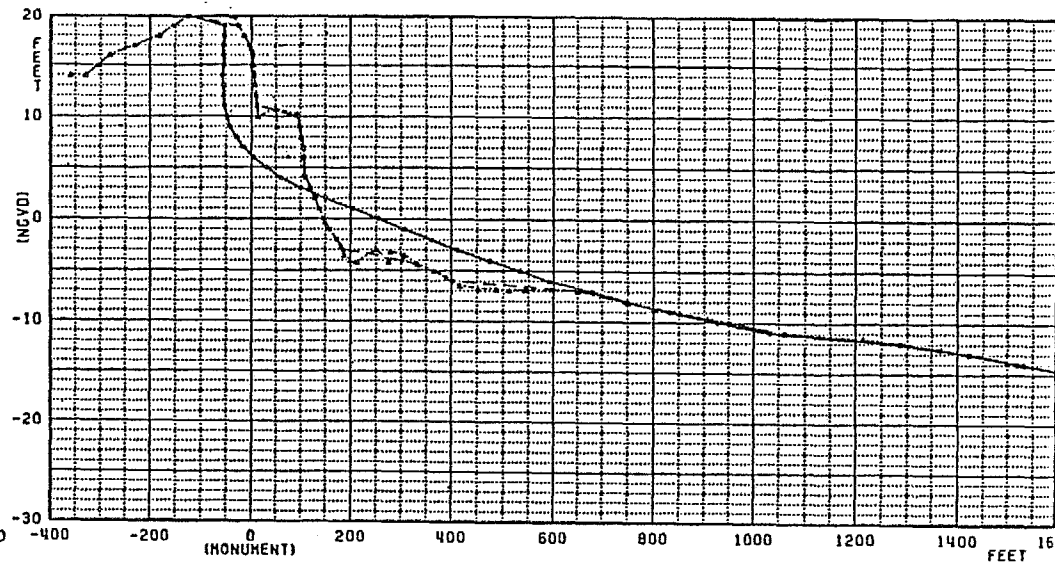
DIVISION OF BEACHES & SHORES
FLA. DEPT. OF NATURAL RESOURCES

RANGE: R-1

1/2

MONUMENT ESTABLISHED:
BEARING: DUE NORTH (MAG. 1)

Figure IV.22 Results of applying erosion model to Range R-1, Martin County (Hutchinson Island), 100 year storm tide, average erosion.



OFFSHORE PROFILE

--- SURVEY
— INITIAL-SMOOTHED
— ERODED-FROM SHO.

COUNTY: MARTIN

DIVISION OF BEACHES & SHORES
FLA. DEPT. OF NATURAL RESOURCES

RANGE: R-89

1/2

MONUMENT ESTABLISHED: R-90
BEARING: DUE NORTH (MAG. 1)

Figure IV.23 Results of applying erosion model to Range R-89, Martin County (Jupiter Island), 100 year storm tide, average erosion.

of erosion is recognized and as documented by Chiu (16) in Hurricane Eloise, the maximum erosion was approximately 2.5 times the average erosion. This factor is incorporated in the erosion considerations employed in the recommended CCCI position by modifying Eq. (IV.15) as follows

$$\Delta x = - (2.5) R_m (1 - e^{-K \Delta t}) \quad (IV.16)$$

which, due to the long beach response time compared to the time scale of storms, results in a profile which is in approximate accord with the 2.5 factor.

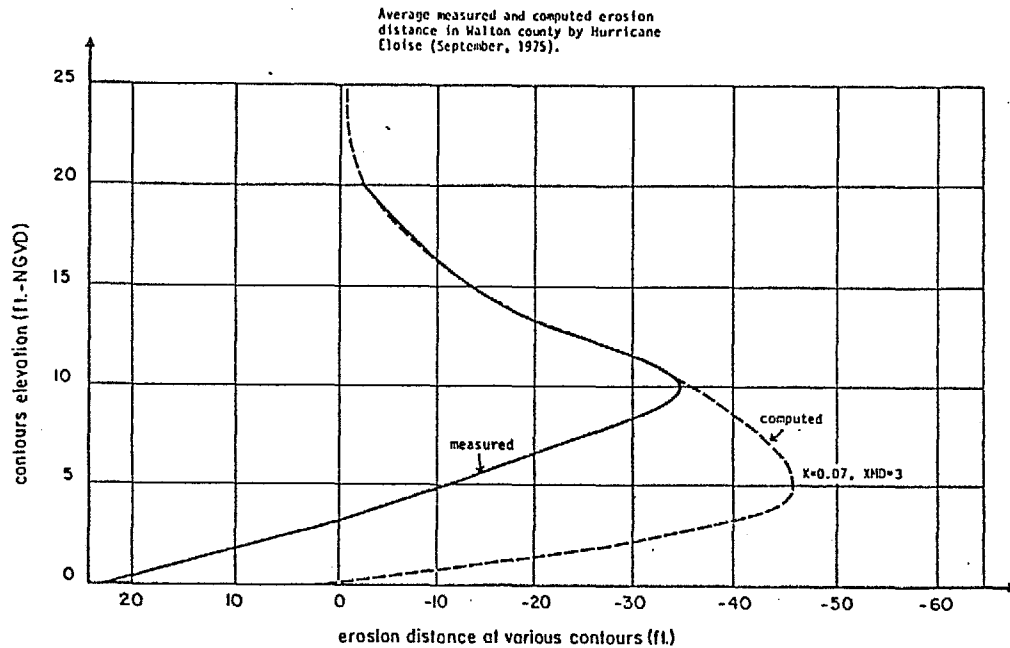


Figure IV. 24 Calibration of Simplified Erosion Model By Comparison with Erosion Occurring at Various Elevation Due to Hurricane Eloise

V WAVE HEIGHT DECAY CALCULATIONS

5.1 Introduction

If calculated erosion is not governing, the final recommended Coastal Construction Control Line position is based on the location where the significant wave height has attenuated to three feet. This three foot criterion is consistent with the Federal Emergency Management Administration (FEMA) criterion for delimiting the so-called "High Velocity Zone" and is considered to be the wave height (significant) at which structural damage is considered to be substantial. This is presumably in recognition of the rather large piling forces and uplift forces that waves of this magnitude can induce. (The wave force is proportional to H^n where $2 < n < 3$.) A potential storm related factor not presently included in the methodology that could cause significant damage is storm-tide induced current across barrier islands (the potential velocity due to a 2 ft tide difference across a submerged barrier island is on the order of 10 ft/sec.).

The following section describes the methodology for calculating wave height decay.

5.2 Methodology

As waves propagate, energy can be added to or removed from the wave system. The most common mechanism for energy addition is by wind blowing over the water surface. Principal mechanisms for energy loss (or dissipation or reflection) include wave breaking due to shoaling water, turbulent losses due to damping by vegetation and wave reflection by buildings. In the present application, energy input by winds is neglected due to the short distances considered, for example the wave height decay usually occurs over a maximum distance of 600-800 ft. The

National Academy of Sciences (NAS) (18) has developed recommended methodology for calculating wave decay due to the various mechanisms noted above. The method employed in the CCCL establishment is basically that recommended by the NAS report. Each of the decay mechanisms is described briefly below; the interested reader is referred to the 1977 NAS report for greater detail.

Wave Height Decay Due to Shoaling Water

The maximum wave height, H , which can be supported in a water depth, h , is

$$H = 0.78 h \quad (V.1)$$

a result developed by McCowan for shallow water waves.

Wave Height Decay Due to Vegetation

Consider waves propagating through a stand of vertical cylindrical elements of diameter, D , (representing for example tree trunks) at a uniform spacing, S . For a water depth, h , an initial wave height, H_I , and a propagation distance, Δx , the wave height, H_T , after propagation through the stand of elements is

$$H_T = \frac{H_I}{1 + AH_I \Delta x} \quad (V.2)$$

in which

$$A = \frac{C_D D}{3\pi S^2 h} \quad (V.3)$$

where C_D is the hydrodynamic drag coefficient (taken as 1.0 in this study) associated with flow about the elements. Equation (V.3) would be modified, for vegetative elements extending only partially over the depth.

Wave Height Decay Due to Buildings

Buildings serve to reduce the transmitted wave energy by blocking the waves and causing energy reflection. For an incident wave encountering buildings with a decimal blockage density, B (perpendicular to the direction of wave propagation), the incident and transmitted wave heights are related by

$$H_T = \sqrt{1 - B} H_I \quad (V.4)$$

If n rows of buildings, each with the same blockage density, are present, the corresponding result is

$$H_T = (1 - B)^{n/2} H_I$$

Combined Effects of Topography, Vegetation and Buildings

For an incident wave height, H_I , and both vegetation and buildings effects present, the transmitted wave height is

$$H_T = \frac{1}{1 + A H_I \Delta x} (1 - B)^{n/2} H_I \quad (V.5)$$

If the transmitted wave height as calculated by Eq. (V.5) is greater than the depth-limited value given by Eq. (V.1), the wave height is set equal to the depth-limited value.

VI LONG-TERM EROSIONAL CONSIDERATIONS

6.1 Introduction

Prior sections have described methodology for calculating the erosion associated with a single severe storm event. In addition to erosion due to relatively short-term events, the recommended location of the CCCL includes consideration of any long-term erosion trends.

6.2 Methodology

The methodology employed presently consists of accessing those studies which have focused on and identified long-term erosional trends. These studies usually incorporate comparison of early surveys (in chart form) and perhaps comparison of early and more recent aerial photography. Additionally, as counties are resurveyed as part of this study, these data are examined to determine long-term trends.

Studies of value may be directed toward a particular county or may be broad in scope, such as the National Shoreline Study (19) of the U.S. Army Corps of Engineers. Some of the early studies by the University of Florida, Coastal Engineering Laboratory quantified long-term erosion around the State, Figure VI.1.

With the long-term erosion rate established, the recommended location of the CCCL includes accounting for a 5 year duration of this erosion. That is, if the long-term erosion rate is 5 ft/year and the methodology described heretofore indicates that the CCCL should be located x feet from shore, then the recommended position is specified at $x + 25$ ft from shore.

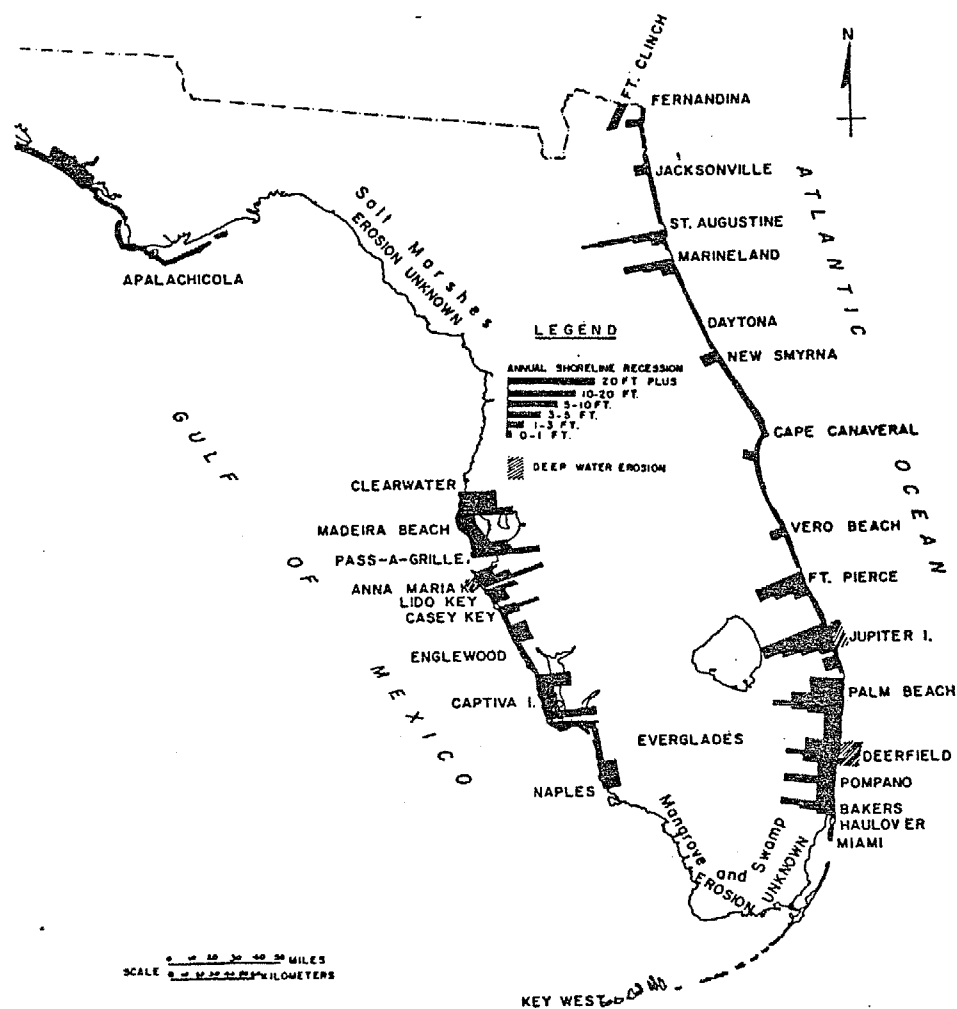


Figure VI.1 General erosion conditions in Florida (Bruun, Chiu, Gerritsen and Morgan, (20)).

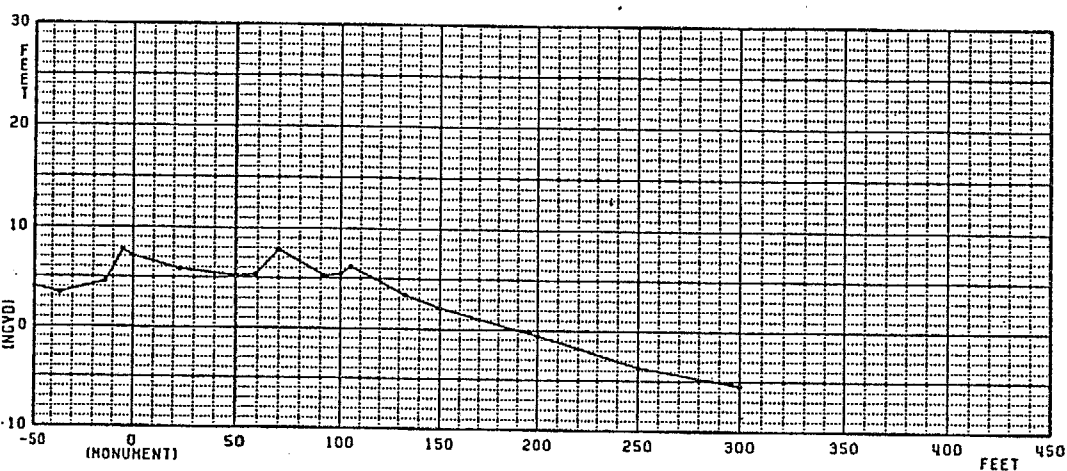
VII OVERALL VERIFICATIONS OF CCCL METHODOLOGY

As might be expected, due to the relative rarity of storms of the 100 year severity level and of the difficulty in conducting meaningful measurement/observations before and after such a storm, there is only limited direct data available to evaluate the CCCL methodology. Two examples which provide varying degrees of evaluation/confirmation are presented below.

7.1 Hurricane Agnes, St. George Island, Franklin County

This example is of interest, in part, because the extent of storm impact was discovered after the recommended position of the CCCL had been established.

Slightly to the west of the center of St. George Island (Range 105-106), the recommended position of the CCCL was some 500 ft landward of the mean sea level contour. The position of the line was challenged by a developer who, by counsel, requested a delay from the Governor and Cabinet to develop proof that the recommended line was too far landward; the delay was granted. After the delay was granted, DNR located aerial photographs flown on June 21, 1972, the day after the passage of Hurricane Agnes, which documented the almost completed destruction of the only road along this portion of St. George Island and landward of Monuments 104 and 105. The roadway is located some 100 ft landward of the recommended position of the CCCL, see Figures VII.1(a) and (b) and photographs on display as a part of this workshop. It is noted that the storm tide accompanying Hurricane Agnes in Franklin County is believed to be on the order of a 40 year event with the erosion event on the same order.



NOTE: THIS DNR SURVEY HAS BEEN EXTENDED UPLAND OF THE MONUMENT BY DOT PHOTOGRAMMETRIC CONTOURS

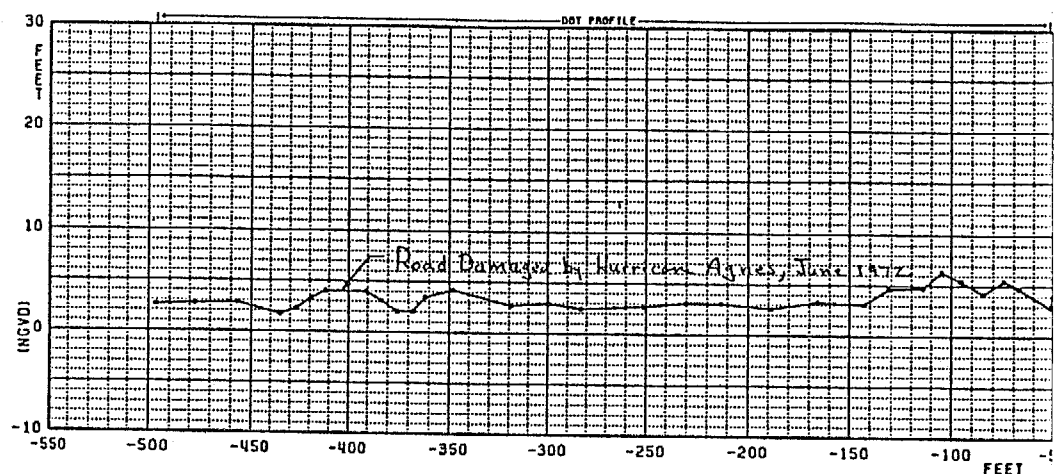
BEACH PROFILE

02 JUL 81

COUNTY: FRANKLIN
DIVISION OF BEACHES & SHORES
FLA. DEPT. OF NATURAL RESOURCES

RANGE: R-105 2/4
MONUMENT ESTABLISHED: MAY 1973
BEARING: S 20°00' E (MAG.)

Figure VII.1(a) Beach profile at Range R-105 on St. George Island. A location of severe overwash and damaged roadway due to Hurricane Agnes, 1972 (see Figure VII.1(b) for extension of this profile).



NOTE: THIS DNR SURVEY HAS BEEN EXTENDED UPLAND OF THE MONUMENT BY DOT PHOTOGRAMMETRIC CONTOURS

BEACH PROFILE

02 JUL 81

COUNTY: FRANKLIN
DIVISION OF BEACHES & SHORES
FLA. DEPT. OF NATURAL RESOURCES

RANGE: R-105 1/4
MONUMENT ESTABLISHED: MAY 1973
BEARING: S 20°00' E (MAG.)

Figure VII.1(b) Continuation of profile across St. George Island, Range R-105, showing location of damaged road, due to Hurricane Agnes, 1972.

Stressing again that the evidence of storm impact cited in this example was located after the CCCL location had been recommended, we interpret the line location in this area to be somewhat too far Gulfward in the vicinity of Monuments 104 and 105.

7.2 Hurricane Eloise Damage in Walton and Bay Counties

The set-back line was established in Walton and Bay Counties in April, 1975, and August, 1974, respectively. Hurricane Eloise made landfall in Walton County on September 23, 1975, as shown in Figure VII.2. The hurricane storm tide is ranked as a 75-100 year occurrence and, due to the relatively high translational speed of the hurricane, the erosion is ranked only as a 20-50 year event.

Two types of information will be presented by way of comparison of the measured zone of impact versus location of the (then) set-back line. Figures VII.3 and VII.4 compare the eroded zone with the location of the set-back lines in Bay and Walton Counties, respectively. The location of the pre-hurricane vegetation line is also shown. It is clear that the limits of erosion correlate reasonably well with the location of the set-back line.

The second type of information available from Hurricane Eloise relates to the per structure damage costs relative to the location of that structure with respect to the set-back line. Of course the quality of construction is very important in terms of the damage that an individual structure will experience.

Based on a survey of 540 structures, Figure VII.5 presents the per structure damage costs as a function of the structure position relative to the set-back line. Of general relevance is the quite steeply rising damage costs as a function of proximity to the shoreline. Of specific

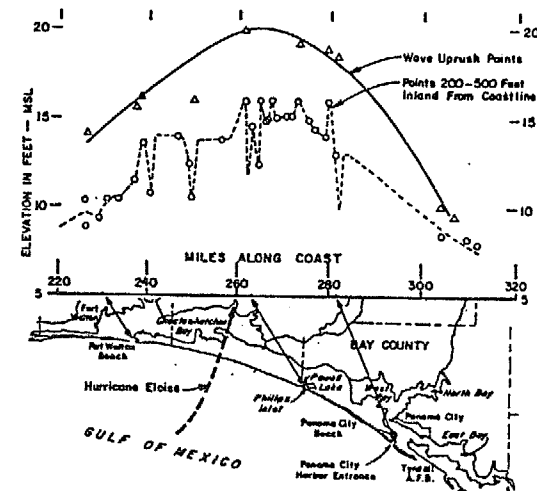


figure VII.2 Landfall location of Hurricane Eloise, September 23, 1975 and some resulting tide and uprush characteristics (from Chiu, (16)).

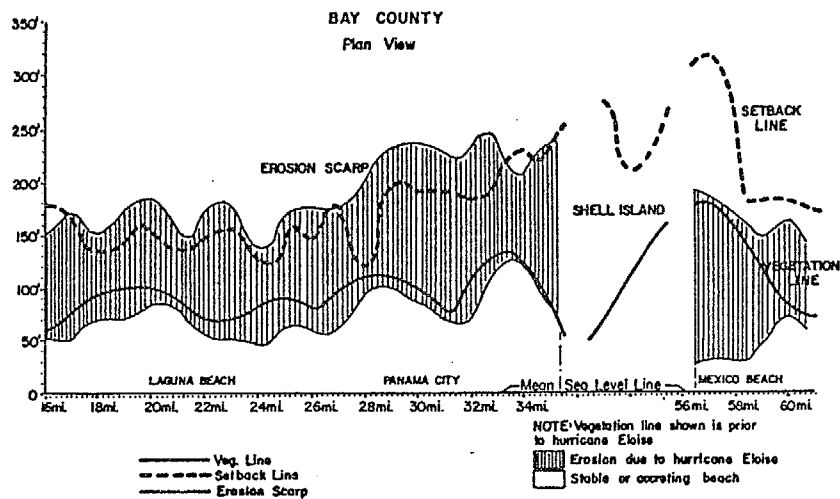


Figure VII.3 Relation of erosional characteristics and pre-Eloise vegetation line to set-back line, Bay County, Florida (from Chiu, (16)).

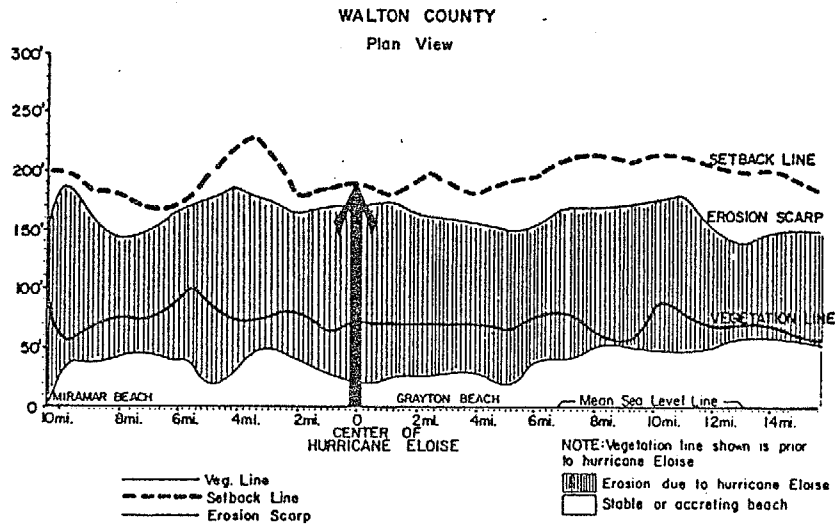


Figure VII.4 Relation of erosional characteristics and pre-Eloise vegetation line to set-back line, Walton County, Florida (from Chiu, (16)).

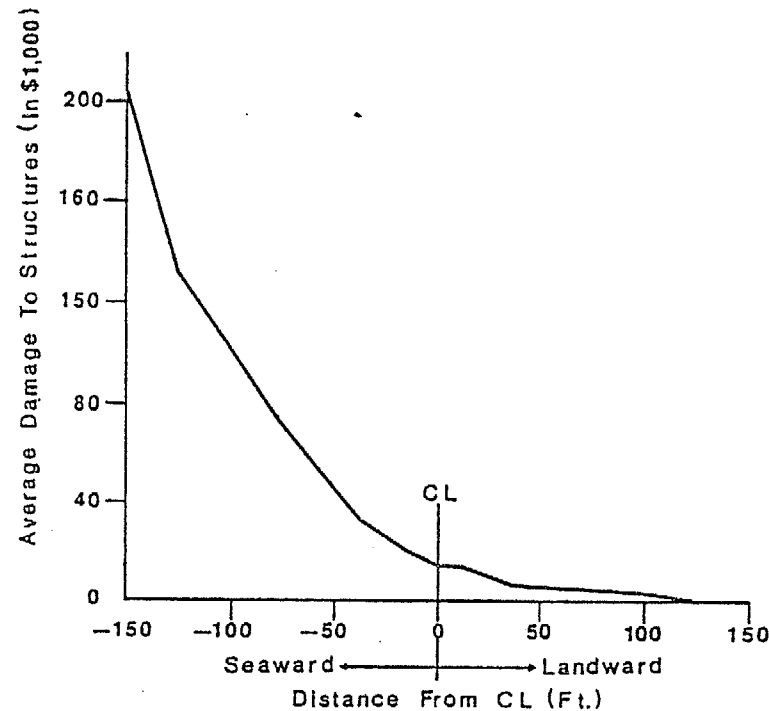


Figure VII.5 Damage to structures in relation to location of set-back control line (based on study of 540 structures in Bay County after Hurricane Eloise, by Shows, (21)).

interest is that average damage costs for a structure situated on the set-back line were approximately \$8,000, whereas the average damage costs for a structure located 150 ft seaward of the set-back line was in excess of \$200,000.

REFERENCES

1. National Oceanic and Atmospheric Administration, "Flood Insurance Study - Sarasota County, Florida," October 1971.
2. U.S. Department of Commerce, National Oceanic and Atmospheric Administration, "Meteorological Criteria for Standard Project Hurricane and Probable Maximum Hurricane Windfields, Gulf and East Coasts of the United States," NOAA Technical Report NWS 23, September 1979.
3. Van Dorn, W., "Wind Stress on an Artificial Pond," Journal of Marine Research, Vol. 12, No. 3, 1953.
4. Christensen, B.A. and Walton, R., "Friction Factors in Flooding Due to Hurricanes," Proceedings, National Symposium on Urban Stormwater Management in Coastal Areas, Blackburg, Virginia, June 19-20, 1980.
5. Saville, T., "Experimental Determination of Wave Set-Up," Proceedings, Second Technical Conference on Hurricanes, 1961, pp. 242-252.
6. Bowen, A.J., Inman, D.L. and Simmons, V.P., "Wave 'Set-Down and Set-Up'," Journal of Geophysical Research, Vol. 73, No. 8, 1968, pp. 2569-2577.
7. Lo, J.M., "Surf Beat: Numerical and Theoretical Analysis," Ph.D. Dissertation, Department of Civil Engineering, University of Delaware, June 1981.
8. U.S. Army Corps of Engineers, "Shore Protection Manual, Volumes I, II and III," U.S. Government Printing Office, 1977.
9. Freeman, J.C., Jr., Baer, L. and Jung, G.H. "The Bathystrophic Storm Tide," Journal of Marine Research, Vol. 16, No. 1, 1957.
10. Hayden, B., et al., "Systemic Variation in Inshore Bathymetry" Tech. Report No. 10, Department of Environmental Science, University of Virginia, 1975.
11. Dean, R.G., "Equilibrium Beach Profiles: U.S. Atlantic and Gulf Coasts," Ocean Engineering Report No. 12, Department of Civil Engineering, University of Delaware, January 1977.
12. Moore, B., "Beach Profile Evolution in Response to Changes in Water Level and Wave Height," M.S. Thesis, University of Delaware, 1982.
13. Saville, T., "Scale Effects in Two-Dimensional Beach Studies," Trans. 7th Meeting of Intl. Assoc. of Hydraulic Research, Lisbon, 1957.
14. Kriebel, D.L., "Beach and Dune Response to Hurricanes," M.S. Thesis, University of Delaware, 1982.
15. Kriebel, D.L., "Beach Erosion Model (EBEACH) Users Manual," Volumes I and II, Division of Beaches and Shores, Florida Department of Natural Resources, 1984.

16. Chiu, T.Y., "Beach and Dune Response to Hurricane Eloise of September 1975," Coastal Sediments '77, ASCE, 1977.
17. Wilson, B.L., "Hurricane Wave Statistics for the Gulf of Mexico," U.S. Army Corps of Engineers, Beach Erosion Board, Technical Memorandum 98, 1956.
18. National Academy Sciences, "Methodology for Calculating Wave Action Effects Associated with Storm Surges," Washington, D.C., 1977.
19. U.S. Army Corps of Engineers, "National Shoreline Study - Regional Inventory Report," South Atlantic Division, Atlanta, Georgia, August 1971.
20. Bruun, P., Chiu, T.Y., Gerritsen, F., and Morgan, W.H., "Storm Tide Study in Florida as Related to Coastal Topography," Bulletin Series No. 109, Florida Engineering and Industrial Experiment Station, University of Florida, 1962.
21. Shows, E.W., "Florida's Coastal Setback Line - An Effort to Regulate Beach Front Development," Coastal Zone Management Journal, Vol. 4, Numbers 1/2, pp. 151-164, Crane, Russak and Company, Inc., 1978.

APPENDIX A
2-D STORM TIDE MODEL*

*This program represents a numerical modeling procedure that is subject to change due to: 1. newly encountered topo-bathymetric and hydraulic boundary conditions, and 2. incorporation of new advancements quantifying coastal processes. This program is applied on a county-by-county basis and is subject to acceptable calibration constraints recommended by the Beaches and Shores Resource Center and approved by the Florida Department of Natural Resources.

PROGRAM: 2-D STORM TIDE

NOTE

DEFINITION OF PARAMETERS:

CASE	20 CHARACTER TITLE TO IDENTIFY A SPECIFIC OUTPUT
DX	HORIZONTAL GRID DISTANCE, IN NAUTICAL MILES
DY	VERTICAL GRID DISTANCE, IN NAUTICAL MILES
DT	TIME INCREMENT FOR EACH TIME STEP, IN HOURS
PINF	REFERENCE PRESSURE(ATMOSPHERIC) USED TO CALCULATE BAROMETRIC TIDES
BF	BOTTOM FRICTION COEFFICIENT(0.02 - 0.002)
RMAX	RADIUS FROM CENTER OF HURRICANE TO THE POSITION OF MAX. WINDS
YS	INITIAL Y-COORD. OF THE HURRICANE CENTER, IN NAUTICAL MILES
DP	HURRICANE CENTRAL PRESSURE INDEX, IN INCHES OF MURCURY
VF	FORWARD VELOCITY OF THE HURRICANE SYSTEM IN KNOTS
NIT	0
WSC	WIND SHEAR STRESS COEFFICIENT
INTERV	≠ TIME STEP INTERVALS AT WHICH TO PRINT OUT AN OUTPUT FOR THE GRID SYSTEM
THETA	LANDFALL HURRICANE TRACK W.R.T. NORTH AND CLOCKWISE IN DEGREES
XHB	INITIAL DIST OF THE HURRICANE, IN NAUTICAL MILES (MAY BE OUTSIDE THE GRID SYSTEM, W.R.T. ORIGIN)
XHE	FINAL DIST OF THE HURRICANE, IN NAUTICAL MILES (MAY BE OUTSIDE THE GRID SYSTEM, W.R.T ORIGIN)
TIDE	ASTRONOMICAL TIDAL ADJUSTMENT IN FEET, POSITIVE ABOVE MSL
XCB	THE X-COORD DIST OF THE LEFT-EDGE OF THE GRID SYSTEM, IN NAUTICAL MILES
XCF	THE X-COORD DIST OF THE RIGHT-EDGE OF THE GRID SYSTEM, IN NAUTICAL MILES
YCB	THE Y-COORD DIST OF THE TOP-EDGE OF THE GRID SYSTEM, IN NAUTICAL MILES
YCF	THE Y-COORD DIST OF THE BOTTOM-EDGE OF THE GRID SYSTEM, IN NAUTICAL MILES
THAX	THE MAX DURATION OF THE PROTOTYPE HURRICANE MODEL SYSTEM, IN HOURS
TMIN	THE TIME AGTER WHICH OUTPUTS ARE GENERATED
NDELT	0

```
C      B4          CORIOLIS PARAMETER (0 OR 0.0000727)
C      NOCVT       SET TO 1, THEN DT,DX,DY IS READ IN SECONDS &
C                  FEET, NO CONVERSION TAKES PLACE
C
CCCCCCCCCCCCCCCCCCCCCCCCCCCCCCCCCCCCCCCCCCCCCCCCCCCCCCCCCCCC
COMMON /A/ UUX(110,110),UUY(110,110),P(110,110),H(110,110),
- DPDX(110,110),DPDY(110,110),DX
COMMON /B/ ETA(110,110),QX(110,110),QY(110,110),NQBX(110),TIDE,
- DY,NXX,IEND
COMMON /C/ IS,J
COMMON /E/ PINF,DT,NNY
COMMON /F/ JJ
COMMON /G/ CVAR(600,3,39),CTIME(600),CASE,IPLOT(78),IC2,
- INTERV,NPLOT
COMMON /H/ IFFACT(110,110)
COMMON /BAR/ NORBAR(50),IBAR(50),JBAR(50),XLBAR(50),HBAR(50),
- WBAR(50),FBAR(50),XKEX(50),NDRINL(50),IINL(50),JINL(50),WINL(50),
- DPINL(50),XKENEX(50),FINL(50),XLINL(50)

DIMENSION Y(110),NQBX(110),ETAT(110),U(110,110),YNM(110),XNM(110)
DIMENSION ETMX(110,110),ISETUP(110)
DIMENSION DXA(110),DYA(110)
DIMENSION D(110,110),DETA(110,110),X(110),UX(110,110),
- UY(110,110),UXR(110,110),
- UYR(110,110),JNET(110),NET(110,110),
- NQX(110,110),NQY(110,110),IB(110)
DIMENSION ETAMAX(39,3)
DIMENSION QS(110,110),ETAS(110,110)
DIMENSION QC(110),ETAC(110)
DIMENSION AC(110),BC(110),CC(110),DC(110)
DIMENSION ACS(110),BCS(110),CCS(110),DCS(110)
DIMENSION ETAS0(110),ETAS1(110),ETAS2(110)
DIMENSION VTIME(15),VDP(15),VVF(15),VRMAX(15),VTHETA(15)
DIMENSION FCTX(110,110),FACTY(110,110),WVXX(110,110),WVYY(110,110)
DIMENSION WSF(110,110)
CHARACTER*20 CASE,SYSTEM
CHARACTER*1 DRY,WET,AREA(110),PER(110,110)
DATA IFLAGZ /1/
DATA DRY,WET /'+','-'/

12000 FORMAT(/)

10 KOUNT=-1
IC2=0
G=32.2
RHOA=0.0024
RHOW=1.99
NFIN=-1
B4=2.33E-08
IICOUN=0

C
***** INPUT GRID SYSTEM DATA (DIMENSIONS, *****
***** CONSTANTS,BATHYMETRY,FRICTION FACTORS) *****
C
READ(5,20) SYSTEM
```



```

      WRITE(6,25) SYSTEM
20  FORMAT(A20)
25  FORMAT(1H1,/,1H ,A20)
      READ(5,30)XCB,XCF,YCB,YCF,DT,PINF,TIDE,B6,INTERV,THETAC
30  FORMAT(7F8.1,E11.4,I3,/,F8.1)
      READ(5,40) NNX,NNY
40  FORMAT(2I3)
      READ(5,50) (DXA(I),I=1,NNX)
      READ(5,50) (DYA(J),J=1,NNY)
50  FORMAT(8F8.0)
      WRITE(6,60)XCB,YCB,PINF,TIDE,DT,XCF,YCF,B6,INTERV,THETAC
60  FORMAT(1H0,'GRID SYSTEM PARAMETERS',/,1H , ' XCB= ',F9.2,
-      ' YCB= ',F9.2, ' PINF= ',F8.2, ' TIDE= ',F8.2, ' DT= ',F10.2,
-      ',1H , ' XCF= ',F9.2, ' YCF= ',F9.2, ' B6= ',E10.4,
-      ' INTERV= ',I6, ' THETAC= ',F6.2)
      WRITE(6,70)NNX,NNY
70  FORMAT(1H0, ' NNX= ',I9, ' NNY= ',I9)
      WRITE(6,80) (DXA(I),I=1,NNX)
      WRITE(6,80) (DYA(J),J=1,NNY)
80  FORMAT(1H0,10F10.0)

      READ(5,90) NBAR,NINL
      WRITE(6,95) NBAR,NINL
90  FORMAT(2I3)
95  FORMAT(1H0,2I3)
      IF (NBAR.EQ.0) GO TO 130
      DO 110 N=1,NBAR
      READ(5,100) NORBAR(N),IBAR(N),JBAR(N),XLBAR(N),HBAR(N),
-      WBAR(N),FBAR(N),XKEX(N)
C      **** ADJUST HEIGHT OF BARRIER TO MEAN SEA LEVEL ****
      HBAR(N)=HBAR(N)+0.8
      WRITE(6,105) NORBAR(N),IBAR(N),JBAR(N),XLBAR(N),HBAR(N),
-      WBAR(N),FBAR(N),XKEX(N)
100  FORMAT(3I3,5F10.3)
105  FORMAT(1H0,3I3,5F10.3)
110  CONTINUE

      IF (NINL.EQ.0) GO TO 130
      DO 120 N=1,NINL
      READ(5,100) NORINL(N),IINL(N),JINL(N),XLINL(N),DPINL(N),
-      WINL(N),FINL(N),XKENEX(N)
      DPINL(N)=DPINL(N)+0.8
C      **** ADJUST DEPTH OF INLET TO MEAN SEA LEVEL ****
      WRITE(6,115) NORINL(N),IINL(N),JINL(N),XLINL(N),DPINL(N),
-      WINL(N),FINL(N),XKENEX(N)
115  FORMAT(1H0,3I3,5F10.3)
120  CONTINUE
130  CONTINUE

C      **** READ IN BATHYMETRY. ELEVATIONS=-H, DEPTHS(WATER)=+H.****
      DO 170 J=1,NNY
      IF(IFLAGZ.EQ.1) READ(5,150)(H(I,J),I=1,NNX)
C      WRITE(6,150)(H(I,J),I=1,NNX)
150  FORMAT(10F7.2)
      H(I,J)=-99.
C      ***** ADJUST BATHYMETRY TO MEAN SEA LEVEL *****

```

```

      DO 160 I=2,NNX
160  H(I,J)=H(I,J)+0.8
170  CONTINUE

C      WRITE(6,180)(I,I=1,25)
180  FORMAT(1H1,'ASSIGNMENT OF FRICTION FACTORS FOR EACH GRID',
-      '/1H0,'I(TOWARDS OCEAN)-)',/1H , 'J(NORTH)'/1H ,
-      '-1'/1H , 'V'/1H ,5X,25I5/)
      DO 210 J=1,NNY
      IF(IFLAGZ.EQ.1) READ(5,190)(IFFACT(I,J),I=1,NNX)
190  FORMAT(10I5)
C      WRITE(6,200) J,(IFFACT(I,J),I=1,NNX)
200  FORMAT(1H ,I2,3X,25I5,/1H ,5X,25I5)
210  CONTINUE

C      C***** INITIALIZE/CONVERT GRID SYSTEM DATA *****
C
      CNM=6076.1
      CHS=3600.0
      XCB=XCB*CNM
      XCF=XCF*CNM
      YCB=YCB*CNM
      YCF=YCF*CNM
      PINF=70.51*PINF
      NNXM1=NNX-1
      NNXF1=NNX+1
      NNYM1=NNY-1
      NNYP1=NNY+1
      IEND=NNX
      IENDM1=IEND-1
      DO 12 J=1,NNY
12  ISETUP(J)=40
      ISETUP(48)=54
      ISETUP(54)=52
      ISETUP(60)=52

      X(1)=XCB
      Y(1)=YCB
      XNM(1)=XCB/CNM
      YNM(1)=YCB/CNM
      DO 220 I=2,NNXP1
      X(I)=X(I-1)+(DXA(I)+DXA(I-1))/2.0
220  XNM(I)=X(I)/CNM
      DO 230 J=2,NNY
      Y(J)=Y(J-1)+(DYA(J)+DYA(J-1))/2.0
230  YNM(J)=Y(J)/CNM
      WRITE(6,240) (J,J=1,10)
240  FORMAT(1H1,/,1H , ' X AND Y DISTANCES (N.MI.)',/,1H0,/1H ,10I10)
      WRITE(6,250) (XNM(J),J=1,NNX)
      WRITE(6,12000)
      WRITE(6,250) (YNM(J),J=1,NNY)
250  FORMAT(1H ,10F10.2)
      WRITE(6,260)
260  FORMAT(1H )

270  DO 300 ISO=1,NNX

```

```

      IF(H(ISO,J).GE.0.0) GO TO 290
      AREA(ISO)=DRY
      PER(ISO,J)=DRY
      GO TO 300
290  AREA(ISO)=WET
      PER(ISO,J)=WET
300  CONTINUE

      DO 310 I=1,NNX
      DO 310 J=1,NNY
      ETA(I,J)=0.0001
      QX(I,J)=0.0001
      QY(I,J)=0.0001
      NET(I,J)=0
      WSF(I,J)=1.0
310  CONTINUE
      DO 315 I=8,35
315  WSF(I,29)=0.0
      DO 316 I=26,30
316  WSF(I,9)=0.0
      DO 317 I=24,26
317  WSF(I,10)=0.0
      DO 320 I=1,NNX
      DO 320 J=1,NNY
      UUX(I,J)=0.001
      UUY(I,J)=0.001
      P(I,J)=0.0001
320  CONTINUE
C
C ***** INPUT HURRICANE PARAMETERS *****
C
325  READ(4,330,END=11130)CASE
330  FORMAT(A20)
      READ(4,340)XHB,YHB,TMIN,TMAX,NPARN
340  FORMAT(4F8.1,I3)
      WRITE(6,345)CASE
345  FORMAT(1H1,/,1H ,A20)
      WRITE(6,350)XHB,YHB,TMIN,TMAX,NPARN
350  FORMAT(1H0,' HURRICANE PARAMETERS ',/,1H0,' XHB= ',F8.1,' YHB= ',
-      F8.1,' TMIN= ',F8.1,' TMAX= ',F8.1,' NPARN= ',I3)
      WRITE(6,360)
360  FORMAT(1H-,20X,'VARIABLE PARAMETERS:',/,1H ,21X,'TIME',8X,'DP',7X,
-      'VF',6X,'RMAX',6X,'THETA',/)
      DO 390 I=1,NPARN
      READ(4,370) VTIME(I),VVF(I),VRMAX(I),VDP(I),VTHETA(I)
370  FORMAT(5F7.2)
      WRITE(6,380) I,VTIME(I),VDP(I),VVF(I),VRMAX(I),VTHETA(I)
380  FORMAT(1H ,13X,I2,5X,F5.2,5X,F4.1,6X,F4.1,6X,F5.1)
      VTIME(I)=VTIME(I)*CHS
      VDP(I)=VDP(I)*70.51
      VVF(I)=VVF(I)*1.69
      VRMAX(I)=VRMAX(I)*CNM
      VTHETA(I)=(VTHETA(I)+90.0-THETAC)/57.2956
390  CONTINUE
      RMAX=VRMAX(1)
      DP=VDP(1)

```

```

      VF=VVF(1)
      THETA=VTHETA(1)
      CTH=COS((THETAC-90.0)/57.2956)
      STH=SIN((THETAC-90.0)/57.2956)
      XHB1=XHB*CTH + YHB*STH
      YHB1=-XHB*STH + YHB*CTH
      XHB=XHB1
      YHB=YHB1
      XHB=XHB*CNM
      YHB=YHB*CNM
C
      THETAC=THETAC/57.2956
      TMAX=TMAX*CHS
      TMIN=TMIN*CHS
      KOUNT=-1
      IC2=0
      IICOUN=0

      READ(4,391) (IPLOT(J),J=1,24)
      IF (IPLOT(24).NE.0) READ(4,391) (IPLOT(J),J=24,48)
391  FORMAT(12(I3,1X,I2))

      NPLOT=0
      DO 392 JPLOT=1,48,2
      IF(IPLOT(JPLOT).EQ.0.OR.IPLOT(JPLOT+1).EQ.0) GO TO 394
      IJ=(JPLOT+1)/2
      J1=IPLOT(JPLOT)
      J2=IPLOT(JPLOT+1)
      ISETUP(J2)=J1
      NPLOT=NPLOT+1
      DO 392 JJJJ=1,3
      ETAMAX(IJ,JJJJ)=0.0
392  CONTINUE
394  CONTINUE
      NPLOT2=NPLOT*2
      WRITE(6,396) (IPLOT(J),J=1,NPLOT2)
396  FORMAT(1H0,'GRIDS FOR PLOTTING: ',/,1H0,
-      15(' ',I2,',',I2,''))
C
C *****
C
      NTIMES=IFIX((TMAX-TMIN)/DT) + 1
      WRITE(6,398)NTIMES
398  FORMAT(1H0,'NTIMES (MAIN LOOP VALUE) = ',I4)
C
C      IB(J) = I DENOTES I INDEX OF FIRST SUBMERGED GRID OF JTH ROW
C      STARTING SECTION TO DETERMINE ACTIVE ETA ELEMENTS
C      NET(I,J)=0 IF DRY AND =1 IF FLOODED.
C
      DO 420 J=1,NNY
      DO 420 I=1,NNX
      IF(ETA(I,J)+H(I,J)) 400,400,410
400  NET(I,J)=0
      ETA(I,J)=-H(I,J)-0.0001
      IB(J)=I+1
      GO TO 420
410  NET(I,J)=1

```

```

420 CONTINUE

C
C   ESTABLISH REFERENCE HURRICANE VALUES FOR WAVE SETUP
C   CALCULATIONS
C
  IS=0
  CALL HURCH(USQ,IS,J,X,Y,VF,PINF,DP,RMAX,THETA,DT,DY,
    RHOW,XHB,YHB)
  USQM=USQ
  UMAX=SQRT(USQ)/1.69
  AA=-RMAX*DP*B4
  AA2=0.160*VF/SQRT(UMAX)
  HMAX=16.5*EXP(AA)*(1.0+AA2)
  TMAX=8.6*EXP(AA/2.0)*(1.0+AA2/2.0)
  IPARM=2
  WRITE(6,430)
430 FORMAT('H0, ' I      THR      ETA NET      QX      QY  D(53,60)',//)
C
C ***** MAIN LOOP *****
C
  DO 10500 JJ=1,NTIMES
    XJ=JJ-1
    T=XJ*DT+TMIN
    THR=T/3600.
    TS=T
    IF (NPARM.EQ.0.OR.IPARM.GT.NPARM) GO TO 2020
    IF (T.LE.VTIME(IPARM)) GO TO 2010
    IF (IPARM.EQ.1) GO TO 2000
    XHB=XHB+(VTIME(IPARM)-VTIME(IPARM-1))*VVF(IPARM-1)
    - *COS(VTHETA(IPARM-1))
    YHB=YHB+(VTIME(IPARM)-VTIME(IPARM-1))*VVF(IPARM-1)
    - *SIN(VTHETA(IPARM-1))
2000 IPARM=IPARM+1
2010 IF (IPARM.GT.NPARM) GO TO 2020
    DPCT=(T-VTIME(IPARM-1))/(VTIME(IPARM)-VTIME(IPARM-1))
    DP=VDP(IPARM-1)+DPCT*(VDP(IPARM)-VDP(IPARM-1))
    RMAX=VRMAX(IPARM-1)+DPCT*(VRMAX(IPARM)-VRMAX(IPARM-1))
    VF=VVF(IPARM-1)
    THETA=VTHETA(IPARM-1)
    TS=T-VTIME(IPARM-1)
2020 CONTINUE
    XH=XHB+TS*VF*COS(THETA)
    YH=YHB+TS*VF*SIN(THETA)
    XHN=XH/CNM
    YHN=YH/CNM
    IF (T.GT.TMAX) GO TO 11000
    DO 2025 J=1,NNY
    DO 2025 I=1,NNX
      QS(I,J)=QX(I,J)
2025 ETAS(I,J)=ETA(I,J)
C
C   ESTABLISH ACTIVE (DISCHARGE) JUNCTIONS
C   USE BOUNDARY CONDITION OF NO FLOW ACROSS A BOUNDARY
C   NQBX(J) IS THE POSITION OF THE NO FLOW COASTLINE ON THE J'TH COLUM
C

```

```

DO 2100 J=1,NNYM1
  DY=DYA(J)
DO 2090 I=1,NNXM1
  DX=DXA(I)
  IF (JJ.NE.1.OR.NET(I,J).NE.1) GO TO 2030
  CALL HURCH(USQ,I,J,X,Y,VF,PINF,DP,RMAX,THETA,DT,DY,
    RHOW,XH,YH)
  ETA(I,J)=0.015625*(PINF-P(I,J))
2030 IF (NET(I,J)*NET(I+1,J)) 2040,2040,2050
2040 NQX(I+1,J)=0.0
  QX(I+1,J)=0.001
  NQBX(J)=I+1
  GO TO 2060
2050 NQX(I,J)=1
2060 IF (NET(I,J)*NET(I,J+1)) 2070,2070,2080
2070 NQY(I,J+1)=0
  QY(I,J+1)=0.001
  GO TO 2090
2080 NQY(I,J+1)=1
2090 CONTINUE
2100 CONTINUE

  CALL ETABCS (XH,YH,T,X,Y,VF,DP,RMAX,THETA,RHOW)
  DO 2110 J=1,NNY
  DO 2110 I=1,NNX
2110 D(I,J)=ETA(I,J)+H(I,J)
C
C   THIS PORTION OF PROGRAM FOR SWEEPS IN THE X-DIRECTION
C
  IMPDIR=1
  DO 3090 J=2,NNYM1
    DY=DYA(J)
    DO 3030 I=2,NNX
      DX=0.5*(DXA(I-1)+DXA(I))
      DX2=DXA(I)
      FACTX=1.0
      CALL HURCH(USQ,I,J,X,Y,VF,PINF,DP,RMAX,THETA,DT,DY,
        RHOW,XH,YH)
      CALL CALLFR(I,J,BF)
      WX=0.5
      CALL INLT(I,J,BF,DT,FACTX,FACTY,WX,WY,IICOUN,NBAR,NINL,IMPDIR)
      FCTX(I,J)=FACTX
      FCTY(I,J)=FACTY
      WXX(I,J)=WX
      WYY(I,J)=WY
      IF (NET(I-1,J)*NET(I,J).NE.0.0.AND.WX.LT.400.0) GO TO 3000
      AC(I)=0.0
      BC(I)=0.0
      CC(I)=0.0
      DC(I)=0.0
      GO TO 3010
3000 DBAR=0.5*(D(I-1,J)+D(I,J))
      IF (ABS(DBAR).LT.0.001) DBAR=0.001
      AC(I)=G*DBAR*DT/DX*FACTX
      QYBAR=0.25*(QY(I-1,J)+QY(I,J)+QY(I-1,J+1)+QY(I,J+1))

```

```

      QQ=SQRT(QX(I,J)**2+QYBAR**2)
      BC(I)=1.0+BF*QQ*DT/(8.0*DBAR**2)
      IF (WX.GT.0.5) BC(I)=WX
      CC(I)=-AC(I)
      DC(I)=QX(I,J)+(-DBAR*DPDX(I,J)/RHOW+UUX(I,J)/RHOW-B6*QYBAR)*DT
3010 IF (NET(I,J).NE.0) GO TO 3020
      ACS(I)=0.0
      BCS(I)=0.0
      CCS(I)=0.0
      DCS(I)=0.0
      GO TO 3030
3020 ACS(I)=DT/(4.0*DX2)
      BCS(I)=1.0
      CCS(I)=-ACS(I)
      DCS(I)=ETA(I,J)-ACS(I)*(QX(I+1,J)-QX(I,J))-DT/(2.0*DY)*
      (QY(I,J+1)-QY(I,J))
3030 CONTINUE
      IDIR=1
      CALL DSWEPT(IDIR,NNX,AC,BC,CC,DC,ACS,BCS,CCS,DCS,ETAC,QC,I,NET)
3050 DO 3060 I=1,NNX
      QX(I,J)=QC(I)
3060 ETA(I,J)=ETAC(I)
3090 CONTINUE
C
C THIS PORTION OF PROGRAM FOR SWEEPS IN THE Y-DIRECTION
C
      IMPDIR=2
      DO 4070 I=2,NNXM1
      DX=DXA(I)
      DO 4030 J=2,NNY
      DY=0.5*(DYA(J-1)+DYA(J))
      DY2=DYA(J)
      FACTY=1.0
      CALL HURCH(USQ,I,J,X,Y,VF,PINF,DP,RMAX,THETA,DT,DY,
      RHOW,XH,YH)
      CALL CALLFR(I,J,BF)
      WY=0.5
      CALL INLT(I,J,BF,DT,FACTX,FACTY,WX,WY,IICOUN,NBAR,NINL,IMPDIR)
      FCTX(I,J)=FACTX
      FCTY(I,J)=FACTY
      WXX(I,J)=WX
      WYY(I,J)=WY
      IF (NET(I,J-1)*NET(I,J).NE.0.0.AND.WY.LT.400.0) GO TO 4000
      AC(J)=0.0
      BC(J)=0.0
      CC(J)=0.0
      DC(J)=0.0
      GO TO 4010
4000 DBAR=0.5*(D(I,J-1)+D(I,J))
      IF (ABS(DBAR).LT.0.001) DBAR=0.001
      AC(J)=G*DBAR*DT/(2.0*DY)*FACTY
      QXBAR=0.25*(QX(I,J-1)+QX(I+1,J-1)+QX(I,J)+QX(I+1,J))
      QQ=SQRT(QXBAR**2+QY(I,J)**2)
      BC(J)=1.0+BF*QQ*DT/(8.0*DBAR**2)
      IF (WY.GT.0.5) BC(J)=WY
      CC(J)=-AC(J)

```

```

      DC(J)=QY(I,J)-AC(J)*(ETAS(I,J)-ETAS(I,J-1))+(-DBAR*DPDY(I,J)/RHOW+
      UUY(I,J)/RHOW+B6*QXBAR)*DT
4010 IF (NET(I,J).NE.0) GO TO 4020
      ACS(J)=0.0
      BCS(J)=0.0
      CCS(J)=0.0
      DCS(J)=0.0
      GO TO 4030
4020 ACS(J)=DT/(2.0*DY2)
      BCS(J)=1.0
      CCS(J)=-ACS(J)
      DCS(J)=ETA(I,J)-DT/(4.0*DX)*(QX(I+1,J)-QX(I,J))+
      (QS(I+1,J)-QS(I,J)))
4030 CONTINUE
      IDIR=2
      CALL DSWEPT(IDIR,NNY,AC,BC,CC,DC,ACS,BCS,CCS,DCS,ETAC,QC,I,NET)
4050 DO 4060 J=1,NNY
      QY(I,J)=QC(J)
4060 ETA(I,J)=ETAC(J)
4090 CONTINUE
C
C REESTABLISH WET AND DRY GRIDS; DRY=0, FLOODED=1
C START AT IEND-1
C DRY UP IF ETA+H<=0.0
C
      DO 5030 J=2,NNYM1
      DO 5030 I=2,NNX
      IS=NNXM1+2-I

      IF (NET(IS,J).EQ.0) GO TO 5030
      ETA(IS,J)=0.67*ETA(IS,J)+0.33*ETAS(IS,J)
      IF (ETA(IS,J) + H(IS,J) 5000,5000,5010)

5000 ETA(IS,J)=-H(IS,J)-0.0001
      D(IS,J)=ETA(IS,J)+H(IS,J)
      NET(IS,J)=0
      GO TO 5020

5010 NET(IS,J)=1
      D(IS,J)=H(IS,J)+ETA(IS,J)

5020 CONTINUE
5030 CONTINUE
C
C REESTABLISH ACTIVE (DISCHARGE) JUNCTIONS
C USE BOUNDARY CONDITION OF NO FLOW ACROSS A BOUNDARY
C NQBX(J) IS THE POSITION OF THE NO FLOW COASTLINE ON THE J'TH COLUMN
C
      DO 5065 J=1,NNYM1
      DO 5060 I=1,NNXM1
      IF (NET(I,J)*NET(I+1,J)) 5035,5035,5040
5035 NQX(I+1,J)=0.0
      QX(I+1,J)=0.001
      NQBX(J)=I+1
      GO TO 5045

```

```

5040 NRX(I,J)=1
5045 IF(NET(I,J)*NET(I,J+1)) 5050,5050,5055
5050 NRX(I,J+1) = 0
      QY(I,J+1)=0.001
      GO TO 5060
5055 NRX(I,J+1)=1
5060 CONTINUE
5065 CONTINUE
C
  DO 6020 J=2,NNYM1
    ICUR=ISETUP(J)
    CALL HURCH(USQ,ICUR,J,X,Y,VF,PINF,DP,RMAX,THETA,
      DT,DY,RHOW,XH,YH)
    H0=HMAX*USQ/USQM
    AAA=SQRT(UUX(ICUR,J)**2+UUY(ICUR,J)**2)
    H0=H0*ABS(UUX(ICUR,J))/AAA
    T0=2.13*SQRT(H0)
    HB=0.936*H0
    IF (UUX(ICUR,J).GT.0.0) HB=0.1
    WSU=0.19*(1.0-2.82*SQRT(HB/(G*T0*T0)))*HB
    WSU1=WSU*1.0
    WSU2=WSU*1.5
    IF(NSETUP.EQ.0) WSU=0.0
    ETAS0(J)=ETA(ICUR,J)
    ETAS1(J)=ETA(ICUR,J)+WSU1
    ETAS2(J)=ETA(ICUR,J)+WSU2
    NQBXT(J)=ICUR
6020 CONTINUE
C
C ESTABLISH MOST SHOREWARD FLOODED STATION.
C NOTE-NEW SHORE ELEMENTS ARE ACTIVATED ONLY BY FLOODING IN X-DIRECTION
C
  DO 6150 J=2,NNYM1
    IC=NQBXT(J)
    DX=DXA(IC-1)
6060 IF(ETA(IC,J)+H(IC-1,J)) 6080,6080,6070
6070 ETA(IC-1,J)=-H(IC-1,J)+0.25*(ETA(IC,J)+H(IC-1,J))
      D(IC-1,J)=ETA(IC-1,J)+H(IC-1,J)
      NET(IC-1,J)=1
      QX(IC,J)=-DX*(ETA(IC-1,J)+H(IC-1,J))/DT
      ETA(IC,J)=-H(IC-1,J)+0.75*(ETA(IC,J)+H(IC-1,J))
6080 IF(NET(IC,J+1)) 6090,6090,6110
6090 IF(ETA(IC,J)+H(IC,J+1)) 6110,6110,6100
6100 ETA(IC,J+1)=-H(IC,J+1)+0.25*(ETA(IC,J)+H(IC,J+1))
      D(IC,J+1)=ETA(IC,J+1)+H(IC,J+1)
      NET(IC,J+1)=1
      DY=DYA(J+1)
      QY(IC,J+1)=DY*(ETA(IC,J+1)+H(IC,J+1))/DT
      ETA(IC,J)=-H(IC,J+1)+0.75*(ETA(IC,J)+H(IC,J+1))
6110 IF(NET(IC,J-1)) 6120,6120,6140
6120 IF(ETA(IC,J)+H(IC,J-1)) 6140,6140,6130
6130 ETA(IC,J-1)=-H(IC,J-1)+0.25*(ETA(IC,J)+H(IC,J-1))
      D(IC,J-1)=ETA(IC,J-1)+H(IC,J-1)

```

```

      DY=DYA(J-1)
      NET(IC,J-1)=1
      QY(IC,J-1)=-DY*(ETA(IC,J-1)+H(IC,J-1))/DT
      ETA(IC,J)=-H(IC,J-1)+0.75*(ETA(IC,J)+H(IC,J-1))
      D(IC,J)=ETA(IC,J)+H(IC,J)
6140 CONTINUE
6150 CONTINUE
      IF(MOD(JJ,1).NE.0) GO TO 10000
C***** STORE ETA VALUES FOR TIME SERIES' OF GRIDS FOR PLOTTING *****
      IC2=IC2+1
      DO 8000 NPLT=1,NPLOT
        JPLOT=(NPLT-1)*2+1
        KPLOT=IPLOT(JPLOT)
        LPLOT=IPLOT(JPLOT+1)
        CVAR(IC2,1,NPLT)=ETA(KPLOT,LPLOT)
        CVAR(IC2,2,NPLT)=ETAS1(LPLOT)
        CVAR(IC2,3,NPLT)=ETAS2(LPLOT)
C***** FIND MAXIMUM ETA'S OF GRIDS FOR PLOTTING *****
      DO 8000 JJJJ=1,3
        IF(ETAMAX(NPLT,JJJJ).LT.CVAR(IC2,JJJJ,NPLT)) ETAMAX(NPLT,JJJJ)=
          CVAR(IC2,JJJJ,NPLT)
8000 CONTINUE
C***** FIND MAXIMUM ETA VALUES (NO SETUP) FOR ALL GRIDS *****
      DO 9000 JJJJ=1,NNY
        DO 9000 IIII=1,NNX
          IF(ETA(IIII,JJJJ).GT.ETMX(IIII,JJJJ)) ETMX(IIII,JJJJ)=ETA(IIII,
            JJJJ)
9000 CONTINUE
      CTIME(IC2)=T/CHS
10000 CONTINUE
      NFIN=NFIN+1
      IF (MOD(JJ-1,18).NE.0) GO TO 10020
      WRITE(6,10010) THR,XHN,YHN
10010 FORMAT(1H0,'*****','THR=',F10.2,' XHN=',F10.2,' YHN=',F10.2)
      IF (MOD(JJ-1,36).NE.0) GO TO 10020
      CTH=COS((90.0-THETAC)/57.2956)
      STH=SIN((90.0-THETAC)/57.2956)
      XHB2=XHN*CTH + YHN*STH
      YHB2=-XHN*STH + YHN*CTH
      WRITE(6,10015)THR,XHB2,YHB2
10015 FORMAT(1H0,' UNROTATED COORDINATES: THR= ',F10.2,
      ' XHN= ',F10.2,' YHN= ',F10.2)
10020 CONTINUE
      IF((NFIN.EQ.7).AND.(XH.LT.45.0.AND.XH.GT.-45.0)) GO TO 10030
      IF (NFIN.EQ.14) NFIN=1
      GO TO 10080
C
C THIS DO LOOP CALCULATES VELOCITY AS A FUNCTION OF FLUX DIVIDED BY
C AVERAGE DEPTH OF TWO ADJACENT GRID ELEMENTS
C
10030 DO 10050 I=1,IEND
      DO 10050 J=1,NNY
        UXR(I,J)=0.001
        UYR(I,J)=0.001
        IF (J.EQ.1) DDUMY=D(I,J)

```

```

      IF(I.EQ.IEND) DDUMX=D(I,J)
      IF(I.EQ.IEND.OR.J.EQ.1) GO TO 10040
      DDUMX=(D(I+1,J)+D(I,J))/2.0
      DDUMY=(D(I,J)+D(I,J-1))/2.0
10040 UX(I,J)=QX(I,J)/DDUMX
10050 UY(I,J)=QY(I,J)/DDUMY
      DO 10070 I=2,IENDM1
      DO 10070 J=2,NNYM1
      IF (I.EQ.2) DUY=2.0/(D(I,J)+D(I,J-1))
      IF (I.EQ.2) GO TO 10060
      DUY=8.0/(D(I+1,J-1)+D(I+1,J)+D(I-1,J-1)+D(I-1,J)+2*D(I,J-1)+
-      2*D(I,J))
10060 DUX=8.0/(D(I,J-1)+D(I+1,J-1)+2*D(I,J)+2*D(I+1,J)+D(I+1,J+1)+
-      D(I,J+1))
      QYR=(QY(I,J)+QY(I,J+1)+QY(I+1,J)+QY(I+1,J+1))/4.0
      QXR=(QX(I,J)+QX(I,J-1)+QX(I-1,J)+QX(I-1,J-1))/4.0
      UXR(I,J)=SQRT(QX(I,J)**2+QYR**2)*DUX
      UYR(I,J)=SQRT(QY(I,J)**2+QXR**2)*DUY
      NTEST=0
10080 CONTINUE
      DO 10110 J=1,NNY
      DO 10100 ISO=1,NNX
      IF(ETA(ISO,J)+H(ISO,J).GE.-0.0001) GO TO 10090
      AREA(ISO)=DRY
      GO TO 10100
10090 AREA(ISO)=WET
10100 CONTINUE
10110 CONTINUE
10500 CONTINUE
C
C ***** END OF MAIN LOOP *****
C
11000 CONTINUE
      WRITE(6,11005)
11005 FORMAT(1H1,/,1H , 'TIME SERIES FOR PLOTTING GRIDS',/)
      I5=-1
      DO 11040 J=1,NFLOT
      I5=I5+2
      WRITE(6,11010) IPLOT(I5),IPLOT(I5+1)
11010 FORMAT(1H , 'GRID (',I2,',',I2,')')
      WRITE(6,11020) (CTIME(K6),(CVAR(K6,I,J),I=1,3),K6=1,IC2)
11020 FORMAT(1H ,F6.2,3F10.3,5X,F6.2,3F10.3,5X,F6.2,3F10.3)
      WRITE(6,11030)
11030 FORMAT(1H1,/)
11040 CONTINUE
      WRITE(33,11050) CASE
11050 FORMAT(A20)
      DO 11090 I=1,NFLOT
      J=(I-1)*2+1
      K=IPLOT(J)
      L=IPLOT(J+1)
      WRITE(33,11060) IPLOT(J),IPLOT(J+1),IC2
11060 FORMAT(2I3,I5)
      WRITE(33,11070) (CTIME(LL),(CVAR(LL,MM,I),MM=1,3),LL=1,IC2)
11070 FORMAT(4F7.2,3X,4F7.2)
      WRITE(6,11080) K,L,(ETAMAX(I,M),M=1,3)

```

```

11080 FORMAT(1H , 'ETAMAX FOR GRID (',I2,',',I2,') = ',3F9.2)
11090 CONTINUE

      WRITE(6,11100)
11100 FORMAT(1H1,/,/, ' MAXIMUM ETA VALUES FOR ALL GRIDS (NO SETUP)',/)
      DO 11120 JJJJ=1,NNY
      WRITE(6,11110) JJJJ,(ETMX(IIII,JJJJ),IIII=1,NNX)
11110 FORMAT(1H0,I3,3X,10F7.2,/,10(1H ,6X,10F7.2,/)
11120 CONTINUE
      IFLAGZ=0
      GO TO 270
11130 STOP
      END
C
C -----
C
      SUBROUTINE HURCH (USQ,I,J,X,Y,UH,PINF,DP,RMAX,THETA,
-      DT,DY,RHO,XH,YH)
      COMMON /A/ UUX(110,110),UUY(110,110),P(110,110),H(110,110),
-      DPDX(110,110),DPDY(110,110),DX
      DIMENSION X(110),Y(110)
C
C ** BEWARE ** SOME SIGNS HAVE BEEN MODIFIED TO ACCOUNT
C FOR LEFTHANDED COORDINATE SYSTEM.
      COR=0.6563E-04
      UCR=23.6
      RHOA=0.0024
      IF(I.NE.0) GO TO 10
      XP=-RMAX*SIN(THETA)
      YP=RMAX*COS(THETA)
      I=1
      J=1
      GO TO 20
10 XI=I
      XJ=J
      XP=X(I)-XH
      YP=Y(J)-YH
20 R=SQRT(XP*XP+YP*YP)
C
      IF(R.LT.2200.0) R=2200.0
      RAT=RMAX/R
      EXP0=EXP(-RAT)
      USG=-DP/(RHOA*R)*RAT*EXP0/COR
      UC=SQRT(-DP/RHOA*RAT*EXP0)
      ALPHA=ATAN2(YP,XP)
      BETA=ALPHA-THETA
      DD=-BETA
      VPRIME=UH*SIN(DD)
      GAMMA=0.5*(VPRIME/UC+UC/USG)
      RATIO=SQRT(GAMMA**2+1.0)-GAMMA
      U=UC*RATIO*0.9
      USQ=U**2
      UXX=-USQ*SIN(-ALPHA+0.31)
      UYY=-USQ*COS(-ALPHA+0.31)
      P(I,J)=PINF+DP*(1.0-EXP0)
      DPDR=-DP*RAT/R*EXP0
      DPDX(I,J)=DPDR*COS(ALPHA)

```



```

COMMON /H/ IFFACT(110,110)
BFSUM=0.0
TFSUM=0.0
DO 5 IP = 1,2
  IFM = IP-1+I
  DVA = ETA(IPM,J)+H(IPM,J)
  D2 = DVA
  IFA = IFFACT(IPM,J)
  CALL FRICT(IFA,DVA,BF,TF,D2)
  BFSUM=BFSUM+BF
5 TFSUM=TFSUM+TF
  BF = BFSUM/2.0
  TF = TFSUM/2.0
C   TF = 1.0
  UUX(I,J)=UUX(I,J)*TF
  UUY(I,J)=UUY(I,J)*TF
  RETURN
END
C-----
SUBROUTINE FRICT(IREM,D1,BF,TF,D2)
  IF(IREM.GE.10) GO TO 10
  I2=1
  GO TO 40
10 IF(IREM.GE.100) GO TO 20
  I2=2
  GO TO 40
20 IF(IREM.GE.1000) GO TO 30
  I2 = 3
  GO TO 40
30 IF(IREM.LT.10000) I2=4
40 BF=0.0
  TF=0.0
  IDIV=10*I2
  DO 90 I=1,I2
    IDIV=IDIV/10
    ITEST=IREM/IDIV
    GO TO (50,60,70,80,85),ITEST
50 PHI=1.0
  IF (D1 .LE. 10.0) D1=10.0
  D2 = D1
  CALL COMP(PHI,0.0,0.0,5.47,1.0,0.0,D1,BF,TF,D2)
  GO TO 90
60 PHI=0.0
  CALL COMP(PHI,0.999,0.34,10.94,0.3,0.0,D1,BF,TF,D2)
  GO TO 90
70 PHI=1.0
  CALL COMP(PHI,0.0,0.0,0.91,1.0,0.0,D1,BF,TF,D2)
  GO TO 90
80 PHI=0.0
  CALL COMP(PHI,0.969,0.5445,10.94,0.3,0.7,D1,BF,TF,D2)
  GO TO 90
85 PHI=0.0
  CALL COMP(PHI,0.64,0.204,10.94,1.0,0.0,D1,BF,TF,D2)
90 IREM=IREM-ITEST*IDIV
  A2=FLOAT(I2)
  TF=TF/A2

```

```

BF=BF/A2
RETURN
END
C-----
SUBROUTINE COMP(PHI,A1,A2,A3,A4,A5,D1,BF,TF,D2)
  A6=A4+A5*D2/10.0
  IF(A6.GT.1.0) A6=1.0
  TF=TF+A6
  D3 = D2
  IF(A3.EQ.5.47) D3=D1
  IF(PHI.EQ.1.0) GO TO 10
  PHI = 1.0/(ABS(A1+A2*ABS(D3)**1.333))**0.5
10 BF = 1.28/((PHI**2)*(ALOG(ABS(A3*D3+1.0)))**2)+BF
  RETURN
END
C-----
SUBROUTINE BARR(N,I,J,F,DT,FACTX,FACTY,WX,WY,IICOUN,NINL)
  COMMON /BAR/ NORBAR(50),IBAR(50),JBAR(50),XLBAR(50),HBAR(50),
  * WBAR(50),FBAR(50),XKEX(50),NORINL(50),IINL(50),JINL(50),WINL(50),
  * DPINL(50),XKENEX(50),FINL(50),XLINL(50)
  COMMON /A/ UUX(110,110),UUY(110,110),P(110,110),H(110,110),
  - DPDX(110,110),DPDY(110,110),DX
  COMMON /B/ ETA(110,110),QX(110,110),QY(110,110),NQB(110),TIDE,
  - DY,NNX,IEND
  G = 32.2
C   THE PRESENT TREATMENT IS FOR SUBMERGED BARRIERS ONLY
C
  NORB=NORBAR(N)
  IM1=I-1
  IC=I
  JM1=J
  JC=J
  DL=DY
  DS=DX
  QC=QX(IC,JC)
  IF (NORB.EQ.1) GO TO 10
  IM1=I
  JM1=J-1
  DS=DY
  DL=DX
  QC=QY(IC,JC)
10 CONTINUE
  D1=H(IM1,JM1)+ETA(IM1,JM1)
  D3=H(IC,JC)+ETA(IC,JC)
C-----
C   AVERAGE WATER SURFACE ELEVATION
C
  ETABAR=0.5*(ETA(IM1,JM1)+ETA(IC,JC))
  W1=DL
  W3=DL
  DX1=0.5*(DS-XLBAR(N))
  DX3=DX1
C
C   THIS NEXT LOOP DETERMINES WHETHER THERE IS AN INLET
C   THROUGH THE BARRIER OF CURRENT INTEREST

```



```

C      DO 20 NI=1,NINL
      IF (IINL(NI).NE.I.OR.JINL(NI).NE.J) GO TO 20
      NINC=NI
      WI=WINL(NINC)
      IF (NORINL(NI).EQ.NORB) GO TO 30
20     CONTINUE
      WI=0.0
C
C-----DEPTH OVER BARRIER
C
30     DBAR=ETABAR+HBAR(N)
      DXB=XLBAR(N)
      FB=FBAR(N)
      WB=WBAR(N)
      IF (DBAR.LE.0.0) WB=0.0
      IF (WI.GT.0.0.OR.WB.GT.0.0) GO TO 40
C
C      IF DBAR IS GREATER THAN ZERO, BARRIER IS OVERTAPPED
C
      WS=500.
      FACT=0.0
      GO TO 70
C
C      THIS SECTION FOR GRID LINES WITH INLET THROUGH BARRIER
C      WHETHER OR NOT BARRIER IS OVERTOPPED
C
40     DI=DPINL(NINC)+ETABAR
      FI=FINL(NINC)
      DXI=XLINL(NINC)
      CONTINUE
      IF (WB.NE.0.0) DX2=DXB
      IF (WI.NE.0.0) DX2=DXI
      T1=DX1/(D1*W1)
      T3=DX3/(D3*W3)
      T4=F*DX1/(8.0*W1*D1**2)
      T5=F*DX3/(8.0*W3*D3**2)
      T21=0.0
      T22=0.0
      T6=10000.0
      T7=10000.0
      T8=10000.0
      T9=10000.0
      T67=10000.0
      T89=10000.0
      IF (WB.EQ.0.0) GO TO 50
      T22=WB/(DBAR*WB)**2
      T8=FB*DXB/(8.0*WB*WB*DBAR**3)
      T9=XKEX(N)/(2.0*DBAR*DBAR*WB*WB)
      T89=(T8+T9)*(WB/(WB+WI))**2
50     IF (WI.EQ.0.0) GO TO 60
      T21=WI/(DI*WI)**2
      T6=FI*DXI/(8.0*DI**3*WI**2)
      T7=XKENEX(NINC)/(2.0*DI*DI*WI*WI)
60     ALPHAI=T6+T7
      ALPHAB=T8+T9

```

```

      SAI=SQRT(ALPHAI)
      SAB=SQRT(ALPHAB)
      T2=(T21*WI*DI+T22*WB*DBAR)*DX2/(WB+WI)
      XMU=T1/(D1*W1)+DX2/(WB+WI)*(T21+T22)+T3/(D3*W3)
      FACT=2.0/(XMU*DL)*(T1+T2+T3)/(D1+D3)
      TEMP=ALPHAI*WI*DI/(1.0+SAI/SAB)**2+ALPHAB*WB*DBAR/(1.0+SAB/SAI)**2
      WS=(DL/DS)*(T4+T5+TEMP)*ABS(QC)
      WS=WS*DT+1.0
70     CONTINUE
      IF (NORBAR(N).EQ.1) GO TO 80
      FACTY=FACT
      WY=WS
      GO TO 90
80     FACTX=FACT
      WX=WS
90     CONTINUE
      NZIP = 0
      IF (NZIP.EQ.0) GO TO 250
100    IF (IICOUN.GE.10) GO TO 250
110    IF (IICOUN.GE.20) GO TO 250
      IICOUN=IICOUN+1
      WRITE(6,120) IICOUN,N,NINC,NORBAR(N),IBAR(N),JBAR(N)
      WRITE(6,130) IM1,JM1,IC,JC,DL,DS,QC,D1,D3
      WRITE(6,140) H(IC,JC),H(IM1,JM1),ETA(IC,JC),ETA(IM1,JM1),ETABAR
      WRITE(6,150) W1,W3,DX1,DX3,DXB,DX2,DBAR,HBAR(N)
      WRITE(6,160) WI,FB,DI,FI,DXI,DX2
      WRITE(6,170) T1,T3,T4,T5
      WRITE(6,180) T21,T22,T8,T9,T89
      WRITE(6,190) T6,T7,T67,T2,XMU,FACT
      WRITE(6,200) WS,DT,FACTX,FACTY,WS,WX,WY
      WRITE(6,210) WB,F
      WRITE(6,220) QX(IM1,JM1),QX(IC,JC),QY(IM1,JM1),QY(IM1,JC+1)
      WRITE(6,230) UUX(IM1,JM1),UUX(IC,JC),UUY(IM1,JM1),UUY(IC,JC)
      WRITE(6,240) DPDFX(IM1,JM1),DPDFX(IC,JC),DPDFY(IM1,JM1),DPDFY(IC,JC)
      FORMAT(1H,'IICOUN=',I3,'/1H0,'N=',I3,' NINC=',I3,' NORBAR(N)='
120    * I3,' IBAR(N)=' ,I3,' JBAR(N)=' ,I3)
130    FORMAT(1H,'IM1=' ,I3,' JM1=' ,I3,' IC=' ,I3,' JC=' ,I3,' DL='
      * F8.1,' DS=' ,F8.1,' QC=' ,F8.3,' D1=' ,F8.3,' D3=' ,F8.3)
140    FORMAT(1H,'H(IC,JC)=' ,F8.3,' H(IM1,JM1)=' ,F8.3,' ETA(IC,JC)='
      * F8.3,' ETA(IM1,JM1)=' ,F8.3,' ETABAR=' ,F8.3)
150    FORMAT(1H,'W1=' ,F8.1,' W3=' ,F8.1,' DX1=' ,F8.1,' DX3=' ,F8.1,
      * ' DXB=' ,F8.1,' DX2=' ,F8.1,' DBAR=' ,F8.3,' HBAR(N)=' ,F8.3)
160    FORMAT(1H,'WI=' ,F8.1,' FB=' ,F8.5,' DI=' ,F8.3,' FI=' ,F8.5,
      * ' DXI=' ,F8.1,' DX2=' ,F8.1)
170    FORMAT(1H,'T1=' ,E12.5,' T3=' ,E12.5,' T4=' ,E12.5,' T5=' ,E12.5)
180    FORMAT(1H,'T21=' ,E12.5,' T22=' ,E12.5,' T8=' ,E12.5,' T9='
      * E12.5,' T89=' ,E12.5)
190    FORMAT(1H,'T6=' ,E12.5,' T7=' ,E12.5,' T67=' ,E12.5,' T2=' ,E12.5,
      * ' XMU=' ,E12.5,' FACT=' ,E12.5)
200    FORMAT(1H,'WS=' ,F8.5,' DT=' ,F8.3,' FACTX=' ,F8.5,' FACTY='
      * F8.5,' WS=' ,F8.5,' WX=' ,F8.5,' WY=' ,F8.5)
210    FORMAT(1H,'WB=' ,F8.1,' DF=' ,F8.5)
220    FORMAT(1H,'QX(IM1,JM1)=' ,E12.4,' QX(IC,JC)=' ,E12.4,
      * ' QY(IM1,JM1)=' ,E12.4,' QY(IM1,JC+1)=' ,E12.4)
230    FORMAT(1H,'UUX(IM1,JM1)=' ,E12.4,' UUX(IC,JC)=' ,E12.3,
      * ' UUY(IM1,JM1)=' ,E12.4,' UUY(IC,JC)=' ,E12.4)

```

```

240  FORMAT(1H,'DPDX(IM1,JM1)=' ,E12.4,' DPDX(IC,JC)=' ,E12.3,
      * ' DPDY(IM1,JM1)=' ,E12.4,' DPDY(IC,JC)=' ,E12.4,////)

```

```

250  RETURN
      END

```

```

C-----
      SUBROUTINE DSWEPT(IDIR,NNI,A,B,C,D,AS,BS,CS,DS,ETAC,QC,JC,NET)

```

```

C      COMMON /B/ ETA(110,110),QX(110,110),QY(110,110),NQBK(110),TIDE,
      -      DY,NNX,IEND

```

```

C      COMMON /F/ JJ
      DIMENSION A(110), B(110), C(110), D(110), E(110), F(110)
      DIMENSION AS(110),BS(110),CS(110),DS(110),ES(110),FS(110)
      DIMENSION QC(110),ETAC(110)
      DIMENSION NET(110,110)
      DATA IICOUN/0/

```

```

C      IF IDIR=1, SWEEP IN X-DIRECTION
C      IF IDIR=2, SWEEP IN Y-DIRECTION

```

```

C      NNM1=NNI-1
      IF (IDIR.EQ.2) GO TO 10

```

```

C      CARRY OUT FIRST SWEEP TO CONDITION COEFFICIENTS

```

```

C      E(NNI)=0.0
      F(NNI)=ETA(NNI,JC)
      ETAC(1)=ETA(1,JC)
      GO TO 20
10  CONTINUE
      E(NNI)=0.0
      F(NNI)=ETA(JC,NNI)
      IF (NET(JC,NNI).EQ.0) F(NNI)=0.0
      ETAC(1)=ETA(JC,NNI)

```

```

20  DO 30 I=2,NNM1
      IC=NNM1+2-I
      ICP=IC+1
      DEN=A(ICP)*E(ICP)+B(ICP)
      IF (DEN.EQ.0.0) DEN=1.0
      ES(IC)=-C(ICP)/DEN
      FS(IC)=(D(ICP)-A(ICP)*F(ICP))/DEN
      DEN=AS(IC)*ES(IC)+BS(IC)
      IF (DEN.EQ.0.0) DEN=1.0
      E(IC)=-CS(IC)/DEN
      F(IC)=(DS(IC)-AS(IC)*F(IC))/DEN
30  CONTINUE

```

```

C      CARRY OUT SECOND SWEEP TO ESTABLISH ETA AND Q

```

```

C      DO 40 I=2,NNI
      IM=I-1
      QC(I)=ES(IM)*ETAC(IM)+FS(IM)
      ETAC(I)=E(I)*QC(I)+F(I)
40  CONTINUE

```

```

      E(1)=ETAC(1)

```

```

      E(NNI)=ETAC(NNI)

```

```

C*****
C

```

```

C      WRITE(6,80) JJ,JC
C 80  FORMAT(1H1,' DSWEPT: JJ=' ,I6,' JC=' ,I6)
C      IF (JJ.NE.07.OR.(JC.NE.40.AND.JC.NE.10)) GO TO 60
C      WRITE(6,90)

```

```

C 90  FORMAT(1H-,' I A(I) B(I) C(I) D(I)
      -E(I) F(I) AS(I) BS(I) CS(I) DS(I) ES(I) FS(I)
C      -) ETAC(I) QC(I)',//)
C      WRITE(6,100) (I,A(I),B(I),C(I),D(I),E(I),F(I),AS(I),BS(I),CS(I),
C      1 DS(I),ES(I),FS(I),ETAC(I),QC(I),I=1,NNI)
C 100  FORMAT(I6,3F9.4,F9.2,5F9.4,F9.2,2F9.3,2F9.2)
      110 RETURN
      END

```

```

C-----
      SUBROUTINE INLT(I,J,BF,DT,FACTX,FACTY,WX,WY,IICOUN,NBAR,NINL,
      -      IMPDIR)

```

```

      COMMON /F/ JJ
      COMMON /BAR/ NORBAR(50),IBAR(50),JBAR(50),XLBAR(50),HBAR(50),
      -      WBAR(50),FBAR(50),XKEX(50),NORINL(50),IINL(50),JINL(50),WINL(50),
      -      DPINL(50),XKENEX(50),FINL(50),XLINL(50)
      FACTX=1.0
      FACTY=1.0
      IF (NBAR.EQ.0) GO TO 20
      DO 10 N=1,NBAR
      IF (IBAR(N).NE.I.OR.JBAR(N).NE.J.OR.NORBAR(N).NE.IMPDIR)
      -      GO TO 10
      CALL BARR(N,I,J,BF,DT,FACTX,FACTY,WX,WY,IICOUN,NINL)
10  CONTINUE
20  RETURN
      END

```

APPENDIX B
1-D STORM TIDE MODEL*

```

CCCCCCCCCCCCCCCCCCCCCCCCCCCCCCCCCCCCCCCCCCCCCCCCCCCCCCCCCCCCCCCC
C
C
C      ONE-DIMENSION NUMERICAL STORM SURGE MODEL
C
C
CCCCCCCCCCCCCCCCCCCCCCCCCCCCCCCCCCCCCCCCCCCCCCCCCCCCCCCCCCCCCCCC
C
      DIMENSION CTS(3,5,1200),COUNTY(4),PROFIL(5),CASE(5),DATE(6)
      DIMENSION H(200),X(200),ETA(200),QY(200),EMXHN(5,2)
10  FORMAT(5A4)
20  FORMAT(5A4,I5,2F7.2)
30  FORMAT(5(F9.0,F7.2))
40  FORMAT(10F7.1,3I3)
100 FORMAT(1H )
110 FORMAT(1H1,'ONE-DIMENSION NUMERICAL STORM SURGE MODEL',T49,
1    'RUN DATE: ',6A4,/1H ,41('-'),///)
120 FORMAT(1H ,4A4,4X,5A4,/1H ,40('-'),///)
130 FORMAT(1H , 'PROFILE DATA -- (DIST,DEPTH):',/)
135 FORMAT(5(1H ,5(F7.0,F7.2,2X),/))
140 FORMAT(1H-,'INPUT PARAMETERS:',//1H ,
1    'PINF=',F8.2,T26,'P0=',F8.2,T51,'DP=',F8.2,/1H ,
2    'ZLAT=',F8.2,T26,'RMAX=',F8.2,/1H ,
3    'COR=',E12.4,T26,'VF=',F8.2,/1H ,
4    'THETAC=',F8.2,T26,'THETAN=',F8.2,T51,'THETA=',F8.2,/1H ,
5    'XSITE=',F8.2,T26,'XHC=',F8.2,T51,'XHB=',F8.2,/1H ,
6    'YSITE=',F8.2,T26,'YHC=',F8.2,T51,'YHB=',F8.2,/1H ,
7    'XOFF=',F8.0,T26,'DIST=',F8.2,/1H ,
8    'DT=',F8.2,T26,'TMAX=',F8.2,T51,'NTIMES=',I5)
145 FORMAT(1H ,4A4,4X,5A4,20X,5A4,/1H ,80('-'),///)
150 FORMAT(1H-,'TIME STEP ',I5,5X,'TIME=',F8.3,' HRS.',5X,'XH=',
1    F9.2,' N.MI.',5X,'YH=',F9.2,' N.MI.',//,1H ,
2    'STORM SURGE, ETA(1) IN FEET ABOVE MSL -- (I,ETA):',//,
3    (1H ,6(I5,F9.3)))
160 FORMAT(1H ,20X,'CONDENSED TIME SERIES OF STORM SURGE ETAS',//1H ,
1    4A4,4X,5A4,20X,5A4,///1H ,
2    2(' TIME SURGE SETUP W/SETUP W/DYNMC      '),/)
170 FORMAT(1H ,F5.2,4F8.3,6X,F5.2,4F8.3)
175 FORMAT(F5.2,4F8.3,6X,F5.2,4F8.3)
180 FORMAT(1H-,'MAXIMUM SURGES FOR ',4A4,2X,5A4,2X,5A4,///1H ,5X,4F8.3)
C
C
C      IUP=0
      RHOA=0.0024
      RHOV=1.99
      G=32.17
      PI=3.1416
      FRICT=0.0025
      CNM=6076.
      CHR=3600.
      CHG=70.51
      CDEG=180.0/PI
      OMEGA=2.0*PI/(24.0*CHR)

```

*This program represents a numerical modeling procedure that is subject to change due to: 1. newly encountered topo-bathymetric and hydraulic boundary conditions, and 2. incorporation of new advancements quantifying coastal processes. This program is applied on a county-by-county basis and is subject to acceptable calibration constraints recommended by the Beaches and Shores Resource Center and approved by the Florida Department of Natural Resources.

```

      BETA2=1.5
      TIDE=0.0
C
C
      READ(5,10) COUNTY
      READ(5,20) PROFIL,IMAX,XSITE,YSITE
      READ(5,30) (X(I+1),H(I),I=1,IMAX)
C
      WRITE(6,110) DATE
      WRITE(6,120) COUNTY,PROFIL
      WRITE(6,130)
      WRITE(6,135) (X(I+1),H(I),I=1,IMAX)
C
C
      IMP1=IMAX+1
      XOFF=XSITE*CNM
      X(1)=0.0
      DO 290 I=1,IMP1
      X(I)=X(I)+XOFF
290  CONTINUE
      DO 295 I=1,IMAX
      H(I)=H(I)+0.8
295  WRITE(6,135) (X(I+1),H(I),I=1,IMAX)
C
C
      XSIT=XSITE*CNM
      YSIT=YSITE*CNM
300 READ(5,10,END=999) CASE
      READ(5,40) DT,THETAC,ZLAT
      READ(5,40) PINF,DP,RMAX,VF,THETAN,XHB,YHB,DIST,TMAX,TMIN,
      1      NFARM,NTIDE,ION
C
      P0=PINF+DP
      THETA=THETAN-THETAC+90.0
      IF (THETA.GT.360.0) THETA=THETA-360.0
      IF (THETA.LT.0.0) THETA=THETA+360.0
      COR=2.0*OMEGA*SIN(ZLAT/CDEG)
      NTIMES=IFIX(TMAX*CHR/DT)+1
      INTERV=IFIX(CHR/DT/2.0)
      INTER4=4*INTERV
      NSTORE=IFIX(180.0/DT)
      IF (NSTORE.EQ.0) NSTORE=1
C
      WRITE(6,110) DATE
      WRITE(6,145) COUNTY,PROFIL,CASE
      WRITE(6,140) PINF,P0,DP,ZLAT,RMAX,COR,VF,THETAC,THETAN,THETA,
      1      XSITE,XHC,XHB,YSITE,YHC,YHB,XOFF,DIST,DT,TMAX,NTIMES
C
      PINF=PINF*CHG
      P0=P0*CHG
      DP=DP*CHG
      RMAX=RMAX*CNM
      VF=VF*CNM/CHR
      THETAC=THETAC/CDEG
      THETAN=THETAN/CDEG

```

```

      THETA=THETA/CDEG
      XHB=XHB*CNM
      YHB=YHB*CNM
C
      DO 310 I=1,IMP1
      QY(I)=0.0
310  CONTINUE
C
      DO 320 I=1,5
      EMXMN(I,1)=0.0
      EMXMN(I,2)=0.0
320  CONTINUE
C
      TIMSC=-DT
      IS=0
C
      CALL HURCH(IS,X,XSIT,YSIT,XH,YH,PINF,DP,RMAX,VF,THETA,
      1      RHOW,RHOA,COR,USQ,P,TAUX,TAUY)
C
      USQM=USQ
      UMAX=SQRT(USQ)*CHR/CNM
      AA=-RMAX*DP/(CNM*CHG*100.0)
      AA2=0.160*VF/SQRT(UMAX)
      HMAX=16.5*EXP(AA)*(1.0+AA2)
      TMAX1=8.6*EXP(AA/2.0)*(1.0+AA2/2.0)
C
C
      DO 600 NTIME=1,NTIMES
C
      WSU=0.0
      TIMSC=TIMSC+DT
      XH=XHB+VF*TIMSC*COS(THETA)
      YH=YHB+VF*TIMSC*SIN(THETA)
      TIMHR=TIMSC/CHR
      XHN=XH/CNM
      YHN=YH/CNM
C
C
      ETASUM=0.0
      SUMSTR=0.0
      CSUM=0.0
C
      DO 500 I=1,IMAX
      IS=IMAX-I+1
      CALL HURCH(IS,X,XSIT,YSIT,XH,YH,PINF,DP,RMAX,VF,THETA,
      1      RHOW,RHOA,COR,USQ,P,TAUX,TAUY)
      ETAPR=1.0/(RHOW*G)*(PINF-P)
      DX=X(IS+1)-X(IS)
      TDPH=H(IS)+ETASUM
      IF (I.EQ.1) TDPH=H(IS)+TIDE
      IF (TDPH.GT.0.0) GO TO 400
      GO TO 450
400  SUMSTR=SUMSTR+TAUX*DX/(RHOW*G*TDPH)
      ETA(IS)=ETAPR-SUMSTR+TIDE
      ETASUM=ETA(IS)
      TDPH=H(IS)+ETASUM

```

```

      RB=1.0+DT*FRIC*ARS(QY(IS))/(TDP*TDPTH)
      QY(IS)=(QY(IS)+DT/RHOW*TAUY)/RB
      CCTIDE=DX*COR*QY(IS)/(G*TDPTH)
      CSUM=CSUM+CCTIDE
      ETA(IS)=ETA(IS)+CCTIDE
      ETASUM=ETA(IS)
C
      IF (IS.NE.1) GO TO 500
450  H0=HMAX*ABS(USQ)/USQM
      IF (USQ.GT.0.0) H0=1.0
      T0=2.13*SQRT(H0)
      HB=0.936*H0
C
      WSU=0.19*(1.0-2.82*SQRT(HB/(G*T0*T0)))*HB
C
      ETASUM=ETASUM+BETA2*WSU
      IF ((ETA(IS)+H(IS)).GT.0.0) GO TO 500
      ETA(1)=0.0
      GO TO 510
C
500  CONTINUE
C
510  CONTINUE
      NTM=(NTIME-1)/NSTORE+1
      CTS(1,1,NTM)=TIMHR
      CTS(1,2,NTM)=ETA(1)
      CTS(1,3,NTM)=WSU
      CTS(1,4,NTM)=ETA(1)+WSU
      CTS(1,5,NTM)=ETA(1)+1.5*WSU
C
      DO 520 I=2,5
      IF (CTS(1,I,NTM).GT.EMXMN(I,1)) EMXMN(I,1)=CTS(1,I,NTM)
      IF (CTS(1,I,NTM).LT.EMXMN(I,2)) EMXMN(I,2)=CTS(1,I,NTM)
520  CONTINUE
C
      IF (MOD(NTIME,INTERV).NE.1) GO TO 600
C
      IF (MOD(NTIME,INTER4).EQ.1) WRITE(6,110) DATE
      IF (MOD(NTIME,INTER4).EQ.1) WRITE(6,145) COUNTY,PROFIL,CASE
      WRITE(6,150) NTIME,TIMHR,XHN,YHN,(I,ETA(I),I=1,IMAX)
      WRITE(6,151) (CTS(1,K,NTM),K=2,5)
151  FORMAT(1H0,'ETA:',F8.3,4X,'WSU:',F8.3,4X,'ETA+WSU:',F8.3,4X,
-      'ETA+1.5*WSU:',F8.3)
C
      600  CONTINUE
      DO 605 I=1,5
      605  CTS(1,I,NTM+1)=0.0
C
      WRITE(8,152)NTM
152  FORMAT(I5)
      DO 610 I=1,NTM,2
      IF (MOD(I,100).EQ.1) WRITE(6,110) DATE
      IF (MOD(I,100).EQ.1) WRITE(6,140) COUNTY,PROFIL,CASE
      IF (MOD(I,10).EQ.1) WRITE(6,100)

```

```

      IF1=I+1
      WRITE(6,170) ((CTS(1,J,K),J=1,5),K=I,IF1)
      WRITE(8,175) ((CTS(1,J,K),J=1,5),K=I,IF1)
610  CONTINUE
      WRITE(11,11) ((CTS(1,J,K),J=1,5,4),K=1,NTM,3)
      FORMAT(2F10.1)
11  C
      WRITE(6,180) COUNTY,PROFIL,CASE,(EMXMN(I,1),I=2,5)
      WRITE(10,180) COUNTY,PROFIL,CASE,(EMXMN(I,1),I=2,5)
C
      ION=1
      GO TO 300
999  RETURN
      END
      SUBROUTINE HURCH(IS,X,XSITE,YSITE,XH,YH,PINF,DP,RMAX,VF,THETA,
1      RHOW,RHOA,COR,USQ,P,TAUX,TAUY)
      DIMENSION X(1)
C BEWARE SOME SIGNS HAVE BEEN MODIFIED TO ACCOUNT FOR LEFT-HANDED COORD
      UCR=23.6
      IF (IS.NE.0) GO TO 4
      XP=-RMAX*SIN(THETA)
      YP=RMAX*COS(THETA)
      GO TO 6
4      XIS=0.5*(X(IS+1)+X(IS))
      XP=XIS-XH
      YP=YSITE-YH
6      R=SQRT(XP**2+YP**2)
      IF(R.LT.2200.0) R=2200.0
      RAT=RMAX/R
      EXPO=EXP(-RAT)
      USG=-DP/(RHOA*R)*RAT*EXPO/COR
      UC=SQRT(-DP/RHOA*RAT*EXPO)
      ALPHA=ATAN2(YP,XP)
      BETA=THETA-ALPHA
      VPRIME=VF*SIN(BETA)
      GAMMA=0.5*(VPRIME/UC+UC/USG)
      RATIO=SQRT(GAMMA**2+1.0)-GAMMA
      IF(RATIO.LT.1.0E-05) RATIO=1.0E-05
      U=UC*RATIO*0.9
      USQ=U**2
      UXX=-USQ*SIN(-ALPHA+0.31)
      UYY=-USQ*COS(-ALPHA+0.31)
      P=PINF+DP*(1.0-EXPO)
      WSC=1.0E-06
      IF(U.LT.UCR) GO TO 20
      WSC=WSC+2.5E-06*(1.0-UCR/U)**2
20  CONTINUE
      AA=1.0
      TAUX=AA*RHOW*WSC*UXX
      TAUY=AA*RHOW*WSC*UYY
      IF (IS.NE.0) USQ=UXX
      RETURN
      END

```

APPENDIX C
BEACH-DUNE EROSION MODEL*

*This program represents a numerical modeling procedure that is subject to change due to: 1. newly encountered topo-bathymetric and hydraulic boundary conditions, and 2. incorporation of new advancements quantifying coastal processes. This program is applied on a county-by-county basis and is subject to acceptable calibration constraints recommended by the Beaches and Shores Resource Center and approved by the Florida Department of Natural Resources.

```

C*****
C      EROSION MODEL
C
C
C
C
C
C
C
C
C      NOTE:  THIS PROGRAM WAS USED FOR CHARLOTTE COUNTY, APRIL 1984.
C
C*****
C      DIMENSION DH(200),DX(200),DPTC(200),
C      -          STAI(120),STA(120),XAO(200),XAW(200),HW(200),
C      -          X(200,2),NCON(200),
C      -          XASAVE(200),HASAVE(200)
C      DIMENSION XTOT(6),DXTOT(6),NTOT(6)
C      COMMON /A/ H1(200),XA(200),HA(200),NELM,X1(200),NP,NELM1
C      CHARACTER*8 RNG,RNGDAT,DOTDAT,BCHDAT,OFFDAT
C      CHARACTER*3 CNTY,CNAME3(5)
C      CHARACTER*10 CNAME(5)
C      DATA NCNTY/5/
C      DATA CNAME3/'WAL','NAS','FRA','CHA','MAR'/
C      DATA CNAME/'WALTON','NASSAU','FRANKLIN','CHARLOTTE','MARTIN'/
C
C      H(N) VALUES ARE DEPTH VALUES TO CENTER OF ELEMENT.
C      ELEVATIONS ABOVE MEAN SEA LEVEL ARE NEGATIVE.
C
C      DATA XK/0.07/,XMD/3.0/,HB/10.0/,A/0.13/,PERIOD/0.5/,DY/1.0/
C      5  FORMAT(/)
C      10 FORMAT(10X,F10.2)
C      15 FORMAT(F8.4)
C      30 FORMAT(5(F7.1,1X,F7.2))
C      37 FORMAT(A3)
C      40 FORMAT(A8,I3)
C      62 FORMAT(1H,5X,F8.1,3X,F8.1,5X,F8.1)
C      65 FORMAT(I3)
C      10050 FORMAT(1H1,/,34X,A10,' COUNTY',
C      -          /,25X,'SIMULATED DUNE EROSION - DEAN-S MODEL',
C      -          /,25X,' FOR DECEMBER 1982',
C      -          /,25X,' 100 YEAR STORM TIDE USED',/)
C      10055 FORMAT(1H0,'NOTE:  XMD/SLOPE=',F3.1,' K VALUE =',F4.2,/,
C      -          1H, ' PROFILES CONTAIN ADDED OFFSHORE DATA',/)
C
C      VOLTOT=0.0
C      PROF=0.0
C      DO 98 I=1,6
C      NTOT(I)=0
C      XTOT(I)=0.0
C      DXTOT(I)=0.0
C      98  DO 100 K = 1,120
C      READ(5,10,END=150) STAI(K)

```

```

100 CONTINUE
150 NTIMES=K-1
C
C   READ H,X VALUES
   WRITE(8,201)
201 FORMAT('INITIAL SURVEY DATA')
   WRITE(9,202)
202 FORMAT('INITIAL SMOOTHED DATA')
   WRITE(10,203)
203 FORMAT('ERODED-SMOOTHED DATA')
   READ(4,37)CNTY
   DO 155 I=1,NCNTY
   IF (CNTY.EQ.CNAME3(I)) GO TO 160
155 CONTINUE
160 ICNTY=I
C
C   175 READ(4,20,END=9999)RNG,RNGDAT,ICODE,YNORTH,XEAST,AZMUTH
   READ(4,25)DOTDAT,BCHDAT,OFFDAT,NP,NPDOT,NPBCH,NPOFF
20 FORMAT(A8,A8,I2,2F12.3,F7.2)
25 FORMAT(A8,A8,A8,4I3,/)
C
   IF (AMOD(PROF,4.0).NE.0) GO TO 1750
   WRITE(6,10050)CNAME(ICNTY)
   WRITE(6,10055)XMD,XK
1750 PROF=PROF+1.0
   DO 176 I=1,200
   X(I,1)=0.0
   X(I,2)=0.0
   X1(I)=0.0
   H1(I)=0.0
   NCON(I)=0
   XA(I)=0.0
176 HA(I)=0.0

   READ(4,30)(X1(I),H1(I),I=1,NP)
   NPOFF=0
   NPDOT=0
   NPBCH=NP
C   FILE 8 CONTAINS INITIAL SURVEY DATA.
   WRITE(8,20)RNG,RNGDAT,ICODE,YNORTH,XEAST,AZMUTH
   WRITE(8,25)DOTDAT,BCHDAT,OFFDAT,NP,NPDOT,NPBCH,NPOFF
   WRITE(8,30)(X1(I),H1(I),I=1,NP)

   IDUNEM = 1
   DO 177 I = 1,NP
   IF (H1(I) .GT. H1(IDUNEM)) IDUNEM = I
177 CONTINUE
   MIN1=1
   DO 178 I = 1,IDUNEM
   IF (H1(I) .LT. H1(MIN1)) MIN1 = I
178 CONTINUE
   MIN2=1
   DO 1781 I = IDUNEM,NP
   IF (H1(I) .LT. H1(MIN2)) MIN2 = I
1781 CONTINUE

```

```

IMAX=IFIX(H1(IDUNEM))
IMIN1=IFIX(H1(MIN1))
IMIN2=IFIX(H1(MIN2))
NELM1=IMAX-IMIN1+1
NELM2=IMAX-IMIN2+1
NELM=NELM1+NELM2
NL=NELM
II=1
IMAXM1=IMAX-1
DO 179 I=IMIN1,IMAX
HA(II)=I
II = II + 1
179 CONTINUE
DO 1791 I=IMAX,IMIN2,-1
HA(II)=I
II = II + 1
1791 CONTINUE
DO 2 I=1,NELM
NCON(I)=1
2 XA(I)=0.0
CALL SMOOTH(IDUNEM,1,2)
CALL SMOOTH(IDUNEM,NP,1)

NELM1M = NELM1 - 1
N2=NELM1+1
N3=NELM-1

DO 17800 M=1,NELM1
XASAVE(M) = -XA(M) + X1(IDUNEM)
HASAVE(M)=-HA(M)
17800 CONTINUE
DO 17820 M=N2,NELM
XASAVE(M) = XA(M) + X1(IDUNEM)
HASAVE(M)=-HA(M)
17820 CONTINUE
C   FILE 9 CONTAINS INITIAL SMOOTHED CURVE.
   NPDOT = 0
   NPBCH = NL
   NPOFF = 0
   WRITE(9,20)RNG,RNGDAT,ICODE,YNORTH,XEAST,AZMUTH
   WRITE(9,25)DOTDAT,BCHDAT,OFFDAT,NL,NPDOT,NPBCH,NPOFF
   WRITE(9,30)(XASAVE(I),HASAVE(I),I=1,NL)

   DO 1780 M=1,NELM1
   I=NELM1-M+1
   NCON(I)=2
   XA(I) = -XA(I) + X1(IDUNEM)
   X(M,1)=XA(I)
1780 CONTINUE
DO 1782 M=N2,NELM
I=M-NELM1
XA(M) = XA(M) + X1(IDUNEM)
X(I,2)=XA(M)
HA(I)=-HA(M)
NLS=1
1782 CONTINUE

```

```

C      INITIALIZE 'ACTIVE' PROFILE
      NL=NLS
      X(NELM1,1)=-1000.0
      DO 1783 I=1,NL
1783    XA(I)=X(I,2)
          NPDOT = 0
          NPBCH = NL
          NPOFF = 0
          CALL SRGCT(ICNTY,RNG,SMULT,SSURGE;IRNG)
      C      WRITE(6,184)ICNTY,RNG,SMULT
184    FORMAT(' ICNTY,RNG,SMULT= ',I3,A8,F7.3)
      DO 185 I = 1,NTIMES
          STA(I) = STAI(I) * SMULT
185    CONTINUE
      C
      C      CALCULATE HSTAR TO NEAREST FOOT
      C
      DO 200 I = 1,NL
          XAO(I) = XA(I)
200    CONTINUE
          HS = (0.667 * A**1.5 / XMD)**2
          DXS = (HS / A)**1.5
          HSTAR = HS
      C
      DO 300 I = 1,NL
          XA(I) = XAO(I)
300    CONTINUE
          XR = 0.0
          DH(1) = 1.0
      C
      C      ESTABLISH INSTANTANEOUS WATER LEVEL, ST
      C
      AMP = 0.0
      P102 = 1.5708
      DT = PERIOD
      DO 400 I = 2,NL
          DH(I) = (HA(I) - HA(I-1) - DH(I-1)/2.0)*2.0
400    CONTINUE
      C
      C      NTIMES LOOP - LOOP FOR EACH SURGE VALUE
      C
      ZZ=1.0-EXP(-XK*DT)
      IBP=1
      NPA=1
      DO 1600 NTIME = 1,NTIMES
          TIME = (NTIME-1)*DT
          ST = STA(NTIME)
          DO 500 I = 1,NL
              DPTC(I) = HA(I) + ST
500    CONTINUE
              DPTB = HB/0.8
              XB = (DPTB / A) ** 1.5
      C
      C      ESTABLISH THE INDICES OF STILL WATER LEVEL AND HSTAR
      C
      IE = 1

```

```

      AA = 100.0
      DO 600 I = 1,NL
          BB = ABS(DPTC(I) - DPTB)
          IF (BB.GT. AA) GO TO 550
          AA = BB
          IE = I
550    IF (ABS(DPTC(I)) .LE. DH(I)/2) IWL = I
          IF (ABS(HSTAR - DPTC(I)) .LE. DH(I)/2) ISTAR = I
600    CONTINUE
          IB=NPA
          DO 1200 IIT = 1,10
              SUM1 = 0.0
              SUM2 = 0.0
              SUM3 = 0.0
              SUM4 = 0.0
              DO 700 I = IB,ISTAR
                  SUM1 = SUM1 + (HA(I) + ST - HSTAR) * DH(I) / XMD + DXS * DH(I)
                  SUM4 = SUM4 + DH(I)
                  SUM3 = SUM3 + XA(I) * DH(I)
700    CONTINUE
                  ISP = ISTAR + 1
                  DO 800 I = ISP, IE
                      SUM4 = SUM4 + DH(I)
                      SUM2 = SUM2 + (DPTC(I)/A)**1.5 * DH(I)
                      SUM3 = SUM3 + XA(I) * DH(I)
800    CONTINUE
                      IEP = IE + 1
                      DO 850 I = IEP,NL
                          IFILL = I-1
                          IF (XR + XB .LT. XA(I)) GO TO 1000
                          SUM3 = SUM3 + XA(I) * DH(I)
                          SUM4 = SUM4 + DH(I)
                          SUM2 = SUM2 + XB * DH(I)
                          IFILL = I
850    CONTINUE
1000   CONTINUE
                      XRO = XR
                      XR = 1.0/SUM4 * (SUM3 - SUM2 - SUM1)
      C
      C      ESTABLISH NEW VALUE OF IB
      C
      IB0 = IB
      BSTAR=(XR+DXS-XA(ISTAR)+DPTC(ISTAR)-HSTAR)/XMD
      BSTAR=BSTAR*ZZ
      XSTAR=XA(ISTAR)+BSTAR
      IB=NPA
      C      WRITE(6,1106)
1106   FORMAT(' NTIME,IIT,I,IB,BB,XSTAR,BSTAR,XA(ISTAR),DPTC(I),
          -HSTAR,XA(I),ZZ ')
          IB=NPA
          DO 1100 I = NPA,IE
              BB=XSTAR+(DPTC(I)-HSTAR)/XMD-XA(I)
              IF (BB.LT.0.0) GO TO 1110
              IB=I+1
      C      WRITE(6,1105)NTIME,IIT,I,IB,BB,XSTAR,BSTAR,
      C      -XA(ISTAR),DPTC(I),HSTAR,XA(I),ZZ

```



```

1105 FORMAT(4I4,BF7.2)
1100 CONTINUE
1110 CONTINUE
      IF (IB.LT.1)IB=1
      IF ((IB.EQ. IBO) .AND. (ABS(XRO - XR) .LE. .01)) GO TO 1300
C+++++
1200 CONTINUE
1300 CONTINUE
C      WRITE(6,1302)
1302 FORMAT(//)
C
C      CALCULATE DX VALUES
C
      DO 1400 I = IB,IFILL
      IF (I.GT. ISTAR .AND. I .LE. IE) GO TO 1325
      IF (I .GT. IE) GO TO 1350
      DX(I) = XA(I) - (XR + DXS + (HA(I) + ST-HSTAR) / XMD)
      GO TO 1400
1325 DX(I) = XA(I) - (XR + ((HA(I) + ST)/A)**1.5)
      GO TO 1400
1350 DX(I) = XA(I) - (XR + XB)
1400 CONTINUE
      VOLCHG = 0.0
      BA = (1.0 - EXP(-XK*DT))
      DO 1500 I = IB,IFILL
      BB = -DX(I) * BA
      VOLCHG = VOLCHG + BB * DH(I)
      XA(I) = XA(I) + BB
      IF (NCON(NPA).EQ.2.AND.XA(NPA).LT.X(NPA,1)) NPA=NPA+1
1500 CONTINUE
C      IF (MOD(NTIME,5).NE.0.AND.NTIME.NE.1) GO TO 1510
C      WRITE(6,1505)NTIME,NPA,IB,IWL,ISTAR,IE,ST,
C      - (I,HA(I),XA(I),NCON(I),
C      - X(I,1),X(I,2),I=1,NP)
1505 FORMAT(1H0,'NTIME NPA IB IWL ISTAR IE ST',/,1H ,
- 2I5,I5,I5,I7,I4,F5.2,/,1H ,
- ' HA(I) XA(I) NCON(I) X(I,1) X(I,2)',/,
- (I5,F5.1,F8.1,I8,F10.2,F10.2))
1600 CONTINUE
C
C *** END OF TIME LOOP ***
C
      DO 1700 I = 1,NL
      DX(I) = XA(I) - XAO(I)
1700 CONTINUE
      S1=0.0
      NPAM=NPA-1
      IF (NPA.EQ.1) GO TO 1721
      DO 1720 I=1,NPAM
      IF (HA(I).GT.0.0) GO TO 1732
1720 S1=S1+(X(I,2)-X(I,1))
1721 DO 1730 I=NPA,NL
      AA=X(I,2)-XA(I)
      IF (HA(I).GT.0.0) GO TO 1732
      IF (AA.LT.0.0) GO TO 1732
1730 S1=S1+AA

```

```

1732 CONTINUE
      VOL=S1/27.0
      VOLTOT=VOLTOT+VOL
C
      WRITE(6,11001)RNG,IMAX
11001 FORMAT(//,6X,AB,'DUNE ELEVATION: ',I2,
- ' LOC. RELATIVE TO MONU.(FT.) DISTANCE ERODED (FT.)',/)
      DO 1550 IJK = 1,NL
      IF (HA(IJK) .NE. -25.0) GO TO 1532
      XTOT(6)=XTOT(6)+XA(IJK)
      DXTOT(6)=DXTOT(6)+DX(IJK)
      NTOT(6)=NTOT(6)+1
      WRITE(6,11000) HA(IJK),XA(IJK),DX(IJK)
11000 FORMAT(1H ,15X,F5.1,' FT. CONTOUR: ',10X,F9.1,17X,F9.1)
1532 IF (HA(IJK) .NE. -20.0) GO TO 1534
      XTOT(5)=XTOT(5)+XA(IJK)
      DXTOT(5)=DXTOT(5)+DX(IJK)
      NTOT(5)=NTOT(5)+1
      WRITE(6,11000) HA(IJK),XA(IJK),DX(IJK)
1534 IF (HA(IJK) .NE. -15.0) GO TO 1536
      XTOT(4)=XTOT(4)+XA(IJK)
      DXTOT(4)=DXTOT(4)+DX(IJK)
      NTOT(4)=NTOT(4)+1
      WRITE(6,11000) HA(IJK),XA(IJK),DX(IJK)
1536 IF (HA(IJK) .NE. -10.0) GO TO 1538
      XTOT(3)=XTOT(3)+XA(IJK)
      DXTOT(3)=DXTOT(3)+DX(IJK)
      NTOT(3)=NTOT(3)+1
      WRITE(6,11000) HA(IJK),XA(IJK),DX(IJK)
1538 IF (HA(IJK) .NE. -5.0) GO TO 1540
      XTOT(2)=XTOT(2)+XA(IJK)
      DXTOT(2)=DXTOT(2)+DX(IJK)
      NTOT(2)=NTOT(2)+1
      WRITE(6,11000) HA(IJK),XA(IJK),DX(IJK)
1540 IF (HA(IJK) .NE. 0.0) GO TO 1550
      XTOT(1)=XTOT(1)+XA(IJK)
      DXTOT(1)=DXTOT(1)+DX(IJK)
      NTOT(1)=NTOT(1)+1
      WRITE(6,11000) HA(IJK),XA(IJK),DX(IJK)
1550 CONTINUE
      WRITE(6,1734)VOL
1734 FORMAT(1H0,13X,'VOLUME ERODED: ',F10.2,' CUBIC YARDS PER FOOT
- MEASURED FROM MSL UP',/)
      NP=NL-NPA+1
C      FILE 10 CONTAINS ERODED SMOOTHED CURVE.
      WRITE(10,20)RNG,RNGDAT,ICODE,YNORTH,XEAST,AZMUTH
      WRITE(10,25)DOTDAT,BCHDAT,OFFDAT,NP,NPDOT,NP,NPOFF
      WRITE(10,30)(XA(KK),HA(KK),KK=NPA,NL)
      GO TO 175
9999 IF (PROF.LE.1.0) GO TO 99999
      WRITE(6,10050)CNAME(ICNTY)
      WRITE(6,10055)XMD,XK
      WRITE(6,1560)
1560 FORMAT(///,6X,'TOTALS FOR ALL PROFILES LOC. RELATIVE TO M
-ONU.(FT.) DISTANCE ERODED (FT.)',/)
      DO 1570 I = 1,6

```

```

      IF (NTOT(I).NE.0) GO TO 1575
      XTOT(I)=0.0
      DXTOT(I)=0.0
      GO TO 1577
1575  XTOT(I)=XTOT(I)/NTOT(I)
      DXTOT(I)=DXTOT(I)/NTOT(I)
1577  CONT=FLOAT(I-1)*5.0
      WRITE(6,1580) CONT,XTOT(I),DXTOT(I)
1580  FORMAT(1H,15X,F5.1,' FT. CONTOUR: ',10X,F9.1,17X,F9.1)
1570  CONTINUE
      VOLT=VOLTOT/PROF
      WRITE(6,1590)VOLTOT,VOLT
1590  FORMAT(1H0,5X,'TOTAL VOLUME ERODED FOR ALL PROFILES: ',F10.2,/
-      1H,5X,'AVERAGE VOLUME ERODED FOR ALL PROFILES: ',F10.2,/)
C
99999 STOP
C
      END
      SUBROUTINE SMOOTH(NBEG,NMAX,ICODE)
C
C      SUBROUTINE TO SMOOTH SURVEY DATA.
C      IF ICODE EQUALS 2, SUBROUTINE HAS BEEN CALLED TO SMOOTH REAR
C      OF DUNE; IF ICODE EQUALS 1, SUBROUTINE HAS BEEN CALLED TO
C      SMOOTH FRONT OF DUNE. SMOOTHING OCCURS FROM HIGHEST ELEVATION
C      TO EITHER FIRST OR LAST SURVEY POINT.
C      SUBROUTINE USES SURVEY H AND X VALUES TO SET VALUES FOR XA,
C      GIVEN PREVIOUSLY SET HA VALUES (FROM MAIN).
C
      COMMON /A/ H1(200),XA(200),HA(200),NELM,X1(200),NP,NELM1
      NSTART=NBEG
      NFINI=NMAX-1
      IF (ICODE .EQ. 2) NFINI = NMAX
      IF (ICODE .EQ. 2) NSTART = NBEG - 1
C
      WRITE(6,10)NSTART,NFINI
10    FORMAT(' NSTART,NFINI ',2I5)
      INC = 1
      IF (ICODE .EQ. 2) INC = -1
C
      DO 800 I = NSTART,NFINI,INC
      H11=H1(I)
      H22=H1(I+1)
      DH=ABS(H11-H22)
      DX=X1(I+1)-X1(I)
      HU=H11
      HL=H22
C
      WRITE(6,20)H11,H22,DH,DX,HU,HL
20    FORMAT(' H1,H2,DH,DX,HU,HL ',6F7.2)
      IF (H22.LT.H11) GO TO 100
C
      HU=H22
      HL=H11
100   NEL1 = NELM1
      NEL2 = NELM
      IF (ICODE .NE. 2) GO TO 200
      NEL1 = NELM1
      NEL2 = 1

```

```

200  DO 300 NEL=NEL1,NEL2,INC
      IF (HA(NEL).LT.HU) GO TO 400
300  CONTINUE
C400  WRITE(6,30)NEL,NEL1,NEL2,HA(NEL),HU
30    FORMAT(' NEL,NEL1,NEL2,HA(NEL),HU',3I5,2F7.2)
400  NB=NEL
      NEL2 = NELM
      IF (ICODE .EQ. 2) NEL2=1
C
      DO 700 N = NB,NEL2,INC
      IF (HA(N).GT.HL) GO TO 600
      XA(N)=XA(N)+DX
      GO TO 700
C
600  DEL1 = (HU - HA(N))/DH
      XA(N) = XA(N) + DX * DEL1
C
      WRITE(6,40)N,HA(N),HL,X(N),XA(N),DEL1
40    FORMAT(' N,HA(N),HL,X(N),XA(N),DEL1 ',15,5F7.2)
700  CONTINUE
C
800  CONTINUE
      RETURN
      END
      SUBROUTINE SRGFCT(ICNTY,RNG,SMULT,SSURGE,IRNG)
C
C      THIS SUBROUTINE CALCULATES A SCALING FACTOR WHICH WILL BE APPLIED
C      TO THE STORM TIDE TIME SERIES.
C
      DIMENSION SSVAL(5),NRNG(5)
      DIMENSION IBND(22,5),SRG(22,5)
      DIMENSION SRGCAL(13)
      CHARACTER*8 RNG
      DATA NRNG/8,6,22,6,0/
      DATA IBND/
1      1,22,43,74,84,98,112,129,14*0.0,
2      1,17,34,50,67,83,16*0.0,
3      1,15,30,60,75,92,101,110,125,138,150,162,172,183,
-      194,200,206,212,217,223,228,240,
4      1,16,31,46,61,69,16*0.0,
5      22*0.0/
      DATA SRG/
1  11.4,11.3,11.2,11.1,10.9,10.7,10.5,10.5,14*0.0,
2  13.9,13.8,13.7,13.45,13.2,13.2,16*0.0,
3  12.05,12.1,12.15,12.2,12.25,12.3,12.4,12.45,12.5,12.6,12.95,13.0,
-  13.15,13.3,14.4,14.55,14.7,14.85,15.0,15.15,15.30,15.30,
4  13.1,13.0,12.9,12.8,12.7,12.7,16*0.0,
5  22*0.0/
      DATA SRGCAL/7.0,7.5,7.9,8.4,8.8,9.3,9.8,10.2,10.7,
-  11.1,11.6,12.0,12.5/
      DATA SSVAL/10.0,13.9,13.78,12.99,1.0/
      DATA ICAL/0/
C
C      CONVERT CHARACTER RANGE TO INTEGER RANGE
C

```

```

      IRNG=0
      DO 50 I=1,3
      J=I+2
      K=ICHR(RNG(J:J))
      IF (K.LT.240) GO TO 100
      IRNG=IRNG*10+(K-240)
50  CONTINUE
100 IF (ICAL.EQ.0) GO TO 150
C
C *** SCALE CALIBRATION STORM SURGE (WALTON COUNTY HURRICANE ELOISE)
C
      DO 110 I=1,13
      IF (IRNG.GE.((I-1)*10).AND.IRNG.LT.((I)*10)) GO TO 120
110 CONTINUE
120 SSURGE=SRGCAL(I)
      SMULT=SSURGE/8.35
      GO TO 300
C
C *** SCALE 100 YEAR STORM SURGE FOR CURRENT RANGE
C
150 N=NRNG(ICNTY)
      DO 160 I=2,N
      IF (IRNG.GE.IBND(I-1,ICNTY).AND.IRNG.LT.IBND(I,ICNTY)) GO TO 170
160 CONTINUE
170 SSURGE=SRG(I-1,ICNTY)
      SMULT=SSURGE/SSVAL(ICNTY)
C
      WRITE(6,99)ICNTY,IRNG,RNG,SSURGE,SMULT
99  FORMAT(I5,I5,A8,2F7.2)
300 RETURN
      END

```